# Optimal Area Triangulation

A Thesis Submitted to the
College of Graduate Studies and Research
in Partial Fulfillment of the Requirements
for the degree of Doctor of Philosophy
in the Departmentof Computer Science
University of Saskatchewan
Saskatoon

By
Tzvetalin Simeonov Vassilev

# Permission to Use

In presenting this thesis in partial fulfilment of the requirements for a Postgraduate degree from the University of Saskatchewan, I agree that the Libraries of this University may make it freely available for inspection. I further agree that permission for copying of this thesis in any manner, in whole or in part, for scholarly purposes may be granted by the professor or professors who supervised my thesis work or, in their absence, by the Head of the Department or the Dean of the College in which my thesis work was done. It is understood that any copying or publication or use of this thesis or parts thereof for financial gain shall not be allowed without my written permission. It is also understood that due recognition shall be given to me and to the University of Saskatchewan in any scholarly use which may be made of any material in my thesis.

Requests for permission to copy or to make other use of material in this thesis in whole or part should be addressed to:

Head of the Department of Computer Science
176 Thorvaldson Building
110 Science Place
University of Saskatchewan
Saskatoon, Saskatchewan
Canada
S7N 5C9

# Abstract

Given a set of points in the Euclidean plane, we are interested in its triangulations, i.e., the maximal sets of non-overlapping triangles with vertices in the given points whose union is the convex hull of the point set. With respect to the area of the triangles in a triangulation, several optimality criteria can be considered. We study two of them. The MaxMin area triangulation is the triangulation of the point set that maximizes the area of the smallest triangle in the triangulation. Similarly, the MinMax area triangulation is the triangulation that minimizes the area of the largest area triangle in the triangulation. In the case when the point set is in a convex position, we present algorithms that construct MaxMin and MinMax area triangulations of a convex polygon in $O(n^2 \log n)$ time and $O(n^2)$ space. These algorithms are based on dynamic programming. They use a number of geometric properties that are established within this work, and a variety of data structures specific to the problems. Further, we study polynomial time computable approximations to the optimal area triangulations of general point sets. We present geometric properties, based on angular constraints and perfect matchings, and use them to evaluate the approximation factor and to achieve triangulations with good practical quality compared to the optimal ones. These results open new direction in the research on optimal triangulations and set the stage for further investigations on optimization of area.

# Acknowledgements

There are three men who had great influence on my mathematical education, and to whom I owe what I have achieved in my academic life. First, I would like to thank my father Dr. Simeon Vassilev, an accomplished matematician himself, who taught me to read and write, and introduced me to most of the concepts of elementary mathematics. Second, I would like to thank Dr. Nikolay Hadjiivanov, who was a great teacher, and most of all a great mentor. Third, I would like to thank my academic supervisor Dr. J. Mark Keil, who introduced me to the field of Computational Geometry, guided and encouraged me during my studies at the University of Saskatchewan, and supported me financially!

To my family and friends with love

# Contents

# List of Tables

# List of Figures

# List of Abbreviations

| | |
|---|---|
| CCW | Counter ClockWise |
| CW | ClockWise |
| DT | Delaunay Triangulation |
| GG | Gabriel Graph |
| LMT | Locally Minimal Triangulation |
| MAT | Maximum Weight Triangulation |
| MST | Minimum Spanning Tree |
| MWT | Minimum Weight Triangulation |
| NE | North East |
| NW | North West |
| RNG | Relative Neighbourhood Graph |

# Chapter 1

# Introduction

## 1.1 Triangulation

**Definition 1 (Triangulation)** *Let $S$ be a set of $n$ points in two-dimensional Euclidean space (plane). A set $T$ of triangles is called a* ***triangulation*** *of the point set $S$ if and only if:*

- *every triangle of $T$ has its vertices in $S$*
- *no triangle of $T$ contains a point from $S$ in its interior*
- *every two triangles in $T$ have disjoint interiors*
- *the union of all the triangles in $T$ is exactly the convex hull of $S$.*

The sides of the triangles in $T$ are called **edges** of the triangulation. It follows from the definition above that no two edges of a triangulation intersect properly. In some texts on computational geometry [19], a triangulation is defined, equivalently, as a set of edges. We prefer the definition given above because triangles and their characteristics are the main focus of our work.
When we talk about a point set, we mean a point set **in general position**, i.e., no three points of the set being collinear, and no four points of the set being co-circular. This assumption is commonly made to avoid degeneracies. There are computational issues arising from and results on dealing with degeneracies, perturbation techniques, etc. These are not a focus of our considerations. We are also considering a special case of a planar point set. We say that the point set is in a **convex position** when all the points of the set are on the convex hull, i.e. the points of the set are vertices of a convex polygon. In this case, the points of the set are also called **vertices**, and the edges of the triangulation are also called **diagonals**.

**Property 2** *Let $S$ be a set of $n$ points in the plane, $h$ of which are on the convex hull of $S$. Every triangulation of $S$ has exactly $2n - h - 2$ triangles and exactly $3n - h - 3$ edges.*

Hence, the triangulation has linear complexity with respect to the size of the point set, considering both the triangles and the edges. This fact is very useful when analyzing time and space require-

ments of various algorithms for optimal triangulation.

Figure 1.1 on the following page shows two different triangulations of a sample point set.

## 1.2 Optimization and optimality criteria

Triangulations of point sets in the plane have been studied for the last three decades as one of the important structures in computational geometry. There are three important characteristics of a triangle: edge lengths, angles and area. While length and angle based optimality criteria are relatively well studied, there are no results on area based optimization. This served as a major motivating factor of this study. As it will be further revealed, it is possible and sometimes useful to consider area as a constraint rather than as a general optimization criterion. The need to study optimal triangulations, apart from the mathematical challenges that are abundant here, is dictated by practical applications. Triangulations with special properties and characteristics are used in computer graphics [46, 50], terrain approximation, multivariable analysis, numerical methods, mesh generation [6, 52, 53], etc. Connected subgraphs of triangulations such as Gabriel Graph and Relative Neighbourhood Graph are used in wireless networking and ad hoc routing [11]. Further, computing a triangulation with particular properties is typically far from trivial. As it is shown in [43], even determining whether a set of edges with vertices in the point set $S$ contains a subset that forms a triangulation of $S$ is an $NP$-complete problem. Part of the complexity of computing a triangulation with particular properties arises from the number of possible triangulations.

**Property 3** *For a point set $S$ of $n$ points in the plane, there are*

$$\Omega(2.33^n) \leq t(S) \leq O(59^{n-\Theta(\log n)})$$

*different triangulations, where $t(S)$ denotes the number of the different triangulations of the point set $S$ [4].*

While the lower bound of $\Theta(2.33^n)$ is attained for special point sets called double circles, establishing a precise upper bound is a very interesting combinatorial problem that is still open. We seek algorithms that run in polynomial time and are capable of selecting or constructing a triangulation with specific properties amongst the exponentially many potential candidates. There are optimality criteria based on edge length, angles, areas and other elements of the individual triangles in a triangulation [6, 52, 54]. Further, in connection with those criteria, we can consider MinMax and MaxMin problems. The first quantifier defines the optimization that is done over all possible triangulations of the given point set, and the second quantifier specifies the optimization that is done within the respective elements (edges, angles, triangles) of a particular triangulation. For example, MinMax angle stands for the triangulation that minimizes the maximum angle in a triangulation over all possible triangulations of the given point set.

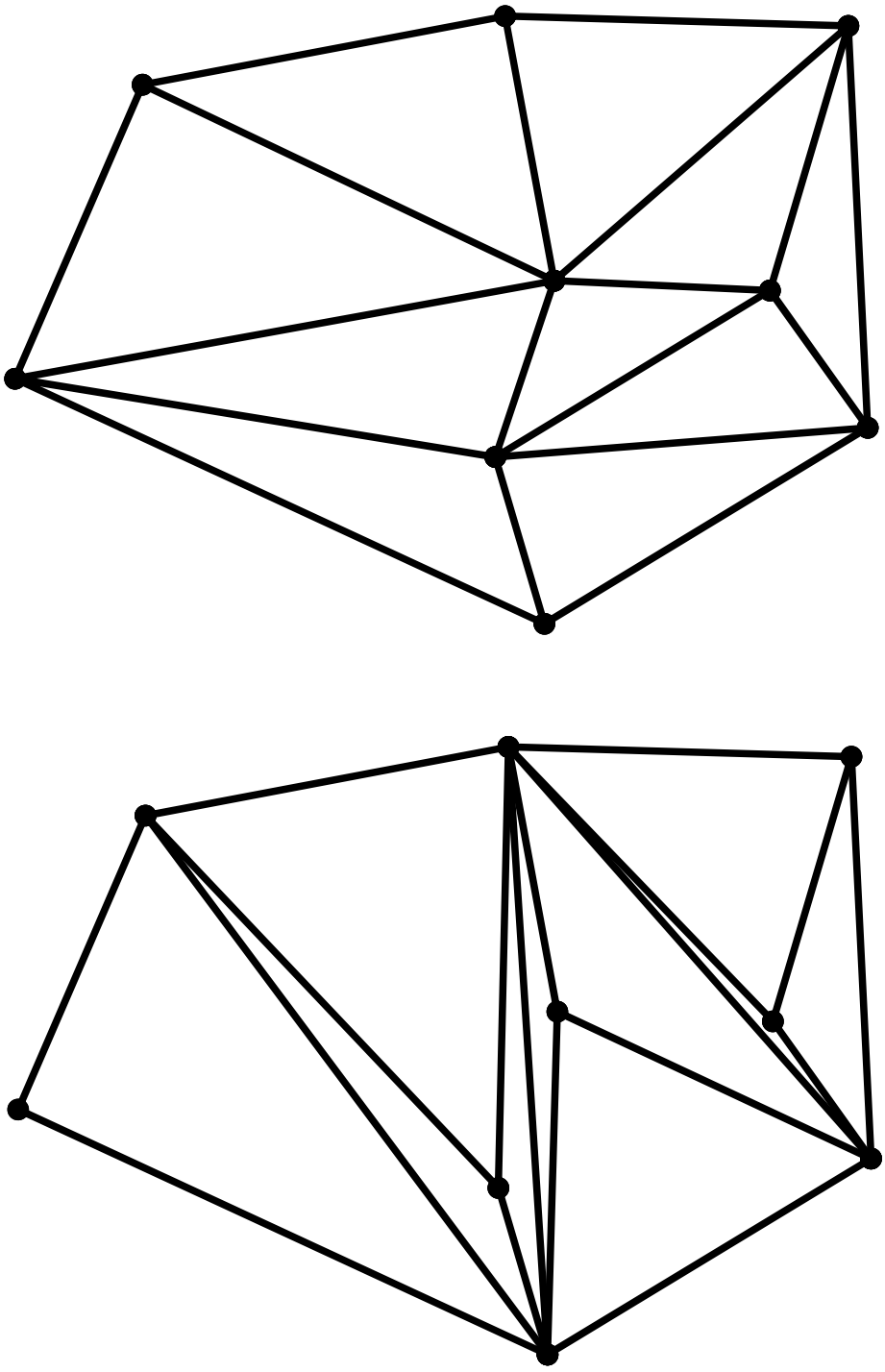

**Figure 1.1:** Two different triangulations of a point set with $n = 9, h = 6$ consisting of $3n - h - 3 = 18$ edges and $2n - h - 2 = 10$ triangles

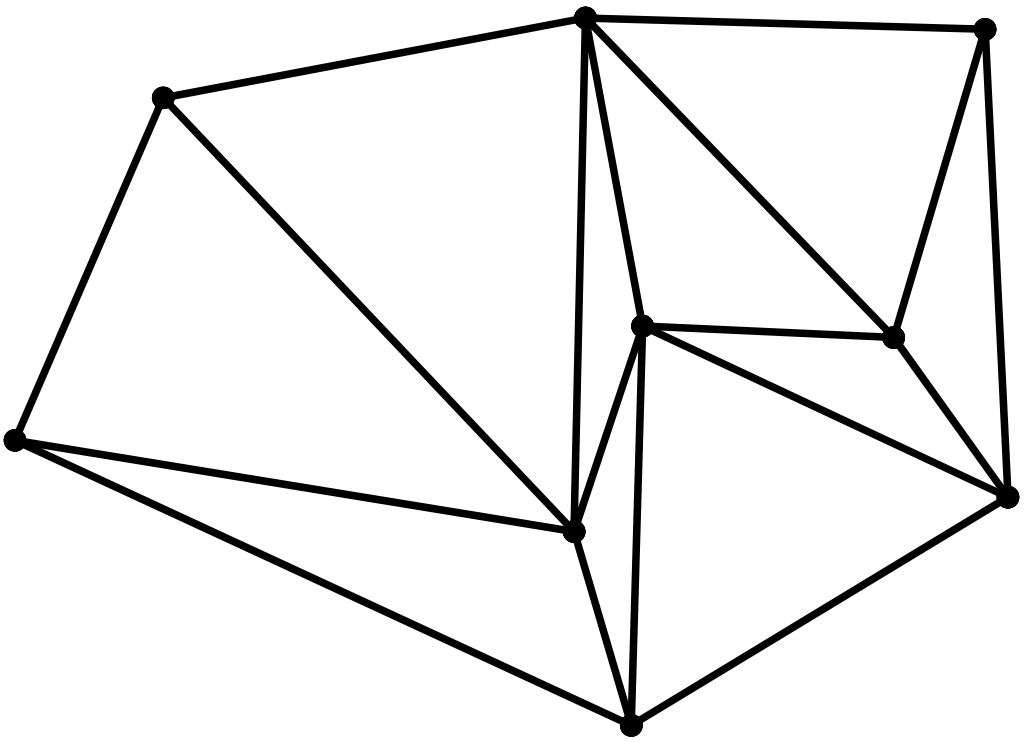

**Figure 1.2:** The Minimum Weight Triangulation of a set of nine points

We can also have global optimization criteria based on the triangulation as a whole, as opposed to the individual elements. For example, the triangulation that has minimum total length of its edges is known in the literature as Minimum Weight Triangulation (MWT). The MWT is important for minimum cost routing/connectivity, but it earned its fame by the numerous attempts to prove or disprove whether computing the MWT is an NP-complete problem. This is by far the most studied problem in the area of optimal triangulations [5, 7, 8, 15, 16, 18, 21, 22, 23, 24, 28, 29, 31, 42, 44, 47] and it is still open [19, 45, 48, 54]. Figure 1.2 gives an illustration of the Minimum Weight Triangulation of the same nine-point set that was presented in Figure 1.1 on the preceding page.
Another global optimization criterion might be exactly the opposite – the triangulation with the maximum total edge length. It is called MAT and interesting results on it were reported recently [30]. It is worth noting that angles and area cannot give meaningful global optimization criteria as their sum is constant for the given point set. However, higher order characteristics such as sums of squares, variances and standard deviations of area have been considered in the literature [17, 54]. An excellent summary of the optimal triangulations studied in the literature can be found in Lambert's thesis [38].

## 1.3 Quality measures

As previously mentioned, practical reasons dictate preference of one optimal triangulation over another for a specific purpose. Thus, the optimality criteria are connected to the quality measures.

**Definition 4 (Quality measure)** *A **quality measure** is a function that allows us to quantitatively compare two triangulations. It can be any reasonable function or composition of functions that arises from our needs. For example, the sum of the lengths of the edges of a triangulation $T$, denoted by $w(T)$, is one quality measure.*

**Definition 5** *A triangulation $T$ of a planar point set $S$ is called **locally optimal** with respect to a quality measure $\eta$ if and only if for each of the triangles in $T$, all the convex quadrilaterals of which it is a part are triangulated in a way that optimizes the quality measure $\eta$.*

Local optimality with respect to $\eta$ does not guarantee global optimality with respect to the same quality measure, i.e. usually there are multiple locally optimal triangulations with different values of their quality measures. There are also situations in which a globally optimal triangulation might not be locally optimal. Generally, in such cases it is algorithmically harder to find the optimal triangulation.

**Definition 6** *A quality measure is called **decomposable** if and only if any optimal trinagulation with respect to it is locally optimal.*

Decomposability is an important property of a quality measure, as it has algorithmic implications. Most of the quality measures that we consider in this thesis are decomposable. Those that are not decomposable are explicitly mentioned as such. In particular, the MaxMin and MinMax Area triangulations are decomposable. In the case of MinMax and MaxMin Area, the quality measures can be defined as follows:

**Definition 7** *Denote by $A_\Delta$ the area of the triangle $\Delta$. Let $\mu(T)$ be the quality measure that represents the minimum area of a triangle in a given triangulation $T$, i.e.*

$$\mu(T) = \mu_0 \Leftrightarrow \forall \Delta \in T : A_\Delta \geq \mu_0, \exists \Delta^{'} \in T : A_{\Delta'} = \mu_0$$

*Similarly, $\lambda(T)$ is the quality measure that represents the maximum area of a triangle in a given triangulation $T$, i.e.*

$$\lambda(T) = \lambda_0 \Leftrightarrow \forall \Delta \in T : A_\Delta \leq \lambda_0, \exists \Delta^{''} \in T : A_{\Delta''} = \lambda_0$$

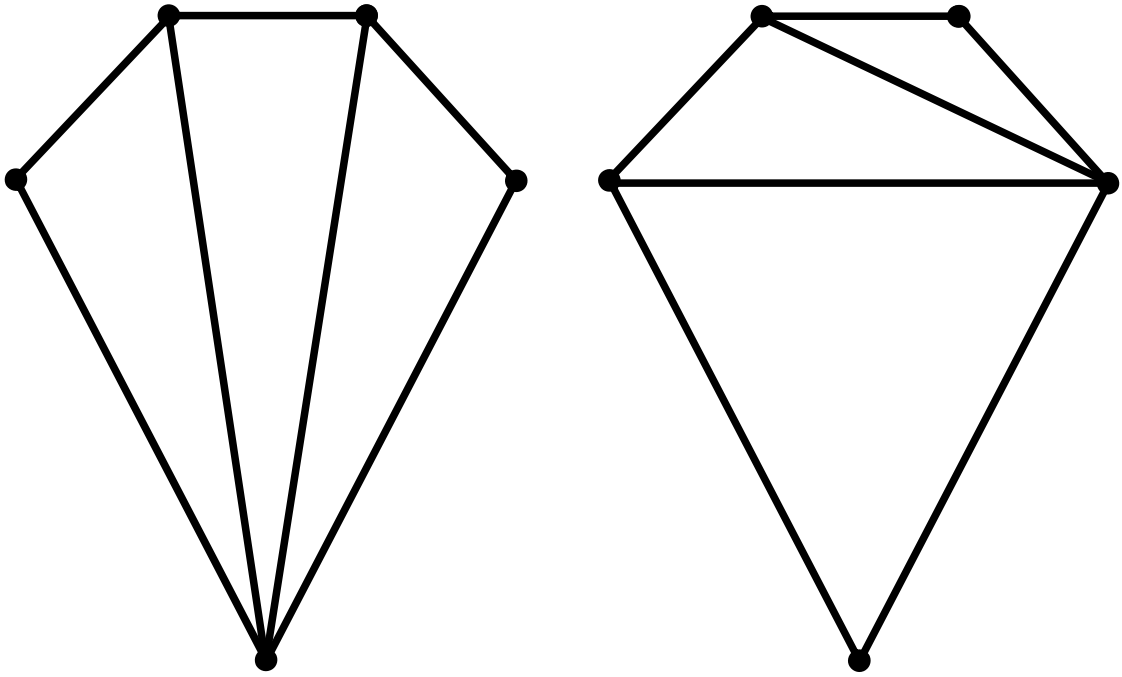

**Figure 1.3:** MinMax Area triangulation (left) and a "fat" triangulation (right) of a five-point set

In the literature on mesh generation, there is an ongoing discussion about the quality of the triangles themselves [6, 52]. Generally a triangle is considered good if it is "fat", i.e. all of its angles are above certain value. In particular, there are two types of triangles that have to be avoided, "flat" triangles (with two angles close to 0°) and "needle" triangles (with two angles close to 90°). The area of an individual triangle has no significance unless compared to the areas of other triangles, to the average area of triangles in the triangulation, or to the area of the (convex hull of the) set. Examples can be constructed that show triangulations containing only fat triangles that have arbitrarily large difference between the largest and smallest areas of their triangles on one hand, and triangulations that contain only equal area triangles that have arbitrarily small angles on the other hand. Figure 1.3 illustrates the difference between optimizing area and optimizing angles. This observation leads to the conclusion that optimizing area might be needed in some cases where optimizing angles does not give nice results (and vice versa), and these two quality measures are not necessarily related. The two optimal area triangulations that we study – MinMax and MaxMin area triangulations – both aim to provide more even distribution of the area between the triangles, which is desirable in many applications: maps, numerical methods, etc.

## 1.4 Optimization and decision problems

We can consider three types of problems with respect to optimal triangulations.

**Definition 8 (Optimization problem)** *Given a planar set of points $S$ and an optimality criterion represented by the quality measure $\eta$, the* ***optimization problem*** *is*
*"Find the triangulation(s) $T$ of $S$ that optimize(s) the value of $\eta$ over all possible triangulations of $S$."*

**Definition 9 (Decision problem)** *Given a planar set of points $S$, a quality measure $\eta$, and a real number $\tau$, the* ***decision problem*** *is*
*"Is there a triangulation $T$ of $S$ such that $\eta(T) \geq \tau$ (or $\eta(T) \leq \tau$)?"*

**Definition 10 (Construction problem)** *Given a planar set of points $S$, an optimality criterion represented by the quality measure $\eta$, and a real number $\tau$, the* ***construction problem*** *is*
*"Find a triangulation $T$ of $S$ such that $\eta(T) \geq \tau$."*

Of course, the optimization, the construction, and the decision problems are interdependent.

**Property 11** *The optimization problem with respect to a single-triangle-based quality measure is decidable in polynomial time if and only if the construction problem is decidable in polynomial time.*

**Proof.** The "only if" direction is trivial. If we can solve the optimization problem in polynomial time, then let $T^*$ be the optimal triangulation found. For each value of $\tau, \tau \leq \eta(T^*)$, the triangulation $T^*$ found by the optimization problem is a solution to the construction problem. For all other values of $\tau, \tau > \eta(T^*)$, there is no solution to the construction problem. In the "if" direction, we use the fact that the quality measure is based on triangles. We can compute all possible triangles with vertices in $S$. There are exactly $\binom{n}{3} \in O(n^3)$ of them in case $S$ is in convex position, and strictly less than that number otherwise. Further, we can sort them, say by descending value of the quality measure. All this takes $O(n^3 \log n)$ time. After that we start binary search for the, say smallest, value of $\tau$, call it $\tau^*$, such that construction problem has a solution. This solution is our optimal solution for the optimization problem. As for the timing, we have $O(\log n)$ calls to the construction problem, which has by our assumption a polynomial time complexity, $O(n^k)$, for some constant $k$. This takes $O(n^k \log n)$ overall time. We also had a preprocessing time of $O(n^3 \log n)$. Finally, the optimization problem is decidable in $O(n^j \log n)$, where $j = \max(k, 3)$. □

Note that the statement of Property 11 can be strenghtened. If, instead of the single-triangle-based quality measure, we had an single-edge-based quality measure then similar reasoning will give us

polynomial time computability in the "if" direction. The proof implies that the same is true for any quality measure, not necessarily edge- or triangle-based, as long as we have a polynomial number of discrete values for the quality measure that have to be checked by invoking the construction problem as a subroutine.

If we can solve the optimization problem, we can solve the decision problem. The converse of this is not generally true. However, if the decision problem can be solved, it can be called as a subroutine to find the "best" triangle in the solution of the optimization problem. If the set $S$ is in convex position, and the quality measure is decomposable, we can then repeat the process. In the convex case removing any triangle with vertices in $S$ will result in at least one and at most three new interior disjoint convex sets. Thus, we have constant number of nested calls to the decision problem subroutine at each level. Moreover, the total number of these calls (levels) will be $O(n)$ as we have to discover $O(n)$ triangles (remember that the number of triangles in each triangulation is $O(n)$). Therefore, in the case of a point set in convex position, a polynomial algorithm for the decision problem yields a polynomial algorithm for the optimization problem.

## 1.5 Delaunay triangulation, flips, locally optimal triangulations

**Definition 12 (Delaunay Triangulation)** *Given a planar set of points $S$, the **Delaunay Triangulation (DT)** of $S$ consists of all triangles with vertices in $S$ such that their circumscribed circles do not have interior points from the set $S$.*

This is only one of the many equivalent ways to define the Delaunay triangulation [49]. It is also known as the dual of the Voronoi diagram, in a sense that there is an edge between two points in the Delaunay triangulation iff their Voronoi regions share an edge. Figure 1.4 on the next page shows the Delaunay triangulation of the same point set that appears in Figure 1.1 on page 3 and Figure 1.2 on page 4. Both the Voronoi diagram and the Delaunay triangulation have been studied extensively [10, 14, 35, 38, 44, 51]. They have nice generalizations in higher dimensions and many interesting properties [49]. For example,

**Property 13** *The Delaunay triangulation of a planar point set $S$ is the MaxMin angle triangulation of $S$. It is also the MinMax circumradius triangulation of $S$ [49].*

The Delaunay triangulation can be computed in optimal $O(n \log n)$ time and $O(n)$ space by a variety of methods, including plane sweep, divide and conquer, etc.
From the point of view of optimization, it is important to mention the flipping algorithm and the properties of the Delaunay triangulation with regard to edge flips.

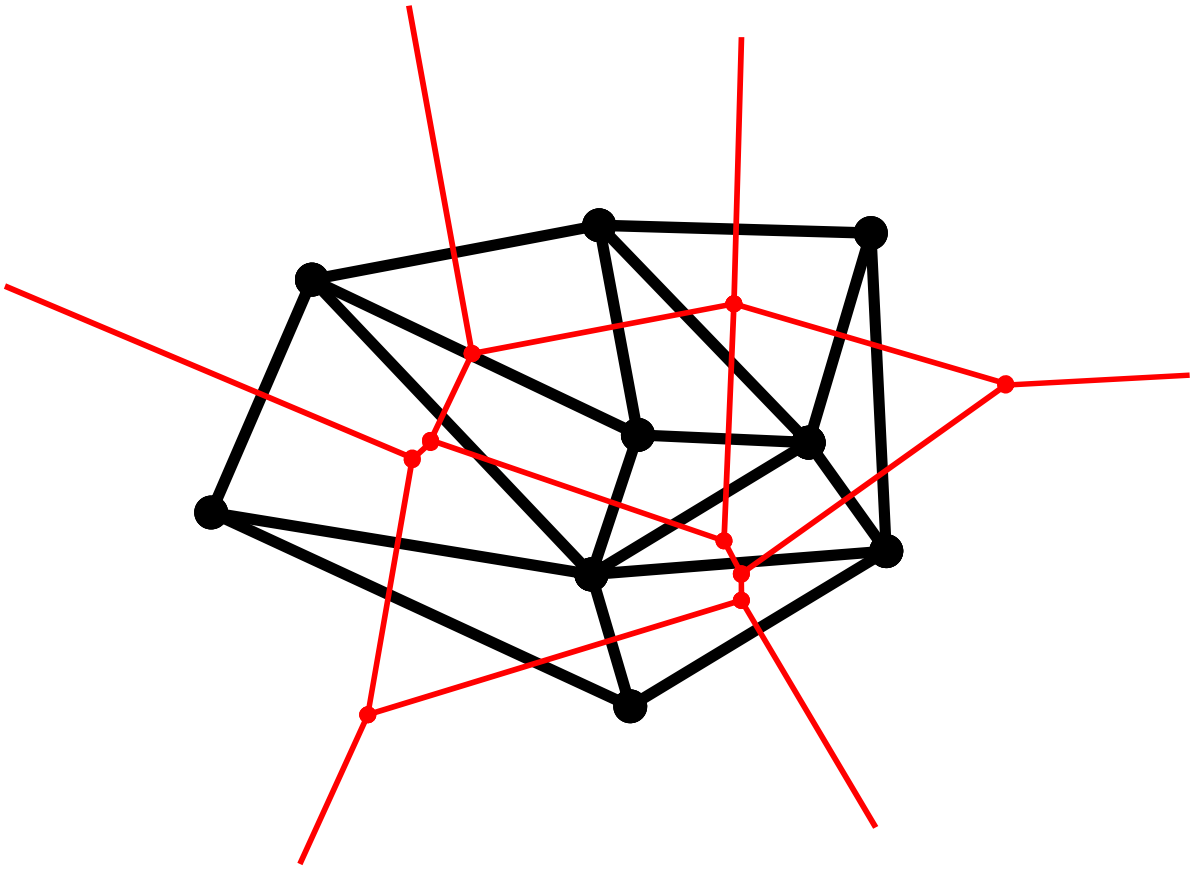

**Figure 1.4:** The Delaunay triangulation (bold lines) and the Voronoi diagram (light lines) of a point set

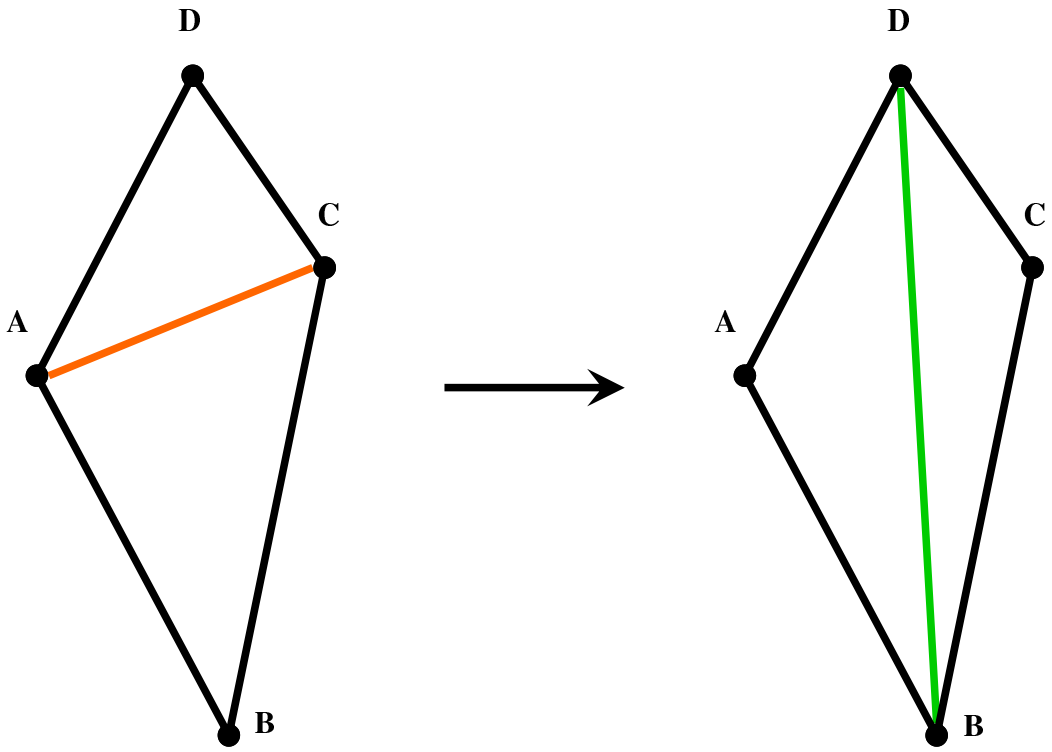


**Figure 1.5:** Edge flip

**Definition 14** *If two triangles $\triangle ABC$ and $\triangle ACD$ in a triangulation share an edge ($AC$ in this case) and form a convex quadrilateral $ABCD$, then replacing the triangles $\triangle ABC$ and $\triangle ACD$ with the triangles $\triangle ABD$ and $\triangle BCD$ is called a* ***flip****.*

A flip is also commonly called **edge flip** in the literature with the understanding that in fact we remove the edge $AC$ from the triangulation, replacing it with the edge $BD$. This is illustrated in Figure 1.5.

The optimization criterion usually indicates whether a flip is beneficial, i.e. which of the two possible triangulations of a convex quadrilateral is preferred. A flip represents the smallest possible local change in a triangulation. The algorithmic idea is simple – we can look at the convex quadrilaterals within the triangulation one at a time, and make flips in order to achieve better triangulation. This technique is very similar to some of the heuristic approaches in linear optimization, where the goal is to achieve a "good" local optimum by improving the current best solution. As it was previously mentioned there is no guarantee that the flips will lead to the globally optimal triangulation. However, there is one notable exception. If a flip has the property that the fourth point is outside of the circumscribed circle of the triangle formed by the other three points, it is called **Delaunay flip**.

**Property 15** *The Delaunay triangulation is the only locally optimal triangulation with respect to the Delaunay flip [48].*

This property gives an interesting algorithmic result, and a connection between all the triangulations of a given point set. From each triangulation, we can obtain every other triangulation using not more than $O(n^2)$ flips. The directed graph whose nodes represent the triangulations of a point set, and arcs reflect the direction of a Delaunay flip is connected and has a unique sink – the Delaunay triangulation. Again, this is under the assumption that we don't have four (or more) co–circular points in the set which leads to multiple Delaunay triangulations. To conclude this subsection, there is no other quality measure known for which the locally optimal triangulation is necessarily globally optimal. Thus, one has to seek more elaborate algorithmic ideas in order to optimize quality measures that are not optimized by the Delaunay triangulation.

## 1.6 Other optimal triangulations

**Definition 16 (Greedy Triangulation)** *The **Greedy Triangulation** of a planar set of points $S$ is produced by the following algorithm: List all possible edges between pairs of points in $S$. Sort the list in ascending order of edge length. Repeat the following step, until the list is empty: add the first edge in the list to the current triangulation, and discard from the list all the edges that intersect properly this edge.*

Although it does not optimize any particular characteristic, the Greedy triangulation is well studied – mainly in connection to MWT [20, 39, 40, 41, 44]. The described algorithm for construction of the Greedy triangulation is not time optimal; it can be computed optimally in $O(n \log n)$ time for general set of points and in linear time for a convex polygon [19, 48, 59].

Figure 1.6 on the next page shows the Greedy triangulation of the sample set of nine points as in Figure 1.1 on page 3, Figure 1.2 on page 4, and Figure 1.4 on page 9. We used the same point set in the figures throughout this chapter in order to illustrate that the optimal triangulations with respect to different optimality criteria have distinct triangle sets, geometric properties, and visual appearance.

A large class of optimal triangulations can be computed using the **edge insertion** method [9]. The idea is to start with an arbitrary triangulation and improve it by inserting an edge that previously was not in the triangulation, removing all edges intersected by the newly inserted edge, and re-triangulating the resulting polygonal regions, see Figure 1.7 on page 14. To be convergent, this procedure requires that particular conditions are in place.

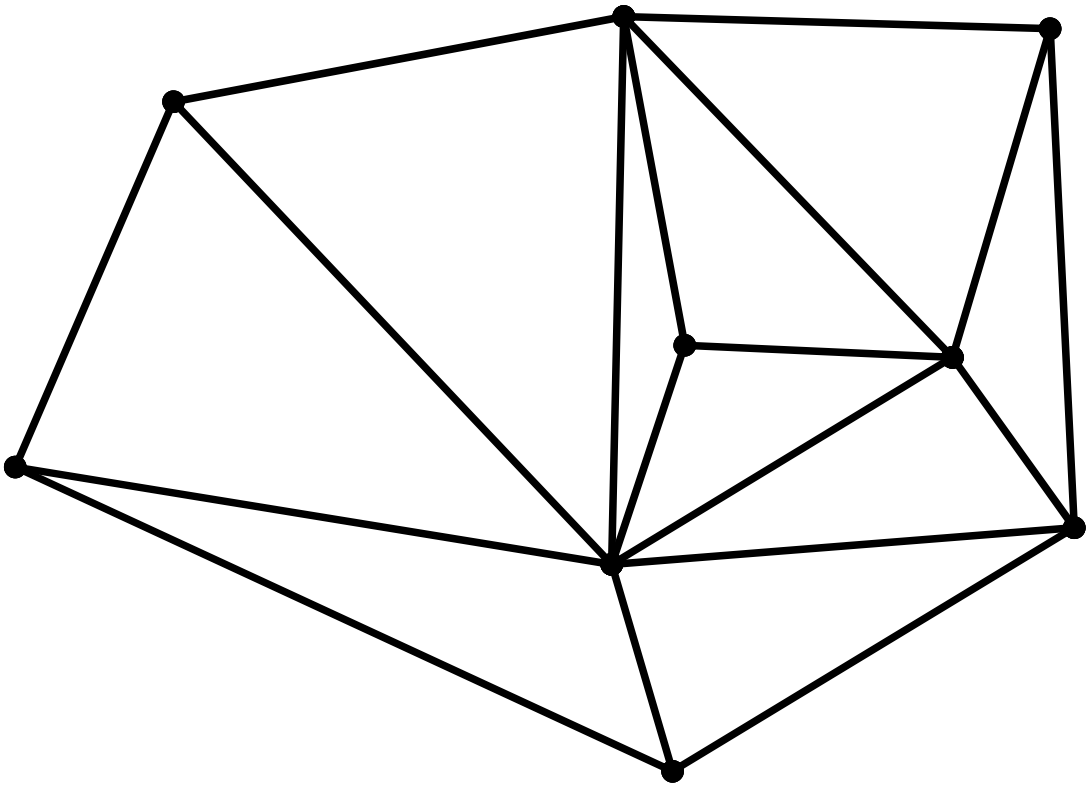

**Figure 1.6:** The Greedy Triangulation of a set of nine points

**Definition 17 (Anchor conditions, [9, 54])** *Given a planar set of points $S$, a quality measure $\eta$, and a triangulation $T$ of $S$, a triangle $\Delta \in T$ has an* ***anchor*** *if $\Delta$ is in the optimal triangulation of $S$ with respect to $\eta$, or in an optimal triangulation the triangle $\Delta$ is intersected by an edge emanating from one of its vertices. This vertex is called an* ***anchor*** *for this triangle. Depending on the quality measure $\eta$, there are two possibilities:*

- *only the worst triangle in a triangulation, with respect to $\eta$, has an anchor* ***(weak anchor condition)***
- *every triangle in a triangulation has an anchor* ***(strong anchor condition)***

**Property 18 ([9, 54])** *The edge insertion algorithm computes the optimal triangulations in*

- *$O(n^2 \log n)$ time and $O(n)$ space if $\eta$ satisfies the strong anchor condition*
- *$O(n^3)$ time and $O(n^2)$ space if $\eta$ satisfies the weak anchor condition.*

Two quality measures that are known to satisfy the strong anchor condition are MinMax angle and MaxMin height of a triangle. Two quality measures that satisfy only the weak anchor condition are MinMax eccentricity and MinMax slope [9, 54].
As a part of our work, we investigated the relationship between the MinMax area, MaxMin area, and the two anchor conditions.
There is another optimal triangulation that is computable in polynomial time by an algorithm that does not use any of the methods described above.

**Property 19** *The triangulation that minimizes the maximum edge length over all possible triangulations (**MinMax Length** triangulation) of a given planar set of points $S$ can be computed in $O(n^2)$ time and space [54].*

The algorithm that computes MinMax Length triangulation uses a variety of methods that were developed in computational geometry, mainly with connection to MWT and the Delaunay triangulation. Those include inclusion/exclusion regions, the relative neighborhood graph, and others. We will discuss them in Chapter 3, in connection with our algorithmic approach to the optimal area triangulations.

## 1.7 Summary of the previous results on optimal triangulations

The results on optimal triangulations, prior to our research on optimization of area, are summarized in Table 1.1 on page 16. There are some "unknown" entries which stand for "no significant research

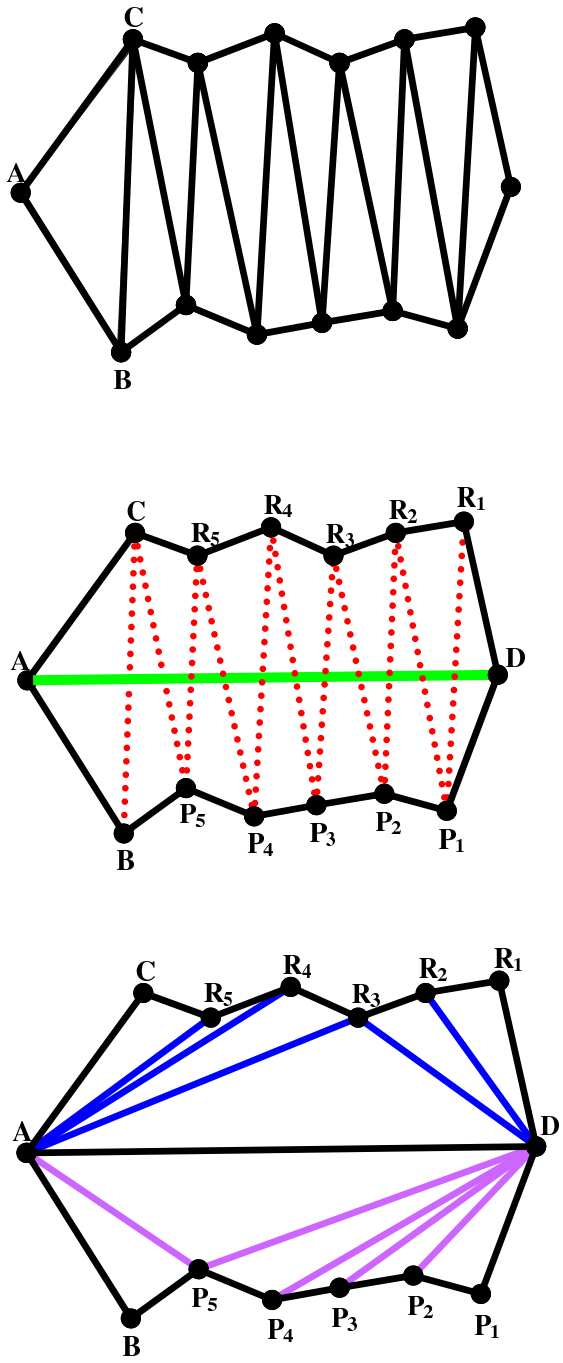


**Figure 1.7:** Edge insertion. Top: part of the existing triangulation surrounding the "worst" triangle $\triangle ABC$. Middle: introduction of the new edge $AD$. Bottom: re-triangulation of the new polygonal regions $ABP_5P_4P_3P_2P_1D$ and $DR_1R_2R_3R_4R_5CA$.

on the problem has been reported, the problem has been defined, known to be interesting, and conjectured to be very hard". The last three optimal triangulations in the table, the so-called $\delta$-triangulations, represent yet another meaningful optimization that can be done. Instead of finding the MinMax area and MaxMin area triangulations, we might want to find a triangulation in which the maximum difference between the area of the largest and smallest area triangles is minimized – this is the MinMax $\delta$-area triangulation. Similarly, it is interesting to know these for length and angles.

**Table 1.1:** Comparison between the known optimal triangulation algorithms

| **Optimal Triangulation** | **General Point Set** | **Convex polygon** | **Algorithms** |
|---|---|---|---|
| Minimum Weight (Min Total Edge Length) | Unsolved, no polynomial time algorithm known | $O(n^3)$ time, $O(n^2)$ space | Heuristics for general case [19, 48], Klincsek's for convex polygon [37] |
| Greedy | $O(n \log n)$ time, $O(n)$ space | $O(n)$ time, $O(n)$ space | Plane sweep, divide and conquer [19, 54, 59] |
| Delaunay (MaxMin Angle) | $O(n \log n)$ time, $O(n)$ space | $O(n)$ time, $O(n)$ space | Plane sweep, divide and conquer, edge flipping [19, 48, 1] |
| MinMax Length | $O(n^2)$ time, $O(n^2)$ space | $O(n^2)$ time, $O(n^2)$ space | Problem specific [54] |
| MinMax Angle | $O(n^2 \log n)$ time, $O(n)$ space | $O(n^2 \log n)$ time, $O(n)$ space | Edge insertion [9, 26, 54] |
| MaxMin Height | $O(n^2 \log n)$ time, $O(n)$ space | $O(n^2 \log n)$ time, $O(n)$ space | Edge insertion [9, 54] |
| MinMax Eccentricity | $O(n^3)$ time, $O(n^2)$ space | $O(n^3)$ time, $O(n^2)$ space | Edge insertion [9, 54] |
| MinMax Slope | $O(n^3)$ time, $O(n^2)$ space | $O(n^3)$ time, $O(n^2)$ space | Edge insertion [9, 54] |
| MaxMin Area | Unknown | $O(n^3)$ time, $O(n^2)$ space | No algorithms published for the general problem, Klincsek's for convex polygon [37, 54] |
| MinMax Area | Unknown | $O(n^3)$ time, $O(n^2)$ space | No algorithms published for the general problem, Klincsek's for convex polygon [37, 25, 54] |
| MinMax $\delta$-angle | Unknown | $O(n^6)$ time, $O(n^2)$ space | No algorithms published for the general problem, modified Klincsek's for convex polygon [13] |
| MinMax $\delta$-area | Unknown | $O(n^6)$ time, $O(n^2)$ space | No algorithms published for the general problem, modified Klincsek's for convex polygon [13] |
| MinMax $\delta$-length | Unknown | $O(n^3)$ time, $O(n^2)$ space | No algorithms published for the general problem, modified Klincsek's for convex polygon [13] |

# Chapter 2

# MinMax and MaxMin area triangulations of a convex polygon

The problem of finding the MinMax Area triangulation of a point set is mentioned as one of the open problems in Edelsbrunner's book [25]. This problem has application to the interpolation of two-dimensional functions. We also study the MaxMin Area triangulation of a point set, which has not been mentioned previously in the literature. In this chapter, we study the particular case of a planar point set – where the points form the vertices of a convex polygon. We first review the best algorithmic solution known for these two problems in section 2.1. In the following section, we provide the necessary geometric background for our algorithms by investigating the properties and structure of the optimal triangulations. In section 2.3 we present algorithms for computing the MaxMin and MinMax area triangulations of a convex polygon, and prove the $O(n^2 \log n)$ time and $O(n^2)$ space bounds. Then in section 2.4 we discuss an algorithm for the MaxMin Area decision problem that runs in $O(n^2 \log \log n)$ time and $O(n^2)$ space.

## 2.1 Klincsek's algorithm

If the point set is in convex position, there is a dynamic programming algorithm by Klincsek [37] that finds the optimal triangulation with respect to a large number of criteria. The algorithm runs in $\Theta(n^3)$ time and requires $\Theta(n^2)$ space. We will review this algorithm, because it illustrates the dynamic programming scheme that is used with modification in our algorithm. It is also useful as an illustration of the inherent structure of the problem of optimally triangulating a convex polygon.

Given a convex polygon $P$ in the plane, let us denote the vertices of $P$ by $v_1, v_2, v_3, \ldots, v_n$. Further, we shall assume for the rest of the chapter that $v_{i+k\cdot n} = v_i$ that is the vertices of the polygon are enumerated modulo $n$, and that the order of the vertices from $v_1$ to $v_n$ is their clockwise order. As it was mentioned before, any line segment connecting two points of our point set is called an edge. In the particular case considered within this chapter, the proper diagonals of $P$ are also called simply **diagonals**. The edges of the convex hull of $P$ are also called **boundary edges**.

**Definition 20 (Subpolygons)** *Given the clockwise ordering of the vertices of a convex polygon $P$, we denote by $P_{ij}$ the subpolygon of $P$ containing vertices $v_i$ through $v_j$. We call the edge $v_iv_j$* ***base edge*** *of $P_{ij}$. Further, we call the angles of $P_{ij}$ adjacent to its base edge, namely $\angle v_{i+1}v_iv_j$ and $\angle v_iv_jv_{j-1}$,* ***base angles*** *of $P_{ij}$. Sometimes we refer to the optimal area triangulation problems associated with the subpolygons of $P$ as* ***subproblems****.*

The algorithm uses dynamic programming with a square table $Best[n, n]$ to record the results. The field $Best(p, q).value$ records the quality measure $\eta$ of the optimal triangulation of the subpolygon $P_{pq}$, which we denote by $\eta(T^\bullet(P_{pq}))$. Another field, $Best(p, q).index$, records the index of the vertex that is connected to the edge $v_pv_q$ in the optimal triangulation of the subpolygon $P_{pq}$ with respect to the quality measure $\eta$. The algorithm computes the optimal triangulations of all subpolygons $P_{pq}$ of $P$ in order of their size, starting with triangles (subpolygons of size 3) and going up to the $n$-gon (polygon $P$ itself). This is done relying on the fact that the base edge of $P_{pq}$ is connected to some other vertex $v_r$ in any triangulation, hence in the optimal triangulation, of $P_{pq}$. Additionally, by the time we need to compare (through the operator denoted by $\prec_\eta$ in the algorithm) the optimal solutions for polygons of smaller size, namely $P_{pr}$ and $P_{rq}$, their optimal values are already computed.

**Algorithm 21 (Klincsek's algorithm)** *Given a simple, not necessarily convex, polygon $P$ with no self-intersections in the plane and a decomposable quality measure $\eta$, the following algorithm finds the triangulation $T^\bullet$ of $P$ that is optimal with respect to $\eta$:*

***for*** $i := 1$ ***to*** $n$ ***do*** {*initializes the table for triangles*}
    $Best(i, i + 2).value := \eta(\triangle v_iv_{i+1}v_{i+2}); Best(i, i + 2).index := i + 1$
***endfor***
***for*** $s := 3$ ***to*** $n - 1$ ***do*** {*gives the size of the subpolygon*}
    ***for*** $i := 1$ ***to*** $n$ ***do*** {*gives the starting vertex of the subpolygon*}
        ***for*** $j := i + 1$ ***to*** $i + s$ ***do*** {*gives the current intermediate vertex under consideration*}
            $CurrentValue := opt(\eta(T^\bullet(P_{ij})), \eta(\triangle v_iv_jv_{i+s}), \eta(T^\bullet(P_{j,i+s})))$;
            ***if*** $CurrentValue \prec_\eta Best(i, i + s).value$ ***then***
            {*compares the best triangulation so far with the current, updates if necessary*}
                $Best(i, i + s).index := j$;
                $Best(i, i + s).value := CurrentValue$
            ***endif***
        ***endfor***
    ***endfor***

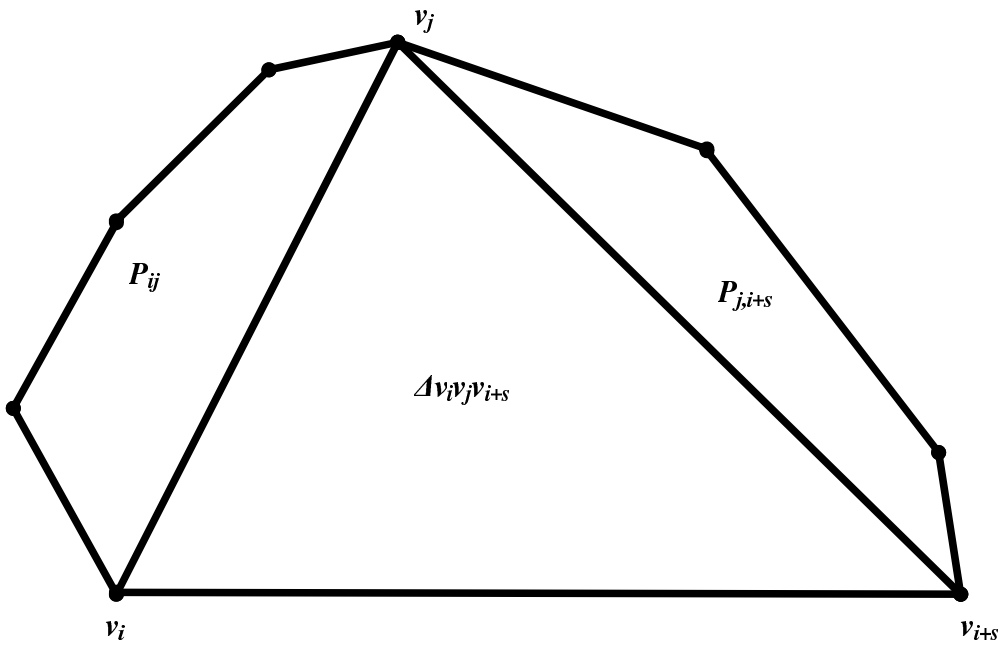


**Figure 2.1:** Klincsek's algorithm: computing the solution for $P_{i,i+s}$ from the subproblems of smaller size $P_{ij}$, $P_{j,i+s}$ and $\triangle v_i v_j v_{i+s}$ at the intermediate vertex $v_j$

***endfor***

***retrieve*** *the optimal triangulation* $T^{\bullet}(P)$ *from* $Best(1, n)$.

**Time and Space Analysis.** Initialization of the table *Best*, which is not mentioned explicitly in the algorithm, takes quadratic time in $n, O(n^2)$, because of its quadratic size. The purpose of the initialization is to set the *value* fields appropriately: with zeros if we have to maximize, and with a large enough value if we have to minimize, depending on the nature of the quality measure $\eta$. The three nested loops are executed in $\Theta(n^3)$ time as each of the indices has $\Theta(n)$ possible values. The optimal triangulation is then retrieved in linear time, $O(n)$, using the information contained in the *index* fields of the subproblems involved.

The fact that the Klincsek's algorithm finds the optimal triangulation by "blindly" computing the optimal triangulations of all subpolygons is its major strength, because it is universal, i.e., it allows optimization over broad class of quality measures. At the same time, it is the major drawback of the algorithm, as it performs too much computation. In some cases, the specifics of the quality measure can be used to reduce the computation. It is our intention to reveal specific properties of the two area-related measures that will allow us to compute the optimal area triangulations more efficiently. In section 2.3 of this chapter, we improve on Klincsek's algorithm for the MaxMin Area and the MinMax Area triangulations of a convex polygon.

It also has to be noted that some of the optimal triangulations admit better problem-specific algorithms that are not based on dynamic programming. The Greedy and the Delaunay triangulations are computable in linear time and space for convex polygons [19, 54, 59]. Some other optimal triangulations can also be computed within time and space bounds that are better than those of the general dynamic programming algorithm, for example by edge insertion [9, 54].

## 2.2 Geometric properties of the MaxMin and MinMax area triangulations

In this section we investigate the structure of the optimal area triangulations. To develop an algorithm that has better running time than the generic algorithm presented in the previous section, we need to establish some properties of the MaxMin and MinMax area triangulations. First, we discuss the location of the worst (smallest area or largest area) triangle within the triangulation. Then, we show that large class of subproblems (called 2-zone subpolygons) admit faster algorithmic solution within the dynamic programming scheme, due to the fact that their optimal area triangulations are sleeves. Further, we show that we can construct the optimal area triangulations, both MaxMin and MinMax, based only on the solutions of the 2-zone subproblems. This relies to the unimodality properties of the optimal triangulations that are proven inside this section. Finally, we show that the optimal triangulation contains specific type of diagonal or triangle, which serve as a basis to our algorithmic approach discussed in the subsequent sections.

Denote by $M_\mu(P)$ the MaxMin area triangulation of the convex polygon $P$ and by $\mu^*(P)$ the area of the smallest area triangle in $M_\mu(P)$. Denote by $M_\lambda(P)$ the MinMax area triangulation of the convex polygon $P$ and by $\lambda^*(P)$ the area of the largest area triangle in $M_\lambda(P)$.

First we recall the following well-known result from elementary geometry [12].

**Property 22** *Given a triangle $\triangle DEF$ in the plane and a triangle $\triangle PQR$ inscribed in it so that $P \in EF, Q \in FD, R \in DE$:*

$$A_{\triangle PQR} \geq \min(A_{\triangle DQR}, A_{\triangle ERP}, A_{\triangle FPQ})$$

In other words, if we inscribe a triangle inside another triangle, the inscribed triangle is not the smallest in terms of area compared to the three other triangles that are adjacent to the sides of the

inscribed triangle. Using this property we will establish a useful fact about the "worst" triangle in the MaxMin area triangulation of a convex polygon.

**Lemma 23** *Given a convex polygon $P$ in the plane and a triangulation $T$ of $P$, the triangle in $T$ that has smallest area has at least one edge on the boundary of $P$.*

**Proof.** Suppose that in the triangulation $T$ the smallest area triangle is $\triangle v_i v_j v_k$, where $i < j < k$ and no two of the vertices $v_i, v_j, v_k$ are adjacent along the boundary of $P$, i.e. $j - i > 1, k - j > 1, i - k > 1$. Please refer to Figure 2.2 on the next page. Let us denote by $D$, $E$ and $F$ respectively the vertices of the other triangles in $T$ adjacent to the edges $v_i v_j$, $v_j v_k$ and $v_k v_i$. Because of the convexity, the edges $DE$, $EF$ and $FD$ properly intersect the interior of $\triangle v_i v_j v_k$. Consider now another triangle, $\triangle D'E'F'$ obtained by the intersection of the lines parallel to the sides of $\triangle DEF$ and passing trough the points $v_i$, $v_j$ and $v_k$. $\triangle v_i v_j v_k$ is inscribed in $\triangle D'E'F'$ and thus, by Property 22 on the preceding page, $A_{\triangle v_i v_j v_k} \geq \min(A_{\triangle D' v_i v_j}, A_{\triangle E' v_j v_k}, A_{\triangle F' v_k v_i})$. But we also have $A_{\triangle D' v_i v_j} > A_{\triangle D v_i v_j}$, since we have enlarged the triangle $\triangle D v_i v_j$. Clearly the point $D$ is inside $\triangle D' v_i v_j$. Similar reasoning can be applied to the other two triangles enlarged: $\triangle E v_j v_k$ and $\triangle F v_k v_i$, showing that $A_{\triangle E' v_j v_k} > A_{\triangle E v_j v_k}$ and $A_{\triangle F' v_k v_i} > A_{\triangle F v_k v_i}$. Thus, for areas we have:

$$A_{\triangle v_i v_j v_k} \geq \min(A_{\triangle D' v_i v_j}, A_{\triangle E' v_j v_k}, A_{\triangle F' v_k v_i}) > \min(A_{\triangle D v_i v_j}, A_{\triangle E v_j v_k}, A_{\triangle F v_k v_i})$$

This contradicts our assumption that $\triangle v_i v_j v_k$ is the smallest area triangle in the triangulation $T$. The contradiction means that at least two of the vertices of $\triangle v_i v_j v_k$ are adjacent, i.e. the triangle has a boundary edge. □

It follows from Lemma 23 that the measure $\mu$ in the case of a convex polygon satisfies the weak anchor condition as per Definition 17 on page 13. This gives as an equivalent result, by edge insertion, to Klincsek's algorithm for MaxMin area triangulation of a convex polygon. More important for the advancement towards our goal is that this lemma reduces the potential candidates for a worst triangle from $O(n^3)$ to $O(n^2)$.

**Definition 24 (Complementary subpolygons)** *We call the subpolygons $P_{ij}$ and $P_{ji}$ complementary. The union of $P_{ij}$ and $P_{ji}$ is $P$.*

Here we recall another classical result about convex polygons.

**Property 25 (Distance unimodality [55])** *The distance between the straight line defined by an edge of a convex polygon and the vertices of the polygon in clockwise (or counterclockwise) order along its boundary is* ***unimodal*** *as a function of the vertex index.*

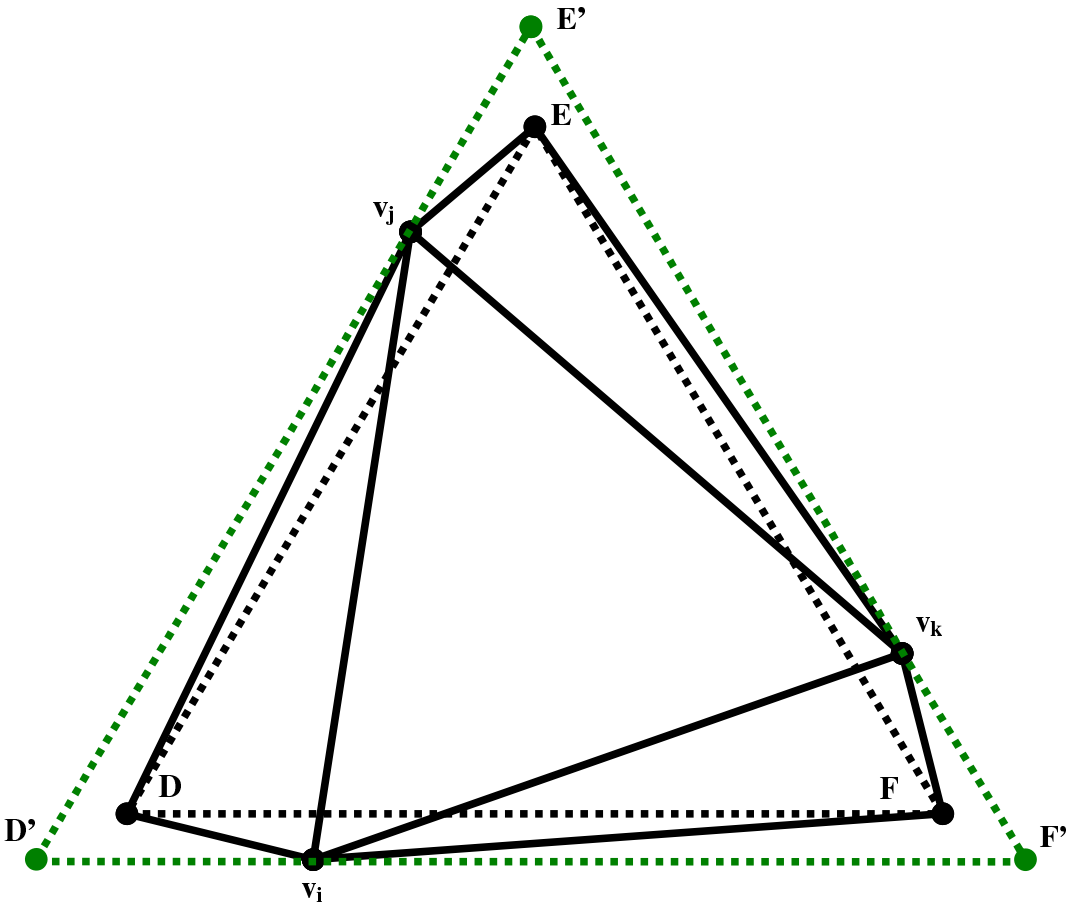


**Figure 2.2:** Lemma 23 on the preceding page, the worst triangle

In other words, for two fixed vertices of $P$, $v_i$ and $v_j$, we have $d(v_k, v_iv_j) = F(k)$, and the function $F(k)$ is unimodal over the interval $[i, j]$. By symmetry, it is also unimodal over the interval $[j, i]$. The above property implies that the area of the triangles with a given base edge in a convex polygon is also unimodal as a function of the (index of) the third vertex. Namely, if we fix the vertices $v_i$ and $v_j$ of $P$, then $A_{\triangle v_iv_jv_k} = G(k)$, and $G(k)$ is unimodal, as a function of $k$, over the intervals $[i, j]$ and $[j, i]$. Another way of looking at this property (the unimodality of area) is by defining the threshold lines. For each value $\tau$ of the threshold, there is a line parallel to the given edge and such that the points on that line form triangles with area equal to $\tau$. We will concentrate only at the threshold line that lies on the same side of the edge as the polygon itself. Then, another way of describing the unimodality with relation to the threshold lines is to say that if the function is unimodal, then its threshold line cuts out of the polygon a contiguous piece (or does not intersect the polygon at all). If the function is not unimodal, the pieces that lie on different sides of the threshold line may alternate more than once as we go along the boundary of the polygon in a chosen direction. One example of such a function is the perimeter of the triangle formed by two fixed vertices $v_i$ and $v_j$ of $P$ and any third vertex $v_k$. We have $P_{\triangle v_iv_jv_k} = H(k)$, and the threshold lines of $H(k)$ are ellipses with foci $v_i$ and $v_j$. They are convex downwards with respect to the line $v_iv_j$, and thus $H(k)$ may not be, and in general it is not, unimodal as a function of $k$ over the intervals $[i, j]$ or $[j, i]$.

**Definition 26** *Given convex polygon $P$, for a diagonal $v_iv_j$ of $P$ we will denote by $Top(v_iv_j)$ the vertex of $P$ in the interval $[v_i, v_j]$ that is farthest from the line through the edge $v_iv_j$. If there are two such vertices, we use the one preceding the other in the clockwise order from $v_i$ to $v_j$ as $Top(v_iv_j)$.*

Note that $Top(v_iv_j)$ and $Top(v_jv_i)$ are two different vertices, lying in different half-planes with respect to the line $v_iv_j$. The value of the function $Top$ for all the diagonals in $P$ can be computed in $O(n^2)$ time by rotating calipers. This approach is due to Toussaint [56]. The important observation is that as we go along the edges of the boundary of $P$ in say counterclockwise order, the $Top$ of the current boundary edge will also move in counterclockwise direction. Consider two edges that are adjacent along the boundary of the polygon $P$ in counterclockwise order, for example $v_2v_1$ and $v_1v_n$. According to Definition 26 if we draw a line, parallel to the line determined by the edge $v_2v_1$ through $Top(v_2v_1)$, the entire polygon $P$ will lie inside the parallel strip formed by these two lines. We claim that $Top(v_1v_n)$ is either equal to $Top(v_2v_1)$ or precedes it in the (clockwise) order. To see this, consider a movement of the line, determined by the edge $v_1v_n$, parallel to itself in the direction of the polygon $P$. Because of the convexity of $P$ at its vertex $Top(v_2v_1)$, and of the relative slope of the edges $v_2v_1$ and $v_1v_n$, by the time this line hits $Top(v_2v_1)$ it would already have gone past all the vertices of $P$ between $v_n$ and $Top(v_2v_1)$.

Algorithmically, this means that we can compute the value of the function $Top$ for the boundary edges of a convex polygon in linear time. We start at an arbitrary edge. We compute the $Top$ vertex for this edge – even using brute force it takes only linear, $O(n)$, time. Further, we follow the edges of the polygon in a chosen direction. We also move the other jaw of the calipers, i.e. keep track of all the vertices along the boundary, following the first $Top$ vertex in the chosen direction. Relative to the currently considered edge, we are interested in a drop in the value of the distance. Once such a drop is detected, the previous vertex was the $Top$ for the considered edge, we record it and proceed. When we return to the edge that we began with, the pointer tracking the $Top$ has done one full rotation around the polygon. Thus, the process takes $O(n)$ time.

In order to compute the value of the function $Top$ for all the diagonals of a convex polygon, we need to slightly modify the previous approach. For each vertex $v_i$, we are going to consider the fan of diagonals, in a chosen (clockwise or counterclockwise) order. It is easy to see that the previous property still holds, the $Top$ vertices of the successive diagonals will rotate in the same direction along the boundary of $P$. Moreover, we are not going to make more than one full rotation around the polygon, as the overall angle at the given vertex $v_i$ is less than $180^\circ$ and the diagonals in the fan are sorted by their slope. The same property was used in the generic rotating calipers approach [56]– the slopes of the edges along the boundary of a convex polygon are sorted and the overall angle (i.e. the sum of the exterior angles of a convex polygon) is $360^\circ$. Note that $Top(v_iv_j)$ is different from $Top(v_jv_i)$ when $v_iv_j$ is a proper diagonal of $P$. Thus, each will be computed separately from the fans of $v_i$ and $v_j$, respectively. Overall, we have $n$ fans of diagonals, computing the value of $Top$ for each fan takes $O(n)$ time, which results in $O(n^2)$ time.

We are going to classify the subpolygons of a convex polygon $P$ according to the sum of their base angles, compared with the integer multiples of $90^\circ$. We call this property **zonality** of the subpolygons.

**Definition 27 (Zonality)** *Given a convex polygon $P$ in the plane and a clockwise ordering of its vertices, we say that the subpolygon $P_{ij}$ containing vertices $v_i$ through $v_j$ is a $k$–zone subpolygon if and only if*

$$k = \left\lceil \frac{\angle v_j v_i v_{i+1} + \angle v_{j-1} v_j v_i}{90^\circ} \right\rceil$$

*Observe that $k \in \{1, 2, 3, 4\}$. Further, the boundary edges, i.e., the polygons $P_{i,i+1}$ have zonality zero.*

**Definition 28 (Zonality function)** *Let $z(P_{ij})$ be a function defined over the subpolygons of the convex polygon $P$ in the plane and having its values in the set $\{0, 1, 2, 3, 4\}$, such that $z(P_{ij}) = k$ iff $P_{ij}$ is $k$-zone subpolygon.*

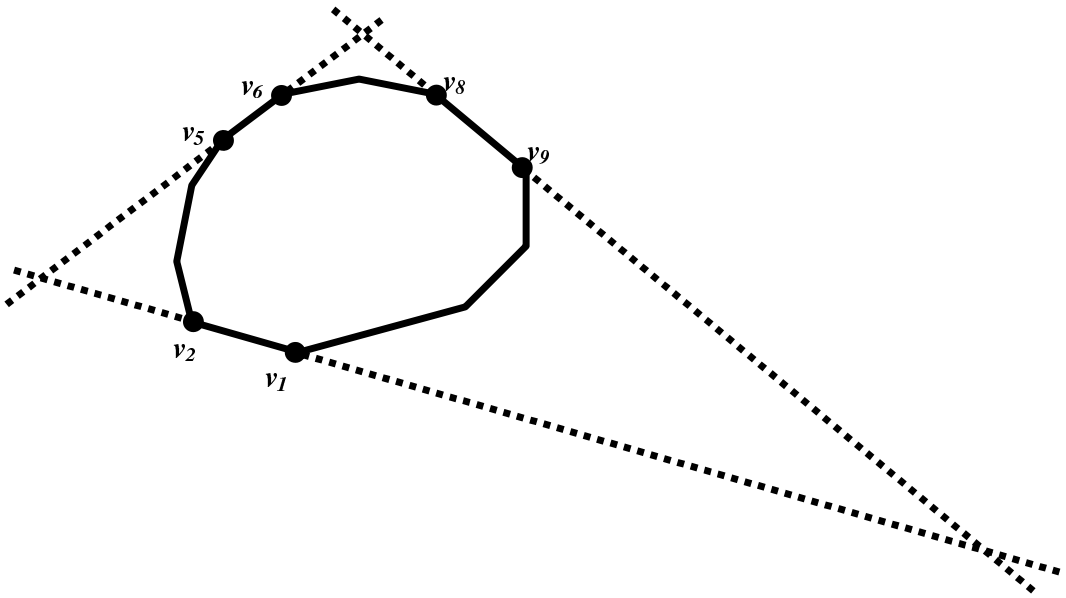


**Figure 2.3:** Definition 27 on the previous page, zonality of the subpolygons: $z(P_{59}) = 1$, $z(P_{82}) = 2$, $z(P_{52}) = 3$, and $z(P_{86}) = 4$

For an illustration of the zonality, please refer to Figure 2.3.

**Property 29**

$$z(P_{ij}) + z(P_{ji}) \leq 5$$

**Proof.** According to Definition 27 on the previous page, $z(P_{ij}) = \left\lceil \frac{\angle v_j v_i v_{i+1} + \angle v_{j-1} v_j v_i}{90^\circ} \right\rceil$. Using the definition of the ceiling function, we can rewrite this as:

$$z(P_{ij}) - 1 < \frac{\angle v_j v_i v_{i+1} + \angle v_{j-1} v_j v_i}{90^\circ} \leq z(P_{ij})$$

Multiplying both sides by $90^\circ$ gives us the following equivalent form:

$$90^\circ \left[ z(P_{ij}) - 1 \right] < \angle v_j v_i v_{i+1} + \angle v_{j-1} v_j v_i \leq 90^\circ z(P_{ij})$$

Similarly, for the zonality of the polygon $P_{ji}$ we can obtain:

$$90^\circ \left[ z(P_{ji}) - 1 \right] < \angle v_{i-1} v_i v_j + \angle v_i v_j v_{j+1} \leq 90^\circ z(P_{ji})$$

Adding together the left hand sides of the last two inequalities gives:

$$90^\circ \left[ z(P_{ij}) + z(P_{ji}) - 2 \right] < \angle v_j v_i v_{i+1} + \angle v_{j-1} v_j v_i + \angle v_{i-1} v_i v_j + \angle v_i v_j v_{j+1}$$

We will rewrite the right hand side of the above inequality, grouping together the first and third term, and respectively the second and fourth term:

$$90^\circ\left[z(P_{ij})+z(P_{ji})-2\right] < (\angle v_j v_i v_{i+1} + \angle v_{i-1} v_i v_j) + (\angle v_{j-1} v_j v_i + \angle v_i v_j v_{j+1})$$

Note that the sums in brackets on the right hand side represent exactly the internal angles of the polygon $P$ at the vertices $v_i$ and $v_j$ respectively:

$$\angle v_j v_i v_{i+1} + \angle v_{i-1} v_i v_j = \angle v_{i-1} v_i v_{i+1}, \angle v_{j-1} v_j v_i + \angle v_i v_j v_{j+1} = \angle v_{j-1} v_j v_{j+1}$$

Since the polygon $P$ is convex, both angles are less than or equal to 180°, or:

$$\angle v_j v_i v_{i+1} + \angle v_{i-1} v_i v_j = \angle v_{i-1} v_i v_{i+1} < 180^\circ, \angle v_{j-1} v_j v_i + \angle v_i v_j v_{j+1} = \angle v_{j-1} v_j v_{j+1} < 180^\circ$$

Adding the two inequalities together yields:

$$(\angle v_j v_i v_{i+1} + \angle v_{i-1} v_i v_j) + (\angle v_{j-1} v_j v_i + \angle v_i v_j v_{j+1}) = \angle v_{i-1} v_i v_{i+1} + \angle v_{j-1} v_j v_{j+1} < 360^\circ$$

Substituting from before, we have:

$$90^\circ\left[z(P_{ij})+z(P_{ji})-2\right] < 360^\circ \Leftrightarrow z(P_{ij})+z(P_{ji})-2 < 4 \Leftrightarrow z(P_{ij})+z(P_{ji}) < 6$$

Which, given the fact that the zonalities $z(P_{ij})$ and $z(P_{ji})$ are integers is equivalent to:

$$z(P_{ij})+z(P_{ji}) \leq 5$$

□

**Property 30** *Let $v_i$, $v_j$ and $v_k$ be three vertices of $P$ in the same clockwise order. Then:*

$$z(P_{ij})+z(P_{jk})+z(P_{ki}) \leq 6$$

The proofs is similar to the proof of Property 29 on the preceding page and is omitted.
We now study area triangulations in 2-zone subpolygons. We can think of a 2-zone subpolygon as subpolygon that is entirely contained in a parallel strip formed by lines through the endpoints of its base edge.

**Lemma 31 (MaxMin area in 2-zone polygons)** *Let $P_{ij}$ be a 2-zone polygon. Given a threshold $\tau$, if there exists a triangulation $T$ of $P_{ij}$ such that $\mu(T) \geq \tau$, then there exists a triangulation $T'$ of $P_{ij}$ such that $\mu(T') \geq \tau$, and the triangulation $T'$ contains one of the triangles $\triangle v_i v_{i+1} v_j$ or $\triangle v_i v_{j-1} v_j$.*

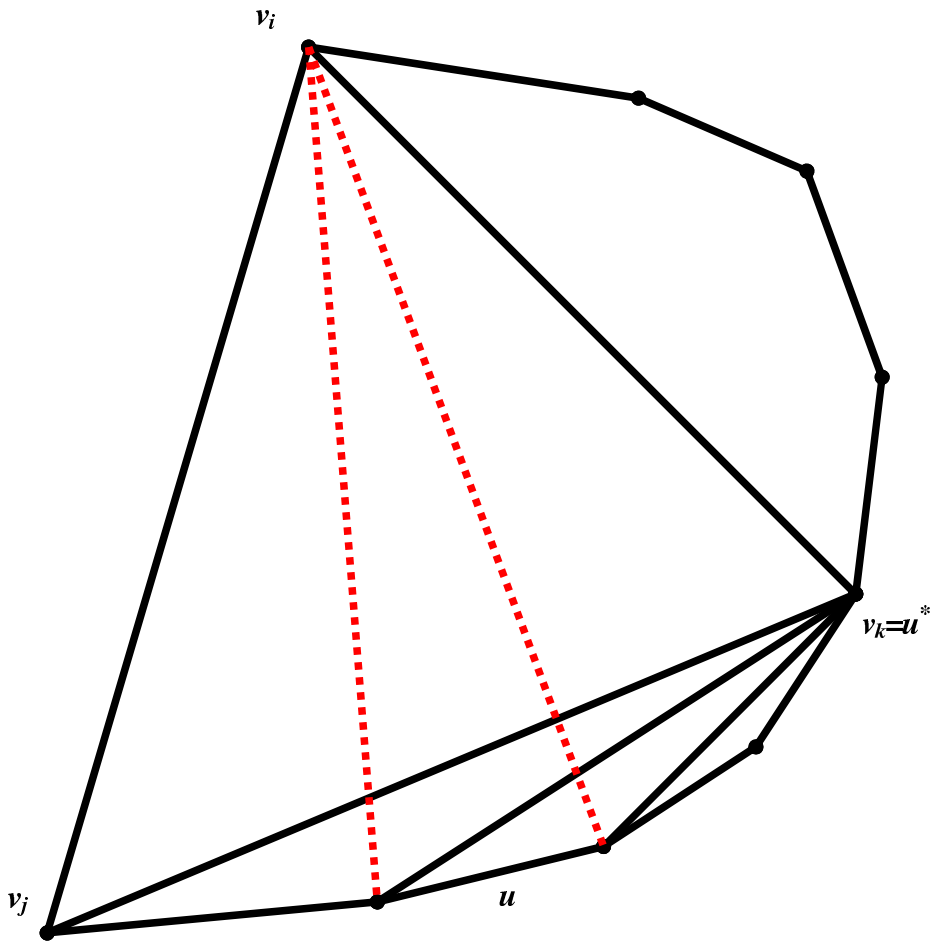


**Figure 2.4:** Retriangulation in a 2-zone polygon, MaxMin area

**Proof.** The triangulation $T$ contains a triangle $\triangle v_i v_k v_j$ for some $i+1 \leq k \leq j-1$, as shown in Figure 2.4 on the previous page. If $k = i+1$ or $k = j-1$ we are done. Otherwise, the vertex $v_k$ will be either between $Top(v_i v_j)$ and $v_j$ or between $v_i$ and $Top(v_i v_j)$. Assume, without loss of generality, that $v_k$ is between $Top(v_i v_j)$ and $v_j$. Since $P_{ij}$ is a 2-zone subpolygon for all edges of the chain between $Top(v_i v_j)$ and $v_j$, the farthest vertex of $P_{ij}$ is $v_i$. We construct $T'$ from $T$ by connecting all the vertices from the range $v_{k+1} \dots v_{j-1}$ to $v_i$. In the triangulation $T$, each of the edges of the chain $v_k \dots v_j$ is connected to another vertex of this chain, since the edge $v_k v_j$ is a part of the triangulation $T$ (remember that $T$ contains $\triangle v_i v_k v_j$). The part of $T$ inside the subpolygon $P_{ik}$ will remain unchanged in $T'$.

To see that $\mu(T') \geq \tau$, consider an edge $u$ from the chain $v_k \dots v_j$. It is connected in $T$ to a vertex $u^*$ from the range $v_{k+1} \dots v_{j-1}$. Because of the fact that the point $v_i$ is farther from $u$ than $u^*$, connecting $u$ to $v_i$ will increase the area of the triangle adjacent to $u$ in the new triangulation $T'$, compared to the area of the triangle that was adjacent to $u$ in the triangulation $T$. Thus, connecting all the edges in the chain $v_k \dots v_j$ to $v_i$ either increases the smallest area triangle (if it was part of $P_{kj}$) or does not influence the value of the smallest area triangle (if it was part of $P_{ik}$). In both cases $\mu(T') \geq \mu(T) \geq \tau$. Thus, the triangle $\triangle v_i v_{j-1} v_j$ will be in $T'$. □

Note that the proof of Lemma 31 on page 26 automatically implies that the same is true for all 1-zone subpolygons.

**Lemma 32 (MinMax Area in 2-zone polygons)** *Let $P_{ij}$ be a 2-zone polygon. Given a threshold $\tau$, if there exists a triangulation $T$ of $P_{ij}$ such that $\lambda(T) \leq \tau$, then there exists a triangulation $T''$ of $P_{ij}$ such that $\lambda(T'') \leq \tau$, and the triangulation $T''$ contains one of the triangles $\triangle v_i v_{i+1} v_j$ or $\triangle v_i v_{j-1} v_j$.*

**Proof.** The triangulation $T$ contains a triangle $\triangle v_i v_k v_j$ for some $i+1 \leq k \leq j-1$, as shown in Figure 2.5 on the next page. If $k = i+1$ or $k = j-1$ we are done. Otherwise, the vertex $v_k$ will be either between $Top(v_i v_j)$ and $v_j$ or between $v_i$ and $Top(v_i v_j)$. Assume, without loss of generality, that $v_k$ is between $Top(v_i v_j)$ and $v_j$. We will show that the triangulation $T^*$, obtained by flipping the edge $v_j v_k$ in $T$, has the property $\lambda(T^*) \leq \tau$. To see this, consider $v_l$ – the other vertex incident to the edge $v_j v_k$ in $T$. Suppose we replace the edge $v_k v_j$ by $v_i v_l$, where $k < l < j$. We have $A_{\triangle v_i v_k v_j} > A_{\triangle v_i v_l v_j}$ because the point $v_l$ is closer to the edge $v_i v_j$ than the point $v_k$. Similarly, $A_{\triangle v_i v_k v_j} > A_{\triangle v_i v_k v_l}$ because the point $v_l$ is closer to the edge $v_i v_k$ than the point $v_j$. Thus, removing the edge $v_k v_j$ and introducing the edge $v_i v_l$, we obtain two triangles $\triangle v_i v_l v_j$ and $\triangle v_i v_k v_l$ that are both smaller in area than the previously existing triangle $\triangle v_i v_k v_j$. Therefore $T^*$ is either strictly better than $T$ if $\triangle v_i v_k v_j$ was the worst triangle of $T$, or of the same quality as $T$ otherwise. In other words $\lambda(T^*) \leq \tau$. If $l = j-1$ we are done, $T'' \equiv T^*$. Otherwise we will repeat the described procedure until we arrive at $v_{j-1}$, the final triangulation obtained will be $T''$. □

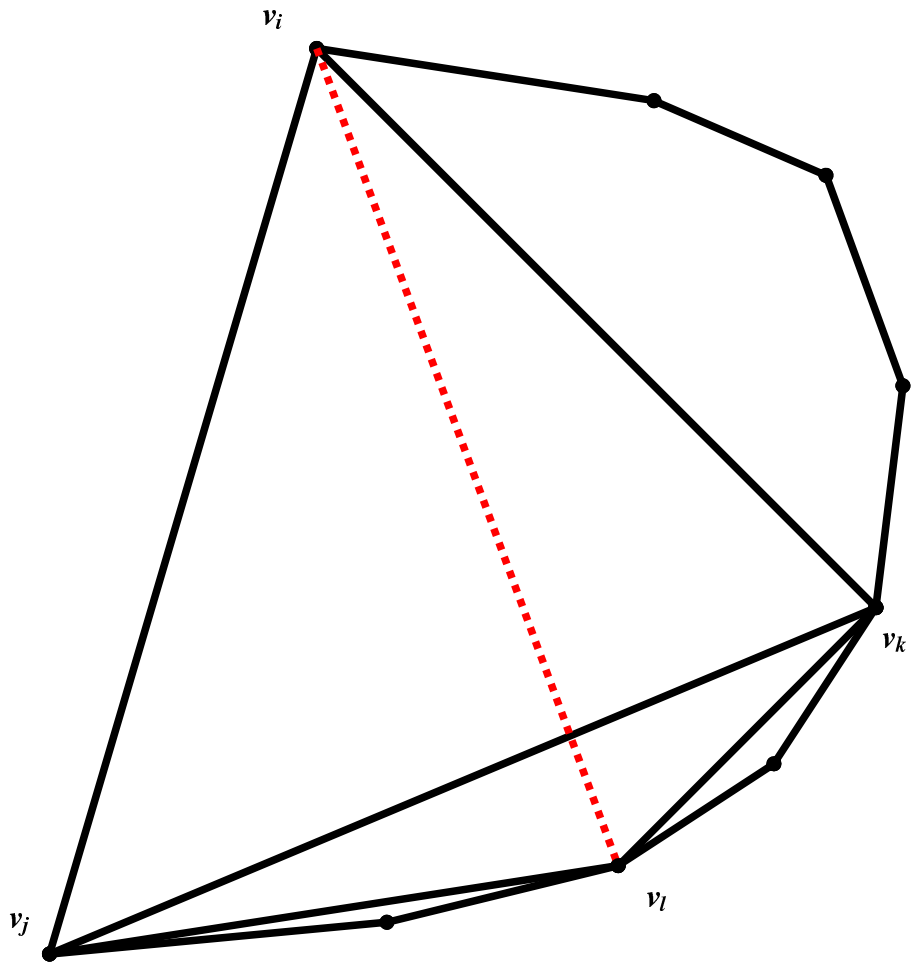


**Figure 2.5:** Retriangulation in a 2-zone polygon, MinMax area

Again, note that the proof of Lemma 32 on page 28 implies that for all zone 1-subpolygons the same property is in place. Furthermore, Lemmas 31 on page 26 and 32 on page 28 establish that the MaxMin and MinMax area triangulations of up to 2-zone polygon $P_{ij}$ always contain one of the triangles $\triangle v_i v_{i+1} v_j$ or $\triangle v_i v_{j-1} v_j$ immediately adjacent to the base edge $v_i v_j$.

**Definition 33** *Let $P$ be a convex polygon with $n \geq 4$ vertices. There are three possible types of triangles in a triangulation of $P$:*

- *Triangles that have two edges from the boundary of the polygon $P$ and one edge that is a proper diagonal of $P$. Triangles of this type are called* ***ears****.*
- *Triangles that have one edge from the boundary of the polygon $P$ and two edges that are proper diagonals of $P$. Triangles of this type are called* ***boundary triangles****.*
- *Triangles whose all three edges are proper diagonals of $P$. Triangles of this type are called* ***internal triangles****.*

**Property 34** *Every triangulation $T$ of a convex polygon $P$ with $n \geq 4$ vertices contains at least two ears.*

**Proof.** This can be proven by either a counting argument or induction. The inductive proof is given here. Note that in case of a triangle (a polygon with three vertices), its only triangulation contains one ear, the triangle itself.
Base case: For $n = 4$ both possible triangulations of a convex quadrilateral contain exactly two ears. The same is true for $n = 5$, all possible triangulations of a convex pentagon contain exactly two ears and one boundary triangle.
Inductive hypothesis: Every triangulation of a convex polygon with up to $n$ vertices contains two ears.
Inductive step: Let $Q$ be a polygon with $n+1$ vertices. Consider a triangulation $T$ of $Q$. It contains a proper diagonal $d$ of $Q$, which divides the polygon into two convex polygons $R$ and $S$ such that $Q = R \cup S$. Let $R$ have $n_1$ vertices, and $S$ have $n_2$ vertices, where $n_1 + n_2 = n + 2$. If $n_1 \geq 4, n_2 \geq 4$ by the inductive hypothesis every triangulation of $R$ and $S$ has at least two ears. Thus, the parts of $T$, $T_R$ and $T_S$ respectively, have at least two ears each. Each ear of $T_R$ and $T_S$ will be an ear in $T$ unless it has $d$ as an edge, as $d$ is a boundary edge of both $R$ and $S$, but a proper diagonal of $Q$. There can be at most two ears containing $d$ – one in $T_R$ and one in $T_S$. Therefore, there will be at least $4 - 2 = 2$ ears in $T$. When either $n_1$ or $n_2$ is equal to 3, the triangulation $T_R$ or $T_S$ is a triangle, but this triangle will be an ear of $T$. The other part will yield at least one more ear, as its triangulation has at least two, and at most one of these is adjacent to $d$. □

**Definition 35** *A triangulation $T$ of a convex polygon $P$ that contains exactly two ears and all other triangles are boundary triangles is called a* ***sleeve****.*

**Corollary 36** *There exist MaxMin and MinMax area triangulations of a 2-zone polygon $P_{ij}$ that are sleeves.*

**Proof.** Lemmas 31 on page 26 and 32 on page 28 show that the optimal area triangulations of $P_{ij}$ contain a triangle with base edge $v_iv_j$ and third vertex immediately adjacent to $v_i$ or $v_j$. This triangle, by Definition 33 on the previous page is an ear of the optimal triangulation. Further, we can see that the remaining polygon is a 2-zone polygon and thus satisfies the premises of the two lemmas. Therefore the optimal triangulation contains an ear adjacent to its base edge, which is a boundary triangle of the optimal triangulation of $P_{ij}$. This is true unless the remaining part is a triangle itself, in which case it will be an ear of the optimal triangulation, its second ear. Thus, the optimal triangulations, both MaxMin and MinMax area, of a 2-zone polygon $P_{ij}$ consist of exactly two ears (the base triangle and some other ear) and all other triangles have exactly one boundary edge. There are no internal triangles, i.e., triangles whose edges are all proper diagonals of the polygon. □

In order to handle 3-zone and 4-zone convex polygons, we introduce the following lemma.

**Lemma 37** *In every triangulation $T$ of a convex polygon $P$, there exists a triangle $\triangle v_iv_jv_k$, such that*

$$z(P_{ij}) \leq 2, z(P_{jk}) \leq 2, z(P_{ki}) \leq 2$$

*If such a triangle is non-degenerate (i.e., has three distinct vertices) we call it a* ***2-2-2-zone triangle****.*

**Proof.** Property 30 on page 26 implies that only one of the subpolygons surrounding an internal triangle can be of zonality 3 or more. Thus, consider any triangle $\triangle v_pv_qv_r$ of $T$. If it has the desired property we are done. If it does not have the property then without loss of generality we can assume that $z(P_{pq}) \geq 3$. By Property 29 on page 25 we have that $z(P_{qp}) \leq 2$. Proceeding into the interior of the subpolygon $P_{pq}$, it contains some triangle $\triangle v_pv_qv_{r_1}$ of $T$. If it has the desired property, we are done. Otherwise, we can repeat this in the interior of the subpolygon $P_{pr_1}$ say, which is a proper subpolygon of the previous polygon $P_{pq}$. This procedure stops whenever a triangle with the desired property is found or if we reach an ear (which will mean in our terms that the polygon $P$ itself has a zonality of 2 and any of its triangles has the claimed property). Note that if we have a proper diagonal such that both subpolygons associated with it have zonality of two or less (call it a **2-2-zone diagonal**), then both triangles adjacent to such a diagonal are 2-2-2-zone triangles. However, it is not always the case that in a triangulation we have a 2-2-zone diagonal. □

One important consequence of Lemma 37 and Corollary 36 on the preceding page is that the structure of the optimal triangulation, in both MaxMin and MinMax area cases is specified. The optimal triangulation contains at most one internal triangle and at most three ears, all other triangles are boundary triangles.

In the next few properties we are going to use the three standard functions for the vertices of the convex polygon $P$: $index()$, $pred()$, and $succ()$, defined as follows:

- $index(v_i) = i$
- $pred(v_i) = v_{(i-1) \mod n}$
- $succ(v_i) = v_{(i+1) \mod n}$

Observe that in the series of subpolygons $P_{i,i+2}, P_{i,i+3}, \ldots, P_{i,i-1} \equiv P$ formed by connecting the vertex $P_i$ to all other vertices of $P$ in clockwise order, the zonality of the subpolygons is monotonically increasing. Since we are going to consider only up to 2-zone subpolygons, we introduce the following:

**Definition 38** *Let $v_i$ be a vertex of $P$. We will denote by $MaxCW(v_i)$ the last (in the clockwise order from $v_i$) vertex of $P$ such that $z(P_{i,index(MaxCW(v_i))}) \leq 2$. In other words, in the series of the subpolygons $P_{i,i+2}, P_{i,i+3}, \ldots, P_{i,index(MaxCW(v_i))}$, all the subpolygons have zonality of 2 or less, and $z(P_{i,succ(index(MaxCW(v_i)))}) \geq 3$. Analogously, we will define $MaxCCW(v_i)$ to be the last vertex in the counterclockwise order from $v_i$, such that $z(P_{index(MaxCCW(v_i)),i})) \leq 2$.*

**Property 39** *$MaxCCW(v_i) = Top(v_{i-1}v_i)$, and $MaxCW(v_i) = Top(v_iv_{i+1})$ or $MaxCW(v_i) = succ(Top(v_iv_{i+1}))$.*

**Proof.** Consider $v_j = Top(v_{i-1}v_i)$, and draw a line through $v_j$ parallel to the edge $v_{i-1}v_i$. By the definition of $Top(v_{i-1}v_i)$ the entire subpolygon $P_{ji}$ will lie in the strip between these two parallel lines. Thus $z(P_{ji}) \leq 2$. Therefore all the subpolygons $P_{ji}, P_{j+1,i}, \ldots, P_{i-2,i}$ will have zonality of 2 or less, and obviously because of the slope of the edge $v_{j-1}v_j$, $z(P_{j-1,i}) \geq 3$. Consequently, $MaxCCW(v_i) = Top(v_{i-1}v_i)$. Repeating the same reasoning with respect to edge $v_iv_{i+1}$, for $MaxCW(v_i)$ two possibilities exist. If there is an edge parallel to $v_iv_{i+1}$ then $MaxCW(v_i) = succ(Top(v_iv_{i+1}))$, otherwise $MaxCW(v_i) = Top(v_iv_{i+1})$. □

Figure 2.6 on the next page illustrates the situation addressed by the following lemma. Recall that $\mu(T)$ represents the minimum area of a triangle in a given triangulation $T$.

**Lemma 40 (Intervals of admissibility for MaxMin Area)** *Let $P_{ij}$ be a subpolygon of $P$ such that $z(P_{ji}) \leq 2$. Consider the interval between $MaxCCW(v_j)$ and $Top(MaxCCW(v_j), v_j)$ of vertices of $P_{ij}$. Given a threshold $\tau$, if there exist two vertices $k_1$ and $k_2$ in the interval such that there*

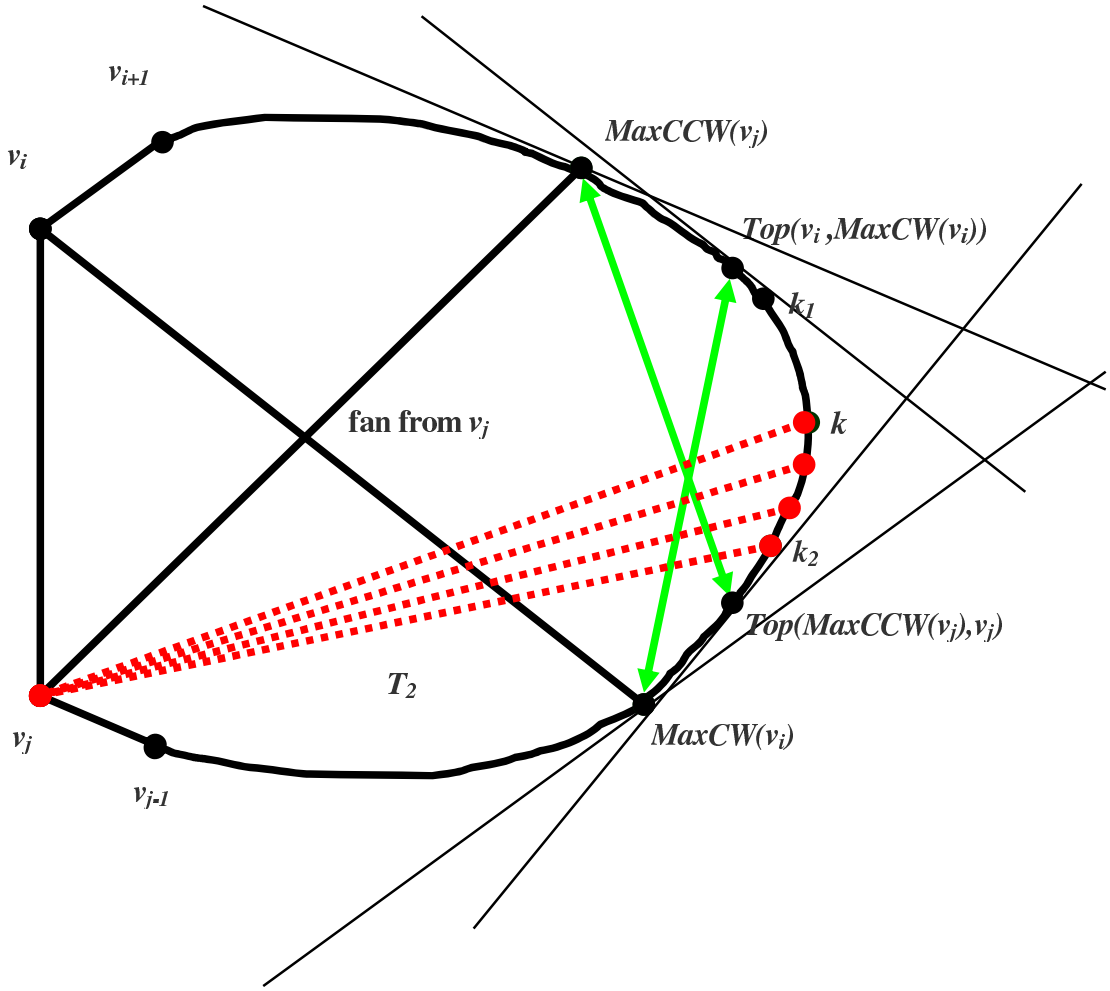


**Figure 2.6:** Intervals of admissibility for MaxMin area

*exist triangulations $T_1$ of $P_{k_1 j}$ and $T_2$ of $P_{k_2 j}$, respectively such that $\mu(T_1) \geq \tau$ and $\mu(T_2) \geq \tau$, then for each vertex $k$ in the interval between $k_1$ and $k_2$ there exists a triangulation $T$ of $P_{kj}$ such that $\mu(T) \geq \tau$. The largest such interval is called the* ***CCW interval of admissibility*** *for MaxMin area with respect to $v_j$ and $\tau$.*

**Proof.** The idea of this proof is similar to that of Lemmas 31 on page 26 and 32 on page 28. We will show how to obtain $T$ from $T_1$ and $T_2$. Please refer to Figure 2.6. The subpolygon between $MaxCCW(v_j)$ and $v_j$ is 2-zone by definition. This means that for all the edges between $MaxCCW(v_j)$ and $Top(MaxCCW(v_j), v_j)$, the vertex $v_j$ is the farthest vertex. Then, we can obtain $T$ by adding to $T_2$ a fan from $v_j$ to the vertices in the chain between $k$ and $k_2$. Because of the existence of $T_1$, we know that all the edges in the chain between $k$ and $k_2$ are contained in

triangles of $T_1$ that have area larger than $\tau$. In $T$ we connect them to $v_j$ that is at least as far as the vertex that they were connected to in $T_1$. Remember that the internal triangles do not matter here as the worst triangle in the MaxMin area triangulation has a boundary edge. □

This argument is symmetric, in the interval between $Top(v_i, MaxCW(v_i))$ and $MaxCW(v_i)$, there is an interval of vertices (possibly empty) such that a triangulation of the subpolygon between $v_i$ and any of these vertices that satisfies the given threshold condition is possible. This is the **CW interval of admissibility** with respect to $v_i$ and $\tau$. It should be mentioned that, depending on the shape of the polygon, $Top(v_i, MaxCW(v_i))$ could precede $MaxCCW(v_j)$ in the clockwise order. Similarly, $Top(MaxCCW(v_j), v_j)$ can be to the right of $MaxCW(v_i)$. However, the key observation here is that $Top(v_i, MaxCW(v_i))$ is to the left of $Top(MaxCCW(v_j), v_j)$, i.e. the interval from $MaxCCW(v_j)$ to $Top(MaxCCW(v_j), v_j)$, and the interval from $Top(v_i, MaxCW(v_i))$ to $MaxCW(v_i)$ completely cover the interval between $MaxCCW(v_j)$ and $MaxCW(v_i)$. Refer to Figure 2.6 on the previous page. Thus, we have a solid basis for checking all possible triangles satisfying the premises of Lemma 37 on page 31 under the measure $\mu$.
There is another important consequence of Lemma 40 on the previous page. Recall that we denoted the value of the minimum area in the MaxMin Area triangulation of the subpolygon $P_{ij}$ by $\mu^*(P_{ij})$.

**Corollary 41 (Unimodality of the optimum)** *Let $v_i$ be a vertex of $P$. $\mu^*(P_{ik})$, as a function of the vertex $v_k$, is unimodal over the interval $[Top(v_i, MaxCW(v_i)), MaxCW(v_i)]$. Similarly, $\mu^*(P_{mi})$, considered as a function of the vertex $v_m$, is unimodal over the respective interval of vertices of $P$ – $[MaxCCW(v_i), Top(MaxCCW(v_i), v_i)]$.*

**Proof.** For any two values of the threshold area, $\tau_1$ and $\tau_2$, such that $\tau_2 > \tau_1$, the admissibility interval of $\tau_1$ will include the admissibility interval of $\tau_2$. This is true since $\mu^*(P_{ij}) \geq \tau_2$ and $\tau_2 > \tau_1$ imply $\mu^*(P_{ij}) > \tau_1$. This geometric inclusion property implies the unimodality of the function. Specifically, for area threshold of zero, $\tau = 0$, the admissibility interval coincides with the entire interval: $[Top(v_i, MaxCW(v_i)), MaxCW(v_i)]$ in CW direction, and $[MaxCCW(v_i), Top(MaxCCW(v_i), v_i)]$ in CCW direction. If we set the threshold value above the area of the polygon $P$, $\tau > A_P$, then obviously the admissibility intervals will be empty. Note that the functions that we defined here are discrete and we use the term unimodality in this sense. □

Recall that $\lambda(T)$ represents the maximum area of a triangle in a given triangulation $T$.

**Lemma 42 (Intervals of admissibility for MinMax Area)** *Let $P_{ij}$ be a subpolygon of $P$ such that $z(P_{ji}) \leq 2$. Consider the interval of the vertices (if any) of $P_{ij}$ following $Top(v_iv_j)$ in the clockwise order and lying in the parallel strip defined by the lines perpendicular to the edge $v_iv_j$ at its endpoints. Given a threshold $\tau$, if there exist two vertices $k_1$ and $k_2$ in the interval such that there exist triangulations $T_1$ of $P_{k_1j}$ and $T_2$ of $P_{k_2j}$, respectively, such that $\lambda(T_1) \leq \tau, A_{\triangle v_i k_1 v_j} \leq \tau$ and*

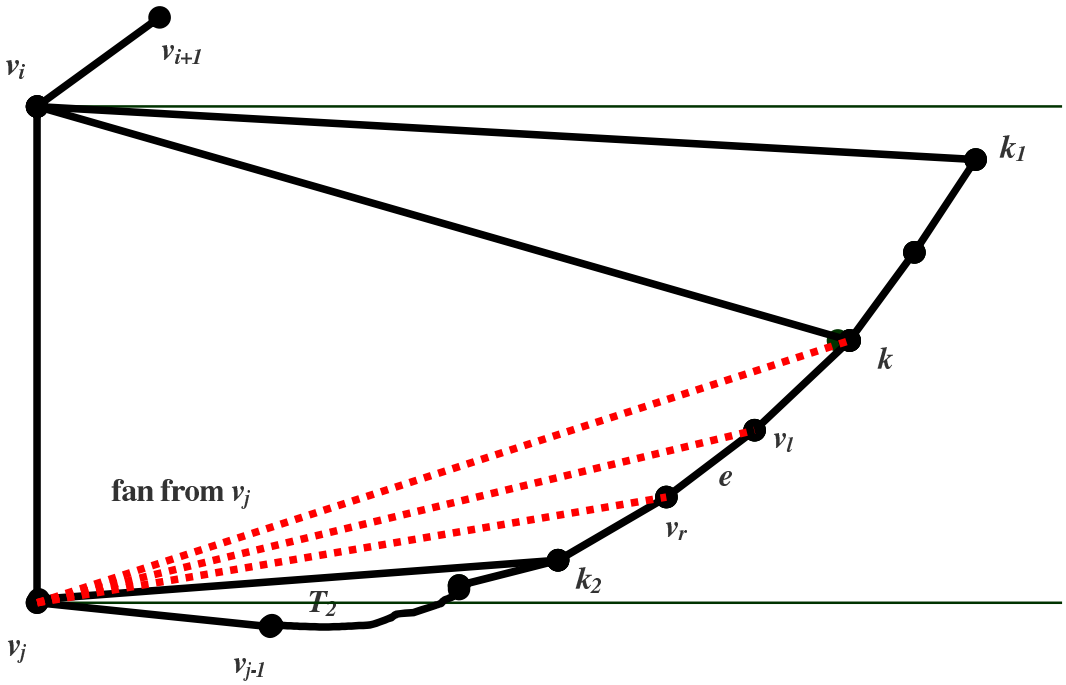


**Figure 2.7:** Intervals of admissibility for MinMax area

$\lambda(T_2) \leq \tau, A_{\triangle v_i k_2 v_j} \leq \tau$, *then for each vertex* $k$ *in the interval between* $k_1$ *and* $k_2$ *there exists a triangulation* $T$ *of* $P_{kj}$ *such that* $\lambda(T) \leq \tau, A_{\triangle v_i k v_j} \leq \tau$. *The largest such interval is called* ***CCW interval of admissibility of*** $\mathbf{v_j}$ *for MinMax area with respect to* $v_i$ *and* $\tau$.

**Proof.** We will show how to construct the triangulation $T$. We will add to the existing triangulation $T_2$ a fan from the vertex $v_j$ to the vertices of the chain between $k$ and $k_2$. Figure 2.7 illustrates this construction. To see that these triangles satisfy the area condition, consider any edge $e$ in the chain from $k$ to $k_2$. In the chain from $k_1$ to $k_2$ each point is closer to the edge $v_i v_j$ than its predecessor. This means that $A_{\triangle(e,v_j)} < A_{\triangle(e,v_i)}$, because the point $v_j$ is closer to the edge $e$ than the point $v_i$. Let us denote the endpoints of the edge $e$ by $v_l$ and $v_r$, where $v_l$ is the one preceding $v_r$ in the clockwise order. Here $l$ and $r$ stand for "left" and "right", respectively. We have $A_{\triangle(e,v_i)} < A_{\triangle v_i v_l v_j}$ since the point $v_r$ is closer to the edge $v_i v_l$ than the point $v_j$. In turn $A_{\triangle v_i v_l v_j} < A_{\triangle v_i k v_j}$ since the point $v_l$ is closer to the edge $v_i v_j$ than the point $k$. For the same reason $A_{\triangle v_i k v_j} < A_{\triangle v_i k_1 v_j} \leq \tau$. Thus, we have established that all the triangles in the fan from $v_j$ to the vertices of the chain between $k$ and $k_2$ have area smaller than the threshold, likewise with the triangle $\triangle v_i k v_j$. Hence, $\lambda(T) \leq \tau$. □

Symmetrically, in the ascending chain of vertices preceding $Top(v_i v_j)$ in the clockwise ordering and lying inside the strip defined above, those vertices $v_m$ that satisfy $\lambda(T) \leq \tau, A_{\triangle v_i v_m v_j} \leq \tau$ for some

triangulation $T$ of the polygon $P_{im}$ form an interval – the **CW interval of admissibility of $\mathbf{v_i}$** for MinMax area with respect to $v_j$ and $\tau$. Of course, here we are restricted by the strip and one or both of these intervals might not exist.

Recall that we denoted the value of the maximum area in the MinMax Area triangulation of the subpolygon $P_{ij}$ by $\lambda^*(P_{ij})$.

**Corollary 43** *Let $v_i$ be a fixed vertex of $P$. $\lambda^*(P_{ik})$ as a function of the vertex $v_k$ is unimodal over the part of the interval $[v_i, Top(v_iv_j)]$ lying inside the parallel strip perpendicular to the edge $v_iv_j$ for every other vertex $v_j$ following $v_i$ in the clockwise order. Similarly, $\lambda^*(P_{mi})$ considered as a function of the vertex $v_m$ is unimodal over the part of the interval $[Top(v_jv_i), v_i]$ lying inside the parallel strip perpendicular to the edge $v_jv_i$ at its endpoints for every other vertex $v_j$ preceding $v_i$ in the clockwise order.*

**Proof.** Identical to the proof of Corollary 41 on page 34. □

To summarize the results of this section, we have shown that the worst triangle in a MaxMin Area triangulation is adjacent to the boundary of the polygon. We have described a way to classify subproblems based on the angles formed by their extreme edges. Some special cases exist. Polygons that can be inscribed in a parallel strip through the endpoints of their base edge can be triangulated using one of the two triangles immediately adjacent to the base edge. Every triangulation contains a triangle such that the three outside parts can be treated more easily than the general case. Based on this, we only need to check small number of possible triangles and these checks are facilitated by the fact that the points that admit triangulations with respect to a given threshold value of area form intervals.

In the case of MinMax Area, although the worst triangle does not necessarily have a boundary edge, the optimal triangulation still uses one of the triangles immediately adjacent to the base edge of a subpolygon for the above described special types of subpolygons. Intervals of admissibility can be constrained to the interior of the parallel strip, perpendicular to the edge and passing through its endpoints. As we shall see further, this is enough to obtain a similar algorithmic result to that of MaxMin Area. Considerations in this section also reveal the specific structure of the two optimal area triangulations.

## 2.3 Algorithmic approach

### 2.3.1 General algorithm

The general algorithm used to compute the MaxMin and MinMax area triangulations of a convex polygon $P$ is based on the dynamic programming approach. We solve all subproblems (i.e. find the optimal area triangulations of the subpolygons) in order of increasing size, starting with the triangles and going up to the polygon $P$ itself. However, we will not solve subproblems with zonality of more than two. Instead, if we detect that a subproblem is not a one- or two-zone problem, we will proceed to the next subproblem. After running through all possible subproblems, we will use the data collected, to determine the answer in the following way. The optimal triangulation contains either a diagonal that has both subproblems associated with it solved or a triangle that has all three subproblems associated with it solved, see Figure 2.8 on the following page. The algorithm will use special data structures to achieve the claimed space and time bounds. The overall scheme used to construct the two optimal triangulations is the same. However, the search for the optimal triangulations after the dynamic programming phase, and the data structures used are different, based on the specific properties of the two triangulations derived in previous section.

The array $SubPr[]$ is used to carry the results of the dynamic programming phase. In the entry $SubPr[i,j]$ we store the index $k$ of the vertex $v_k$ that is connected to the edge $v_iv_j$ in the optimal triangulation of $P_{ij}$, or zero if $z(P_{ij}) \geq 3$. In addition, if the index is non-zero, the $SubPr[i,j]$ entry also stores the value of the maximal/minimal area for the subproblem. Thus the entries in $SubPr[i,j]$ have two fields – for the indices and areas of the optimal triangulations being computed. All these data structures are global for the described algorithm. The searching phase, performed in step *iv.*, creates and uses additional data structures, which will be introduced and explained later in this section. These are all of quadratic size, $O(n^2)$, as it will be shown in the subsequent analysis.

**Algorithm 44 (Optimal Area Triangulation)**

***Input:*** *Convex polygon $P$ represented by the list of its $n$ vertices in clockwise order.*

***Output:*** *Triangulation $T_1$ (MaxMin Area triangulation) of $P$ such that the minimum area triangle in $T_1$ has maximum area over all triangulations of $P$, and triangulation $T_2$ (MinMax Area triangulation) of $P$ such that the maximum area triangle in $T_2$ has minimum area over all triangulations of $P$.*

*i. Compute, for each edge and diagonal of $P$, the most distant vertex of $P$.*

*Store the results in the array $Top[1..n, 1..n]$.*

*Compute the arrays $MaxCW[1..n]$ and $MaxCCW[1..n]$ from $Top[1..n, 1..n]$.*

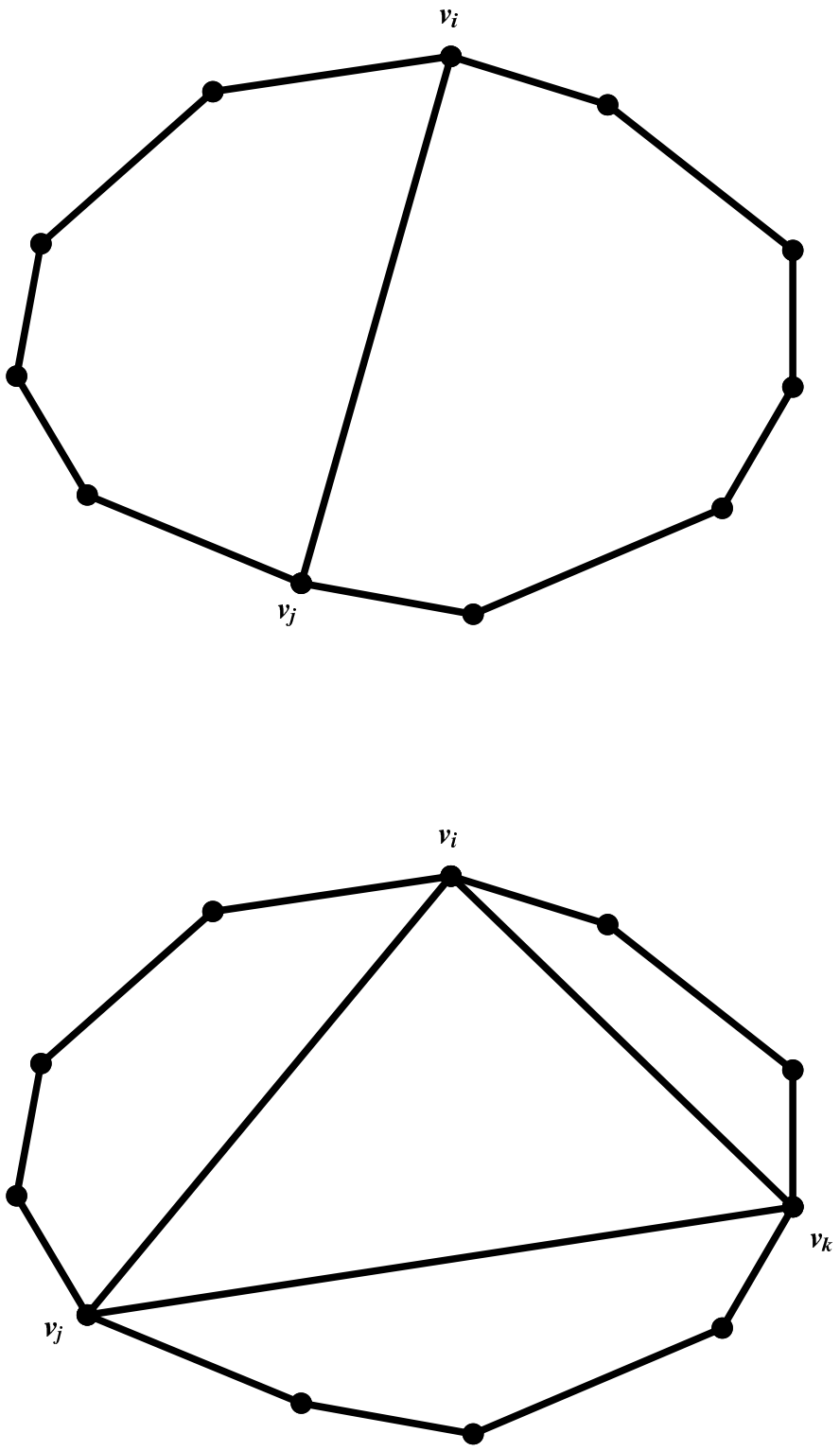


**Figure 2.8:** Top: for the diagonal $v_iv_j$ both $P_{ij}$ and $P_{ji}$ are 2-zone subpolygons. Bottom: for $\triangle v_iv_jv_k$, all three polygons $P_{ij}$, $P_{jk}$, and $P_{ki}$ are 2-zone subpolygons

*ii. Initialize the array* $SubPr[1..n, 1..n]$ *with zeros.*

**for** $i := 0$ **to** $n$ **do**

*set the area fields of* $SubPr[i, (i+2) \mod n]$ *with the area of* $\triangle v_i v_{i+1} v_{i+2}$*;*

*set the index fields of* $SubPr[i, (i+2) \mod n]$ *with* $(i+1) \mod n$*.*

*iii.* **for** $l := 3$ **to** $n-1$ **do**

**for** $i := 1$ **to** $n$ **do**

**if** $z(P_{i,i+l}) \leq 2$ **then**

*set the area fields of* $SubPr[i, (i+l) \mod n]$ *with the minimum/maximum area in the optimal triangulations of* $P_{i,i+l}$*;*

*set the index fields of* $SubPr[i, (i+l) \mod n]$ *with the index of the vertex adjacent to* $v_i v_l$ *in each of the optimal triangulations of* $P_{i,i+l}$

*iv.* **for** $i := 1$ **to** $n$ **do**

**for** $j := 1$ **to** $n$ **do**

**if** $SubPr[j, i] \neq 0$ **then**

**if** $SubPr[i, j] \neq 0$ **then**

*compare to the current best triangulations and update if necessary*

**else**

*search in* $[i, j]$ *for a* $k$ *such that the triangle* $\triangle v_i v_k v_j$ *yields a solution;*

*compare to the current best triangulations and update if necessary*

*v. Construct the two optimal triangulations* $T_1$ *and* $T_2$ *obtained from the search in iv.*

**Lemma 45** *Steps i. to iii. of Algorithm 44 are performed in* $O(n^2)$ *time, using* $O(n^2)$ *space.*

**Time and Space Analysis.** As it was mentioned earlier in the text, the computation of the values in the array $Top[]$ in step i. can be performed in $O(n^2)$ time. The idea used is again the rotating calipers [56], but instead of considering edges on the boundary of $P$ one after another and moving the calipers accordingly, we consider the fan of edges that are incident to one particular vertex and move the calipers to compute the $Top[]$ of the edges in this fan. This is done in $O(n)$ time since the calipers do not make more than one full rotation around the boundary of $P$. We have $n$ vertices, and for each vertex we perform two rotations, as we consider the fan of diagonals adjacent to the vertex in both the clockwise and the counterclockwise directions, hence there are $2n$ such passes and the task is completed in $O(n^2)$ time.

The computation of $MaxCW[]$ and $MaxCCW[]$ requires linear time, due to their relationship with the values in $Top[]$ given by Property 39 on page 32. The initialization of $SubPr[]$ in step ii. takes $O(n^2)$ time. In step ii. we also initialize the entries in $SubPr[]$ that correspond to triangles. This takes linear time. Step iii. performs the dynamic programming and solves all subproblems of zonality up to two reflecting the solutions in $SubPr[]$ as discussed. There are two nested loops, in

each of the iterations through the inner loop, we only perform constant number of checks and value assignments. This is based on the fact that for each subproblem we only have to compare the two possible triangulations containing the triangles immediately adjacent to the base, as it was proven in Lemmas 31 on page 26 and 32 on page 28. Thus, step iii. also takes $O(n^2)$ time.
The claimed time and space bounds follow.

Further we will analyze in detail step iv. of the Algorithm 44 on the preceding page, separately for MaxMin and MinMax area triangulations, as they are performed differently. We will show that step iv. takes $O(n^2 \log n)$ time and $O(n^2)$ space in both cases. To achieve efficient search for the optimal triangulations, within the claimed time and space bounds, we use specific data structures that are different for the MaxMin and MinMax area triangulations. We explain the data structures and properties that are used to find the MaxMin and MinMax area triangulations based on the data gathered during the dynamic programming, starting with the MaxMin area triangulation.

### 2.3.2 MaxMin Area triangulation

Lemma 23 on page 21 establishes that the worst triangle, in the case of MaxMin area, contains a boundary edge. If the optimal MaxMin area triangulation contains a non-degenerate 2–2–2–zone triangle, we do not have to account for its area as it is not going to be the worst triangle. We may also assume that we discover the desired 2–2–2–zone triangle from the edge $v_iv_j$ such that $\mu^*(P) = \mu^*(P_{ji})$. We try to find a vertex $v_k$ in the interval $[v_i, v_j]$ such that $\mu^*(P_{ik}) \geq \mu^*(P_{ji})$ and $\mu^*(P_{kj}) \geq \mu^*(P_{ji})$. In fact it is sufficient to know that the desired vertex $v_k$ exists in the interval $[v_i, v_j]$. We do not need to find the exact vertex until we need the optimal triangulation. Remember that the subinterval of $[v_i, v_j]$ that contains vertices forming 2–2–2–zone triangles with base $v_iv_j$ is completely covered by the intervals of unimodality of $\mu^*(P_{ik})$ and $\mu^*(P_{kj})$, as shown in Corollary 41 on page 34. Thus, if we have to check whether there is triangulation of a certain quality, we may divide this task into two parts. Check whether there is a vertex with the desired property in $[Top(v_i, MaxCW(v_i)), MaxCW(v_i)]$, and whether there is such a vertex in $[MaxCCW(v_j), Top(MaxCCW(v_j), v_j)]$. Let's consider the first part. We are looking for a vertex $v_k$ in $[Top(v_i, MaxCW(v_i)), MaxCW(v_i)]$. $\mu^*(P_{ik})$ will be unimodal over this interval. Thus we have to find the portion of this interval in which $\mu^*(P_{ik}) \geq \mu^*(P_{ji})$. According to Lemma 40 on page 33 this portion is a subinterval. Now we are interested in whether there is some $v_k$ in the interval of admissibility of $v_i$ and $\mu^*(P_{ji})$ such that $\mu^*(P_{ik}) \geq \mu^*(P_{ji})$. It is important to emphasize that $\mu^*(P_{kj})$ is generally not unimodal in this interval. A natural way to represent this problem is a two-dimensional range search with a 3–sided open query rectangle. Please refer to Figure 2.9 on the following page for illustration.

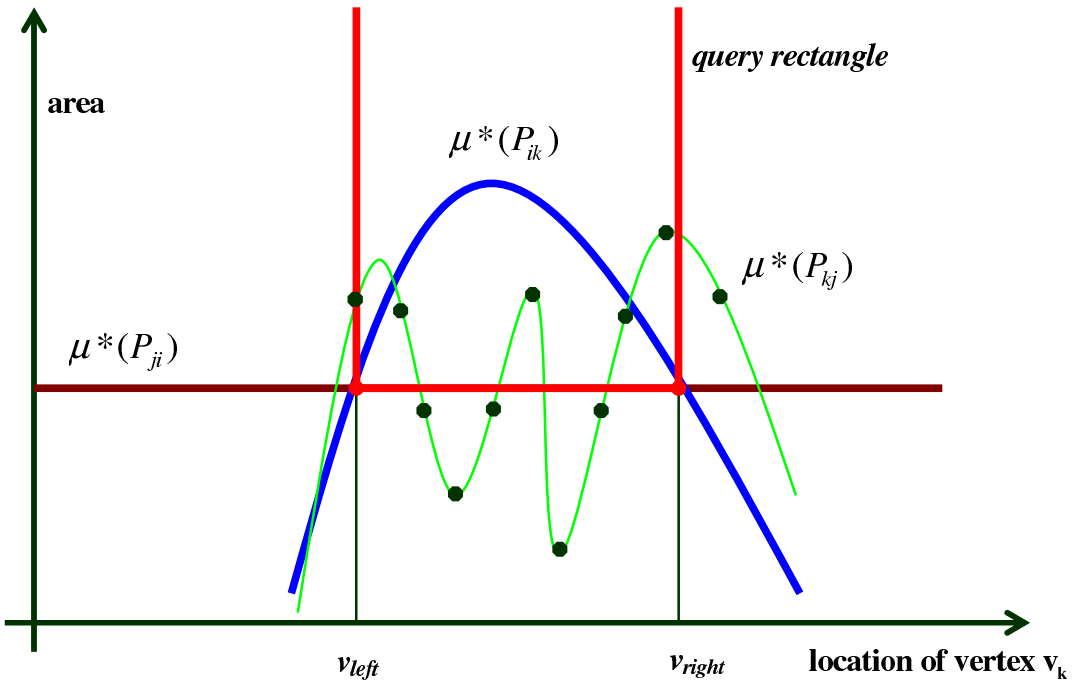


**Figure 2.9:** Range searching, MaxMin area triangulation

If we represent $\mu^*(P_{ji})$, $\mu^*(P_{kj})$ and $\mu^*(P_{ik})$ as functions of $k$ over the interval of vertices between $Top(v_i, MaxCW(v_i))$ and $MaxCW(v_i)$, then the query rectangle will be given by the lines $y = \mu^*(P_{ji})$, $x = v_{left}$ and $x = v_{right}$, where $v_{left}$ preceding $v_{right}$ are the endpoints of the interval of admissibility of $v_i$ and $\mu^*(P_{ji})$. The $x$ coordinate axis represents the indices of the vertices of the original polygon $P$ in $[Top(v_i, MaxCW(v_i)), MaxCW(v_i)]$, and the $y$ coordinate axis represents area. Once again, we only need to check whether there is a point from the curve $y = \mu^*(P_{kj})$ (green curve in the figure) inside the query rectangle. This kind of range searching can be performed using the approach of [19]. For a data set of $n$ points in the plane, we can build a tree structure of linear size, $O(n)$. The time required to build the data structure, i.e., the preprocessing time is $O(n \log n)$. Then, the queries of the specified type, 3–sided open rectangle, can be answered in logarithmic time, $O(\log n)$, by a search in the tree.

The preprocessing of the polygon is done using the data from the dynamic programming phase. For each vertex $v_i$, we are going to keep four data structures: two arrays containing the values of $\mu^*(P_{ik})$ (solutions of the subproblems starting from $v_i$ in clockwise order) and $\mu^*(P_{mi})$ (solutions of the subproblems ending at $v_i$ in counterclockwise order); and two data structures that correspond to the first two arrays preprocessed in a way that is required to answer range searching queries of the specified type. As we have $n$ vertices, we have to build $4n$ data structures of linear size. Thus the space used will be quadratic, $O(n^2)$, and the preprocessing will require $O(n^2 \log n)$ time. Compu-

tationally, there is one more issue. We have to find the sides of the query rectangle. The bottom is given by $\mu^*(P_{ji})$, found by lookup in the $SubPr[j,i]$. We also have to compute the sides of the rectangle, $v_{left}$ and $v_{right}$. Using the unimodality of $\mu^*(P_{ik})$, this can be done by three binary searches in the array representing values of $\mu^*(P_{ik})$: one to determine the point of the maximum, and two in each of the parts to find the two intersection points with the given value of area, $\mu^*(P_{ji})$. Thus, per diagonal we only spend $O(\log n)$ time inside the nested loops of step iv. in Algorithm 44 on page 39.

**Lemma 46** *Step iv. of Algorithm 44 on page 39 computes the MaxMin Area triangulation in $O(n^2 \log n)$ time and $O(n^2)$ space.*

### 2.3.3 MinMax Area triangulation

In the case of MinMax area triangulation the approach is a bit different. We are not guaranteed that the worst triangle has a boundary edge. In fact it is easy to construct a six point example where the largest area triangle in MinMax area triangulation has no boundary edge. As Figure 2.10 on the next page shows, the optimal triangulation (dotted edges) contains an internal triangle which is largest in terms of area. All other possible triangulations of this point set, using either dashed or solid edge(s) have larger value of $\lambda$. Therefore, we cannot use the value of $\lambda^*(P_{ji})$ to guide the search.

Furthermore, we are restricted to unimodality within a parallel strip, perpendicular to the diagonal of reference, $v_iv_j$ at its endpoints. The intervals of unimodality of $\lambda^*(P_{ik})$ and $\lambda^*(P_{kj})$ do not necessarily share more than the vertex $Top(v_iv_j)$. Together though, they still cover the parallel strip. Nevertheless, this is enough to guarantee an algorithmic result with the same time and space complexity as in MaxMin area case. Instead of using the value of $\lambda^*(P_{ji})$, we are going to use the fact that for each triangle at least one of its vertices lies in the parallel strip perpendicular to the opposite side in its endpoints. This is true for the vertex opposite the largest side of the triangle. To see that, recall that in a triangle the larger side is opposite the larger angle. Therefore we have two cases: the largest side is opposite an acute angle, and the largest side is opposite a non-acute angle. In the first case, each of the vertices of the triangle (which is an acute triangle, given that its largest angle is acute) lies within the parallel strip perpendicular to its opposite side. In the second case, the vertex of the triangle opposite its largest side lies in the parallel strip perpendicular to the largest side since the two angles adjacent to the largest side are acute. Thus, if the optimal MinMax Area triangulation contains a non-degenerate 2–2–2–zone triangle, we will discover it from its largest side $v_iv_j$ with the third vertex $v_k$ lying within the parallel strip. Otherwise, there will be a diagonal that has both subproblems associated with it solved, and $M_\lambda(P)$ will be found when the named diagonal is examined.

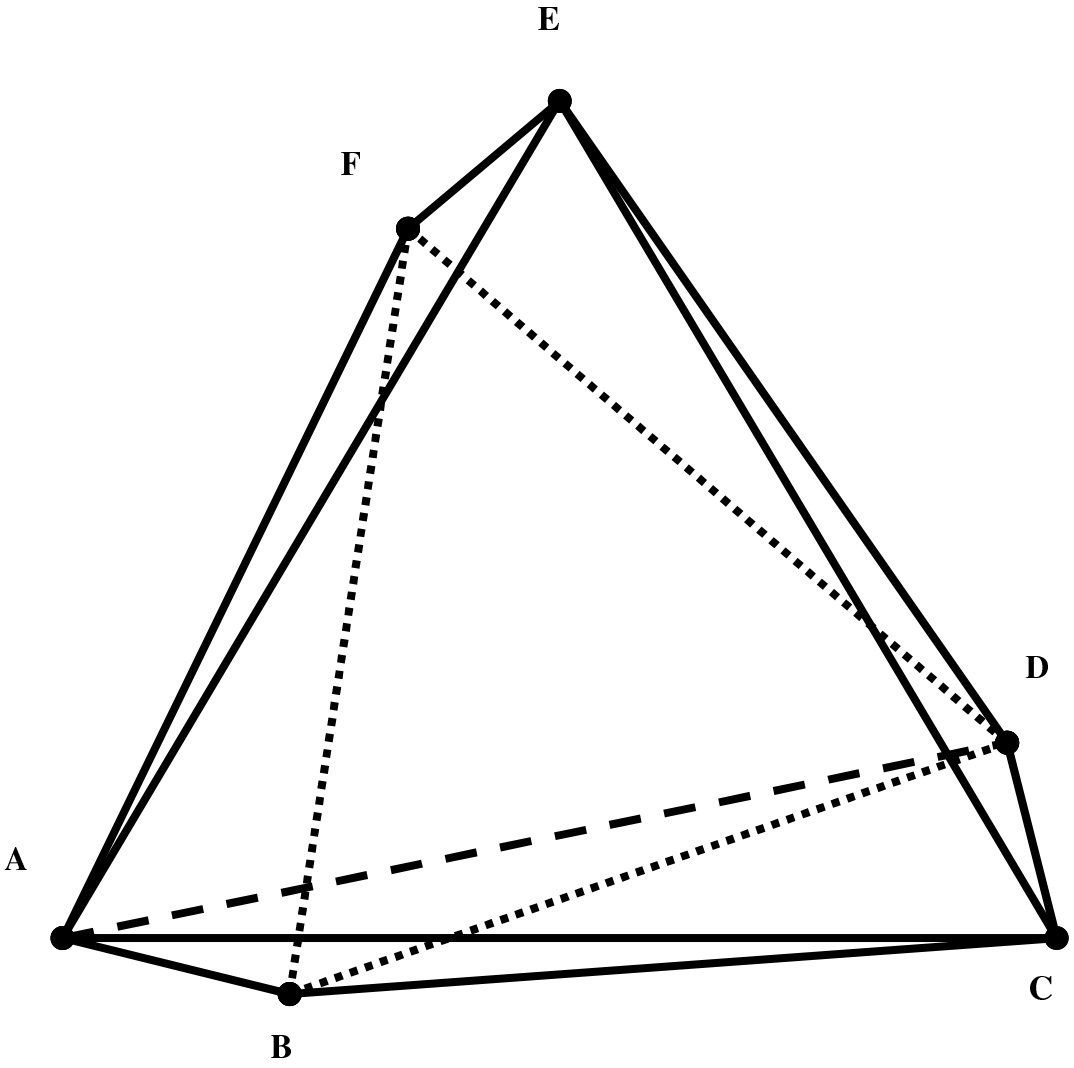


**Figure 2.10:** Six-point counterexample for the anchor condition

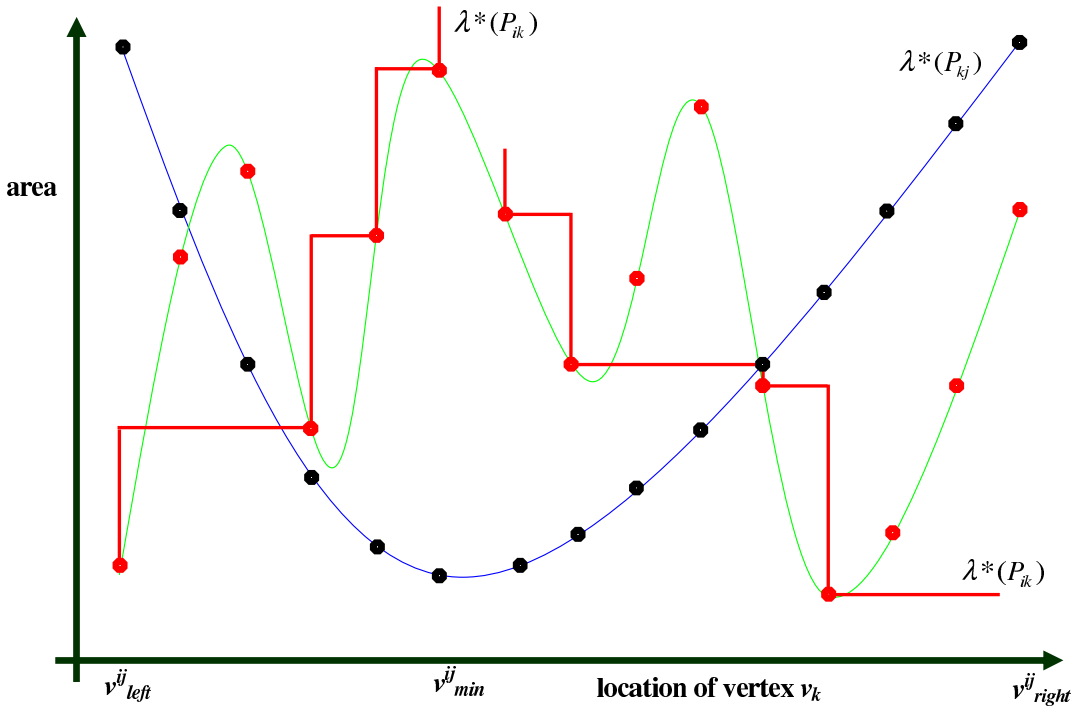


**Figure 2.11:** Staircase structures and the search for MinMax pair

It remains to consider the problem of finding vertex $v_k$ in the strip perpendicular to $v_iv_j$ so as to minimize $\max(\lambda^*(P_{ik}), \lambda^*(P_{kj}))$. Let $v^{ij}_{left}$ and $v^{ij}_{right}$ be respectively the leftmost and the rightmost vertices of $P$ in the perpendicular strip of the edge $v_iv_j$. Depending on the position of $Top(v_iv_j)$ with respect to the interval $[v^{ij}_{left}, v^{ij}_{right}]$, we have two possibilities. If $Top(v_iv_j) \in [v^{ij}_{left}, v^{ij}_{right}]$, then $\lambda^*(P_{ik})$ will be unimodal over $[v^{ij}_{left}, Top(v_iv_j)]$ and $\lambda^*(P_{kj})$ will be unimodal over $[Top(v_iv_j), v^{ij}_{right}]$ by Corollary 43 on page 36. Otherwise, exactly one of the two functions will be unimodal over the entire interval $[v^{ij}_{left}, v^{ij}_{right}]$: it will be $\lambda^*(P_{kj})$, if $Top(v_iv_j)$ precedes $v^{ij}_{left}$ in the clockwise order of vertices of $P$, and $\lambda^*(P_{ik})$, if $Top(v_iv_j)$ follows $v^{ij}_{right}$ in the clockwise order of vertices of $P$, again by Corollary 43 on page 36.

Without loss of generality, we can illustrate the algorithmic approach with the case where $\lambda^*(P_{kj})$ is unimodal over the entire interval $[v^{ij}_{left}, v^{ij}_{right}]$. Denote the vertex where the minimum of $\lambda^*(P_{kj})$ over this interval is attained by $v^{ij}_{min}$. This situation is illustrated in Figure 2.11.

To be able to find the index $k$ for which $\max(\lambda^*(P_{ik}), \lambda^*(P_{kj}))$ is minimum we need to introduce some monotonicity in $\lambda^*(P_{ik})$. It seems natural to use staircase structures for this purpose. In the interval of increase of $\lambda^*(P_{kj})$, we need the staircase structure for $\lambda^*(P_{ik})$ that represents only the points of $\lambda^*(P_{ik})$ that decrease the area, i.e., points are rejected that lie NE (in the I quadrant) relative to a point of $\lambda^*(P_{ik})$. Please, refer to Figure 2.12 on the next page for an illustration

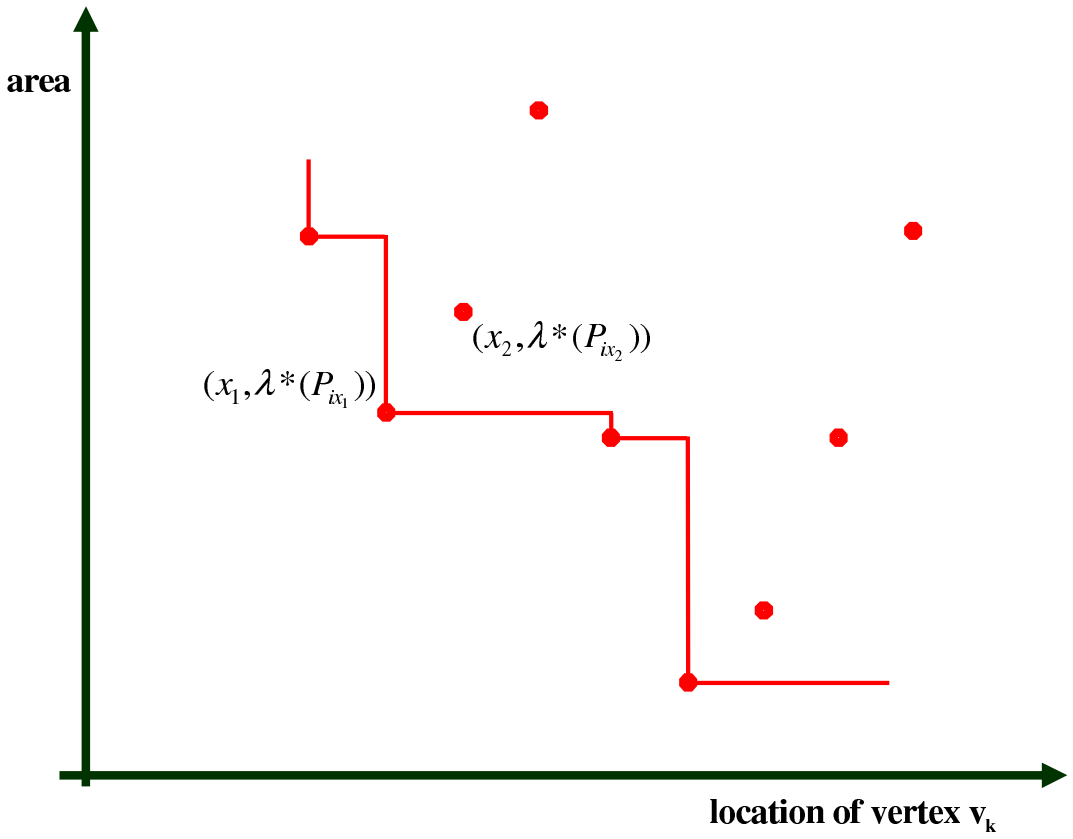


**Figure 2.12:** Rejection of points in the staircase structures, NE case

of the rejection rule. To see that this is true, consider two points on $\lambda^*(P_{ik})$: $(x_1, \lambda^*(P_{ix_1}))$ and $(x_2, \lambda^*(P_{ix_2}))$ for $x_1 < x_2$. Assume that $\lambda^*(P_{ix_1}) \leq \lambda^*(P_{ix_2})$, that is the point $(x_2, \lambda^*(P_{ix_2}))$ for $x_1 < x_2$ lies in the I quadrant relative to a coordinate system with an origin at $(x_1, \lambda^*(P_{ix_1}))$. Keeping in mind that $\lambda^*(P_{kj})$ is increasing in the interval, we can see that $\lambda^*(P_{x_1 j}) \leq \lambda^*(P_{x_2 j})$ and therefore $\max(\lambda^*(P_{ix_1}), \lambda^*(P_{x_1 j})) \leq \max(\lambda^*(P_{ix_2}), \lambda^*(P_{x_2 j}))$. As we need to minimize the maximum, the point $(x_2, \lambda^*(P_{ix_2}))$ can be rejected from our considerations. Analogously, for the interval of decrease of $\lambda^*(P_{kj})$ we need the staircase structure for $\lambda^*(P_{ik})$ that represents points of $\lambda^*(P_{ik})$ that increase the area, i.e., points are rejected that lie NW (in the II quadrant) relative to a point of $\lambda^*(P_{ik})$. We call a staircase NE if it is built by the NE (I quadrant) rejection rule and NW if it is built by the NW (II quadrant) rejection rule.

It is the intersection points between the two staircase filtered versions of $\lambda^*(P_{ik})$ and the unimodal $\lambda^*(P_{kj})$, i.e., the points where the two functions change their dominance one over the other, where we find the locally best MinMax Area triangulation. Only the two entries adjacent to each point

of intersection, either to the left or to the right, have to be compared to determine the MinMax Area triangulation for each part of the interval. Using binary search, we need $O(\log n)$ time to determine $v_{min}^{ij}$ in the interval $[v_{left}^{ij}, v_{right}^{ij}]$. In addition, we have to perform at most two binary searches to find the intersection points and MinMax points in each of the two parts $[v_{left}^{ij}, v_{min}^{ij}]$ and $[v_{min}^{ij}, v_{right}^{ij}]$, respectively. In order to do this, we need to compute the data structures representing the staircase filtered versions of $\lambda^*(P_{ik})$ and $\lambda^*(P_{kj})$. Thus, for each vertex $v_i$ we are going to keep seven arrays: two arrays containing the values of $\lambda^*(P_{ik})$ (solutions of the subproblems starting from $v_i$ in clockwise order) and $\lambda^*(P_{ki})$ (solutions of the subproblems ending at $v_i$ in counterclockwise order), and four arrays that correspond to the staircase filtered versions of the first two arrays - NW and NE in both directions. One additional array per vertex stores the values of $v_{min}^{ij}$ sorted in clockwise order. This array is used to guide the construction of the staircase arrays. For each diagonal $v_iv_j$, we can find the vertex $v_{min}^{ij}$, a binary search achieves this in $O(\log n)$ time. Thus, we have $O(n \log n)$ time per vertex to precompute all the values of $v_{min}^{ij}$ and we can sort them within the same time. Given the fact that we have to build $n$ such arrays of linear size, we will be within $O(n^2 \log n)$ time and $O(n^2)$ storage space. The arrays representing the solutions of the subproblems starting and ending at $v_i$ will also be precomputed, and this takes $O(n^2)$ time and $O(n^2)$ space. The arrays representing the staircase structures will be built during the process of examining diagonals adjacent to $v_i$.

When we examine the diagonal $v_iv_j$ we have to find the points $v_{left}^{ij}$ and $v_{right}^{ij}$ – the ends of the interval of vertices of $P$ lying inside the strip. This can be done by two binary searches over the indices of the interval $[v_i, v_j]$, hence in $O(\log n)$ time. To be able to build and handle staircase structures efficiently we need to examine the diagonals adjacent to the vertex $v_i$ in a particular order. This order is given by the location of the vertex $v_{min}^{ij}$.

We need to consider the two intervals $[v_{left}^{ij}, v_{min}^{ij}]$ and $[v_{min}^{ij}, v_{right}^{ij}]$ separately, find their MinMax points, and compare them to find the overall MinMax point for the interval $[v_{left}^{ij}, v_{right}^{ij}]$. Consider computing the NE staircase structure that is used to determine the local MinMax point in the interval $[v_{min}^{ij}, v_{right}^{ij}]$. We examine the diagonals $v_iv_j$ adjacent to $v_i$ in a special order – the order of decreasing of their $v_{min}^{ij}$, instead of their clockwise (or counterclockwise) order. This special order gives us the opportunity to efficiently compute and update the staircase structures, which is central to the efficiency of the algorithm. For the first diagonal in the mentioned order, we compute the NE staircase structure by examining all the points from $v_{min}^{ij}$ down to $v_{i-1}$ rejecting some according to the NE rejection rule. The points that represent the staircase structure will be kept in an array. When each subsequent diagonal is examined, its respective $v_{min}^{ij}$ is going to be to the left of the previous one, so we have to examine the points between these two consecutive locations of $v_{min}^{ij}$ and to update the staircase structure at its left end. It might be necessary, in doing this, to go over the points in the beginning of the array and reject them, if they are dominated by a point to

the left. The key here is to notice that we are going to examine each point exactly twice, i.e., each point can enter the staircase structure once and leave the staircase structure exactly once. However, once rejected, a point can never reappear. This guarantees that over all diagonals adjacent to a vertex, we spend linear time on updates in the staircase structures, leading to overall $O(n^2)$ time and space spent on this process. Finally, given the current staircase structure, we can find its intersection with $\lambda(P_{kj})$ in logarithmic time by binary search. The binary search should be guided by the indices of the points represented in the staircase structure as these indices are a subset of the indices in $\lambda(P_{kj})$. It remains to mention that trimming the array representing NE staircase structure from right (effectively finding the position of $v^{ij}_{right}$) is also a logarithmic time operation, done by a simple binary search in the array representing the staircase structure. The intervals $[v^{ij}_{left}, v^{ij}_{min}]$ are handled in one more pass through the diagonals adjacent to $v_i$ in the opposite order – increase of $v^{ij}_{min}$. During this pass the NW staircase structures are used analogously to determine the intersection points with $\lambda(P_{kj})$. Thus, for each diagonal $v_iv_j$, we can find the vertex $v_k$ that gives the MinMax Area triangulation of $P_{ij}$ in logarithmic time. Therefore, the overall time spent is $O(n^2 \log n)$. After examining each diagonal, we have to keep the index of the vertex to which it is connected in the 2–2–2–zone triangle that is part of the optimal triangulation. Moreover, we are able to do so because we compute the exact best triangulation for each diagonal. After the completion of the process, the MinMax area triangulation can be retrieved in linear time given the information about the index without any further checks. This settles our final claim.

**Lemma 47** *Step iv. of Algorithm 44 on page 39 computes the MinMax Area triangulation in $O(n^2 \log n)$ time and $O(n^2)$ space.*

**Theorem 48** *Algorithm 44 on page 39 computes the MaxMin and MinMax Area triangulations of a convex polygon $P$ in $O(n^2 \log n)$ time and $O(n^2)$ space.*

**Proof.** It was established by Lemma 45 on page 39 that steps i. through iii. of Algorithm 44 on page 39 take quadratic time and space. Lemma 46 on page 42, and Lemma 47 showed that step iv. takes $O(n^2 \log n)$ time and $O(n^2)$ space. It remains to consider the step v. of the algorithm. This last step of the algorithm is done in linear time, $O(n)$. In fact, during the search phase, in iv., we do not maintain a complete triangulation as currently best. Once we know which diagonal generates the optimal triangulation and the value of the optimal area, we can retrieve the whole triangulation (list of its edges, for example) in linear time. In fact, each edge within a solved subproblem is retrieved in constant time per edge. In the unsolved part we can allow ourselves to test each vertex once to find the one that yields the best triangulation. □

## 2.4 Better solution to the MaxMin decision problem

The MaxMin and MinMax area decision and construction problems can be solved in $O(n^2 \log n)$ time and $O(n^2)$ space by solving the optimization problem as shown in previous section. However, the MaxMin Area decision and construction problems can be solved more efficiently. This is due to the fact that the function $\mu^*$ is unimodal from both sides over a large interval of the boundary of the subpolygon as shown in Corollary 41 on page 34. To achieve the better time bound of $O(n^2 \log\log n)$, we have to use special data structure, called Van Emde-Boas priority queue during the search phase of the algorithm. Van Emde-Boas priority queues [57, 58] are data structures that operate over a universe of keys (usually integers) of size $N$ in a way that the operations insertion, deletion, membership testing, finding predecessor and successor are performed in $O(\log\log N)$ time. The size of the priority queue is $O(N)$. We can use as universe of keys the set of indices of the vertices of the polygon $P$, i.e. $[1..n]$. Here we outline in detail the algorithmic approach that was first presented in [32].

We will define a function $M(\tau)$ that returns *true* if there is a triangulation $T$ of $P$ such that $\mu(\tau) \geq \tau$ and $false$ otherwise.

$M(\tau)$ uses an array $Table[n, n]$. It is similar to the arrays $Best[n, n]$ and $SubPr[n, n]$, used by Algorithm 21 on page 19 and Algorithm 44 on page 39, respectively. In the entry $Table[i, j]$, we store the index $k$ of the vertex $v_k$ that is connected to the edge $v_i v_j$ in a triangulation (if such triangulation exists) of an up to 2–zone subpolygon $P_{ij}$ that satisfies the threshold condition, or zero otherwise. The algorithm will set to zero all entries in $Table[]$ that correspond to subproblems of zonality three or higher. The information in $Table[]$ is duplicated in two arrays of priority queues $R$ and $C$. The array $R$ has $n$ priority queues that encode the non-zero entries of the rows of $Table[]$, and the array $C$ has $n$ priority queues that encode the non-zero entries of the columns of $Table[]$. In $R[i]$, we insert all indices $j$ that correspond to an element $Table[i, j] > 0$. Similarly, in the priority queue $C[j]$, we insert all indices $i$ that correspond to an element $Table[i, j] > 0$. Again, the zero entries in the rows and columns of $Table[]$ are not represented in $R$ and $C$.

**Algorithm 49 (The function M($\tau$):)**

(a) *Initialize $Table[]$ with zeros, initialize $R$ and $C$ with empty queues.*

(b) *For every possible pair $(i, j)$, in the order of dynamic programming, if $z(P_{ij}) \leq 2$, check whether an admissible triangulation exists and if so – update $Table[i, j]$, $R[i]$ and $C[j]$ accordingly. Use the method of Lemma 31 on page 26.*

(c) *Check for each entry in* $Table[]$*, whether both* $Table[i,j]$ *and* $Table[j,i]$ *are non-zero, if so – return* **true**.

(d) *Check for every non-zero entry* $Table[j,i]$*, whether there exists* $k \in (i,j)$ *such that* $Table[i,k]$ *and* $Table[k,j]$ *are non-zero and* $A_{\triangle v_i v_k v_j} \geq \tau$*, if so – return* **true**. *Lemma 37 on page 31 allows us to search only for a* $k$ *that yields 2–zone subproblems and Lemma 40 on page 33 allows us to do this efficiently.*

(e) *Return* **false**.

**Lemma 50** *The function* $M(\tau)$ *is computed in* $O(n^2 \log\log n)$ *time and* $O(n^2)$ *space by Algorithm 49.*

**Time and Space Analysis.** Each individual entry in the arrays $R$ and $C$ is a van Emde–Boas priority queue. These priority queues are a central part of the efficiency of the algorithm. As it was mentioned, Van Emde–Boas priority queues work with a universe of keys of size $N$ so that the operations of insertion, deletion, membership testing, finding predecessor and successor are performed in $O(\log\log N)$ time. The size of the priority queue is linear in $N$ – $O(N)$. In our algorithm, the universe of keys is the set of indices of the vertices of the polygon $P$, i.e. $[1,n]$. Thus, the size of each individual priority queue is $O(n)$ and the overall size of the arrays $R$ and $C$ is $O(n^2)$. Now, we analyze the timing of the computation of the function $M(\tau)$. Initializations of $Table[]$ and the arrays $R$ and $C$ in **(a)** is done in $O(n^2)$ time. After that, in **(b)**, we have two nested loops that compute the values of $Table[]$ for all subproblems of zonality two or less. There are $O(n^2)$ iterations through this program segment. In every iteration, we perform a constant number of checks and logical operations and at most two insertions in the priority queues, if the subproblem has an admissible triangulation. Therefore, the total time for the execution of the two nested loops is $O(n^2 \log\log N)$. If the subproblem is a triangle, we only need to check whether the area of this triangle is larger than the threshold value $\tau$. If so, we reflect this in the queues $R$ and $C$ and in the $Table[]$. If the subproblem is larger in size than a triangle but has zonality of two or less, Lemma 31 on page 26 imples that we only need to check the two triangles that are immediately adjacent to the base edge, if any of them is larger in area than the threshold value $\tau$ and the rest of the subpolygon has admissible triangulation, we have to record the admissible triangulation of the subproblem in the queues and $R$ and $C$ and in the $Table[]$. When the algorithm has gone through all subproblems and has identified all subproblems that have admissible triangulations, we have to obtain the answer for the polygon $P$ as a whole. This is done in **(c)** and **(d)**.
In **(c)** we have two nested loops, both of $O(n)$ iterations, giving us $O(n^2)$ overall iterations. In each

iteration we check one of the induced subproblems. If both the subproblem and its complementary subproblem have been found to have an admissible triangulation, we can return **true** and thus exit the computation of the function $M(\tau)$. So, the time for **(c)** is $O(n^2)$. In **(d)** we have to look for the possibility of the current edge $v_iv_j$ being a base of a triangle with the property of Lemma 37 on page 31. To check this, we use the results and procedure of Lemma 40 on page 33. Namely, if such a triangle exists, with the given edge as a base, we only have to check certain intervals. We know, from the discussion following Lemma 40 on page 33, that admissible subproblems that start from $v_i$ and end between $Top(v_i, MaxCW(v_i))$ and $MaxCW(v_i)$, if any, form an interval. Thus, we can look in the priority queue $R[i]$ for these subproblems. This is done by insertion of the two ends of the interval – $Top(v_i, MaxCW(v_i))$ and $MaxCW(v_i)$ in $R[i]$ and then querying $R[i]$ about their respective successor and predecessor. If those exist, we denote them by $k_1$ and $k_2$ and use them to find an admissible subproblem that starts between $k_1$ and $k_2$ and ends at $v_j$. Again, this is done efficiently by inserting $k_1$ and $k_2$ in the priority queue $C[j]$. We also insert $Top(v_iv_j)$ there, and then query the queue $C[j]$ about the successor or/and predecessor of $Top(v_iv_j)$ in the interval $[k_1, k_2]$. If either of these vertices is found to give admissible triangulation, we have to record it in the queues $R$ and $C$, and in the $Table[]$ and return **true** for $M(\tau)$. If we cannot find such a vertex, we have to symmetrically try to find a vertex in the admissible interval $[k_3, k_4]$ of subproblems ending at $v_j$, such that the triangulation of $P$ is admissible. If such a vertex exists we return **true** for $M(\tau)$. Otherwise, we exit this iteration. If none of the iterations has resulted in the return of **true** for $M(\tau)$, we have to conclude that a triangulation of $P$ given this threshold is impossible, and return **false** for $M(\tau)$. As we have mentioned, there are $O(n^2)$ overall iterations. Within each iteration we only have a constant number of constant time operations or van Emde–Boas priority queue operations that are performed in $O(\log\log n)$ time. Thus, the total time complexity of the fragment in **(d)** and therefore of the computation of $M(\tau)$ is $O(n^2 \log\log n)$. The space that data structures use is $O(n^2)$. Finally, the triangulation can be recovered from the data in $Table[]$ in linear time, $O(n)$ , because it has linear complexity and each time we look up in $Table[]$ we add at least one (and at most two) new edge(s) to the triangulation.

From the analysis in this section we can conclude the following:

**Theorem 51** *The MaxMin Area decision problem for a convex polygon can be solved within $O(n^2 \log\log n)$ time and $O(n^2)$ space. The MaxMin Area construction problem can be solved within the same time and space bounds.*

## 2.5 Open problems and directions for future research

Our approach, based on dynamic programming, leads to algorithms that have time complexity of more than $O(n^2)$ due to the fact that the search phase is separate from the dynamic programming

phase. Moreover, an exhaustive search of $O(n^2)$ possibilities is required. It is interesting to know whether an algorithmic approach to MaxMin and MinMax area triangulations is possible that combines the two phases. The problem has no apparent complexity of more that quadratic. Thus, we strongly believe that further geometric and algorithmic results are likely to improve the bounds achieved here.

Further, assuming that these two problems admit a quadratic time solution, it is interesting to know whether they belong to the class of 3-SUM HARD problems [45]. These are problems that have been shown to have quadratic time solution, but no better solution is known. One problem, that is related to the two problems considered in this chapter and is known to be 3-SUM HARD, is finding the minimum (maximum) area triangle with vetices in a given set of $n$ points [19].

# Chapter 3

# MaxMin and MinMax area triangulations of general point sets

In the previous chapter, we outlined algorithms that efficiently compute the MaxMin and MinMax area triangulations of a convex polygon. They were based on geometric properties that are specific for this situation. In the case of general point set, we cannot derive similar properties that will help us to efficiently search for the optimal triangulation. Although it has been conjectured [9, 54] that a condition similar to, but weaker than, the weak anchor condition exists for a class of quality measures, the MaxMin and MinMax area do not appear to belong to such a class. Being unable to decide whether the general problem is computable in polynomial time, we take another approach – to find a reasonable in quality, and practical in terms of computational effort, approximation of either of the two optimal area triangulations. We derive upper bounds for the approximations computed. This has not been previously done in the literature. Experimental results on Minimum Variance Area triangulation are obtained in [17]. The authors use so-called LMT-skeletons in angularly-restricted triangulations, and dynammic programming to complete the triangulation once a connected subgraph has been computed. No discussion is provided about the quality of the triangulations obtained by this method.

## 3.1 Angular constraints, $\alpha$-triangulations, forbidden zones

**Definition 52 ($\alpha$-triangulation)** *Given a planar point set $S$ and an angle $\alpha$ such that $0^\circ < \alpha \leq 60^\circ$, a triangulation $T$ of $S$ is called an $\alpha$-triangulation if and only if all the angles in the triangles of $T$ are greater than or equal to $\alpha$. Note that all the angles (of the triangles) in an $\alpha$-triangulation are in the interval $[\alpha, 180^\circ - 2\alpha]$.*

For example, the bottom triangulation of Figure 1.1 on page 3 is a 4°-triangulation and the top one is a 17°-triangulation. Only the vertices of a regular triangular grid represent a point set that admits a 60°-triangulation.

As it was pointed out in the introductory chapter, there is no guarantee for the quality in terms of area of a "fat" triangulation, and reciprocally there is no guarantee for the "fatness" of a good

area triangulation. We will show that a reasonable compromise can be achieved. The rest of this chapter will be devoted to this.

Knowing that all the angles are in some interval, we can derive an interesting property of the edges of an $\alpha$-triangulation. We are going to define a region of the plane surrounding each possible edge of the triangulation with the property that if this region contains some point(s) of $S$ then we can reject the edge as a possible part of an $\alpha$-triangulation.

**Definition 53 (i-th order triangles)** *Given a planar point set $S$ and an angle $\alpha$ such that $0° < \alpha \leq 60°$, we call an edge $AB$, $A, B \in S$, **internal** if there are points from $S$ in both half-planes with respect to the line $AB$. For an internal edge $AB$, we define the isosceles triangle $\triangle AV_1B$ with angles $\angle V_1AB = \angle ABV_1 = \alpha$ as a **first order triangle** with respect to the edge $AB$. We call the point $V_1$ a **first order vertex** with respect to the edge $AB$. Similarly, we call the edges $AV_1$ and $V_1B$ **first order edges** with respect to the edge $AB$. Note that the point $V_1$ is generally not a point from the set $S$. It is just a part of an auxiliary construction. Recursively, on each $i$-th order edge, we can build an isosceles triangle with base angles of $\alpha$, and it will be $(i+1)$-th order triangle with respect to the original edge $AB$. As it is clear from the construction method, for $i > 1$, there are multiple $i$-th order triangles, edges and vertices. The vertices in particular can be enumerated by double indexing $V_{ij}$ meaning that $V_{ij}$ is the $j$-th vertex of $i$-th order, where $i = 2, 3, \ldots, j = 1, 2, \ldots, 2^{i-1}$, and the index $j$ is running clockwise from the leftmost $i$-th order triangle (which is incident to $A$) to the rightmost $i$-th order triangle (which is incident to $B$). The construction is illustrated in Figure 3.1.*

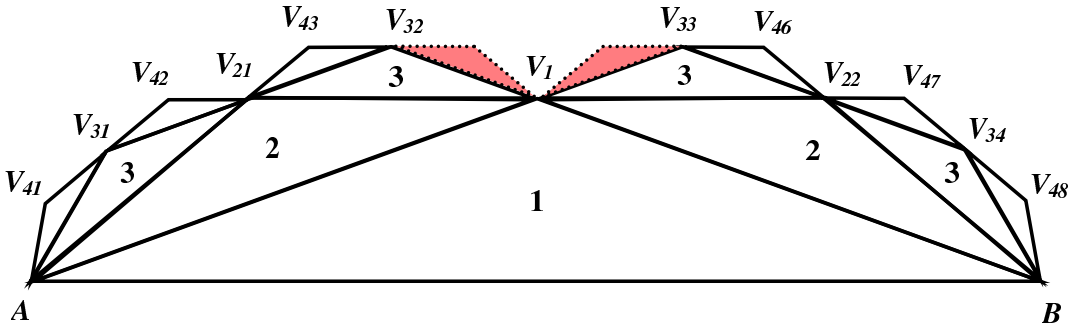


**Figure 3.1:** Construction of the $i$-th order ($i \leq 4$) triangles that form part of the forbidden zone of the edge $AB$ for $\alpha = 20°$

**Definition 54 (Free zone)** *For each triangle of $i$-th order, we can define its* ***free wedge*** *as the interior of the angle opposite of its internal angle of $180° - 2\alpha$, as illustrated in Figure 3.2. The union over all values of $i, i = 1, 2, \ldots$ of all free wedges for all $i$-th order triangles of the edge $AB$ is the* ***free zone*** *of the edge $AB$. Note that some of the $i$-th order triangles lie entirely in the free wedges of triangles of lower order. Such triangles are not needed in the recursive construction of the free zone. So, they are not recursively considered, although the numbering of vertices treates them and their recursive descendants as existing. In Figure 3.1 on the preceding page it can be seen that two potential $4^{\text{th}}$ order triangles (shaded interior, dotted lines) are not considered as they lie inside the free wedge of the $1^{\text{st}}$ order triangle. The recursion also stops whenever we reach a triangle whose interior is properly intersected by the line $AB$. The part of such a triangle's free zone that is in the same half-plane with respect to $AB$ as the first order triangle is also a part of the free zone of the edge $AB$. The free zone lies in both half-planes with respect to the edge $AB$, thus the construction above has to be applied twice, in each of the half-planes defined by the line $AB$.*

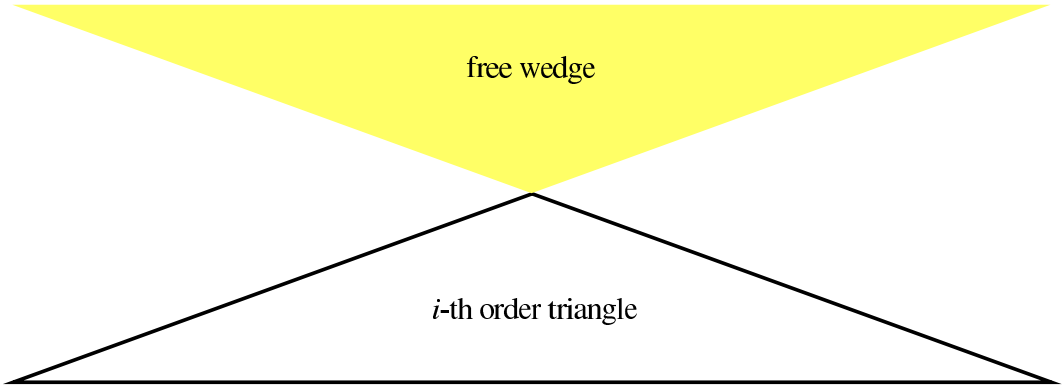


**Figure 3.2:** Free wedge of an $i$–th order triangle

**Definition 55 (Forbidden zone)** *The complement of the free zone of the edge $AB$ is the* ***forbidden zone*** *of the edge $AB$. Points for which all local circular neighbourhoods contain both points from the free zone and from the forbidden zone are called* ***boundary points*** *of the forbidden zone. They form the* ***boundary*** *of the forbidden zone.*

We now introduce additional notation that will help us in the following considerations of the geometry of the forbidden zone throughout this chapter. Denote by $V_L$ and $V_R$ the two intersection points of the boundary of the free wedge of first order (i.e., angle opposite $\angle AV_1B$) with the boundaries of the left and the right free wedges of second order (i.e., angles opposite $\angle AV_{21}V_1$ and $\angle V_1V_{22}B$), respectively. In a similar fashion, denote by $V_{L1}$ the intersection point of the boundary of the free

wedge of the leftmost triangle of third order (the angle opposite $\angle AV_{31}V_{21}$) with the boundary of the free wedge of the leftmost triangle of second order; denote by $V_{R1}$ the intersection point of the boundary free wedge of the rightmost triangle of third order (the angle opposite $\angle V_{22}V_{34}B$) with the boundary of the free wedge of the rightmost triangle of second order. We are going to use extensively the points $V_L$, $V_R$, $V_{L1}$, and $V_{R1}$ in the discussion throughout the rest of this chapter. Please, refer to Figure 3.3 on page 57 for an illustration. In general, the other "breakpoints" of the boundary of the forbidden zone can be defined as follows. Denote by $V_{Li}$ the intersection point of the boundary free wedge of the leftmost triangle of $(i+2)$-th order (the angle opposite $\angle AV_{i+2,1}V_{i+1,1}$) with the boundary of the free wedge of the leftmost triangle of $(i+1)$-th order; denote by $V_{Ri}$ the intersection point of the boundary free wedge of the rightmost triangle of $(i+2)$-th order (the angle opposite $\angle V_{i+1,2^i}V_{i+2,2^{i+1}}B$) with the boundary of the free wedge of the rightmost triangle of $(i+1)$-th order. Here the subscripts $L$ and $R$ stand for left and right, respectively.

Assume that the edge $AB$ is horizontally aligned, with $A$ to the left of $B$, and the words "above" and "below" have their usual meaning. Now we can specify the boundary of the top part (the one that is above the line $AB$) of the forbidden zone of the edge $AB$ as a chain of line segments.

**Property 56** *The boundary of the forbidden zone of the edge $AB$, above $AB$, as per Definition 55 on the preceding page consists on the left of the chain of line segments $V_1V_L$, $V_LV_{21}$, $V_{21}V_{L1}$, $V_{L1}V_{31}$, $V_{31}V_{L2}$, ..., as many edges as needed until the chain intersects the line $AB$ to the left of $A$. On the right, the boundary of the forbidden zone consists of the line segments $V_1V_R$, $V_RV_{22}$, $V_{22}V_{R1}$, $V_{R1}V_{34}$, $V_{34}V_{R2}$, ..., as many as necessary until the chain intersects the line $AB$ to the right of $B$.*

**Proof.** To show that the named chains form the boundary of the forbidden zone, we have to show that:

(1) no free wedge of a generated triangle of any order shares interior points with the region bounded by the chains and $AB$, and

(2) every point on the named chains is contained in the boundary of the free wedge of a triangle of some order.

Certainly, the free wedge of the first order triangle is exterior to the region, and shares with it only the boundary segments $V_1V_L$ and $V_1V_R$. Similarly, for the free wedge of the left second order triangle $\triangle AV_{21}V_1$, it shares with the region only the boundary segments $V_LV_{21}$ and $V_{21}V_{L1}$. We have to consider the interior of the triangle $\triangle V_{21}V_LV_1$, as it might share interior points with free wedges of triangles of higher order. According to the construction of the forbidden zone, the angles of $\triangle V_{21}V_LV_1$ are as follows: $\angle V_{21}V_1V_L = \alpha$, $\angle V_1V_{21}V_L = 2\alpha$, $\angle V_{21}V_LV_1 = 180^\circ - 3\alpha$. Therefore, the third order triangle that is built on $V_{21}V_1$ as a base, will have its vertex $V_{32}$ on the segment

$V_1V_L$. The free wedge of this triangle, consequently, will lie entirely inside the free wedge of $\triangle AV_1B$ and will share only the line segment $V_{32}V_L$, which is a proper part of the segment $V_1V_L$, with the boundary of the region. Further, the fourth order triangle, built on $V_{21}V_{32}$ as a base, will have its vertex $V_{43}$ on the segment $V_{21}V_L$. The free wedge of this triangle, consequently will lie entirely inside the free wedge of $\triangle AV_{21}V_1$ and will share only the line segment $V_{43}V_L$, which is a proper part of the segment $V_{21}V_L$, with the boundary of the region. From these two steps we can see that the subsequent higher order triangles will have their vertices on the segments $V_1V_L$ and $V_{21}V_L$, alternately, and their free wedges will lie entirely inside the free wedges of the triangles $\triangle AV_1B$ and $\triangle AV_{21}V_1$, respectively. Taking infinitely many steps, we reach the conclusion that no interior point of a free wedge of a higher order triangle lies inside the triangle $\triangle V_{21}V_LV_1$. Thus, triangle $\triangle V_{21}V_LV_1$ lies entirely inside the forbidden zone of $AB$. Note that this serves also as a proof of the fact that the triangle $\triangle V_{21}V_LV_1$ is completely covered by higher order triangles. This fact will be used in the proof of the next Property 57. A similar argument establishes that the triangles containing all the convex corners of the boundary are completely contained in the forbidden zone of $AB$, e.g. $\triangle V_{31}V_{L1}V_{21}$. Although trivial, it should be mentioned that the generated $i$-th order triangles themselves are completely inside the forbidden zone since they are interior disjoint with their own free zones. □

To summarize the results of this proof, we have established that the boundary of the forbidden zone contains certain line segments. Along the boundary, convex vertices of angle $180° - 3\alpha$ alternate with reflex vertices of angle $180° + 2\alpha$, and the forbidden zone is in fact the region tiled by the $i$-th order triangles, $i = 1, 2, \ldots$, that do not lie inside the free wedges of lower order triangles. The last fact is very useful as it helps to intuitively understand the geometry of the forbidden zone, and it can be used as an alternative definition of it from here onwards.

**Property 57** *If there is a point of the set $S$ in the forbidden zone of the internal edge $AB$, then $AB$ is not a part of any $\alpha$-triangulation of $S$.*

**Proof.** In fact, the forbidden zone was defined to ensure this property. Using the notation from Definition 53 on page 53 which is also used in Figures 3.1 on page 53 and 3.3 on the following page, we are going to prove the claim by induction. Assume the edge $AB$ is part of some $\alpha$-triangulation of $S$, call this triangulation $T_{AB}$. For the triangles of $T_{AB}$, we recursively define the distance from $AB$ as follows:

- A triangle that has $AB$ as a side has distance one from $AB$.
- All the triangles that have an edge of a triangle at distance $i$ from $AB$ as a side, and whose distance has not been defined yet, have distance $i + 1$ from $AB$.

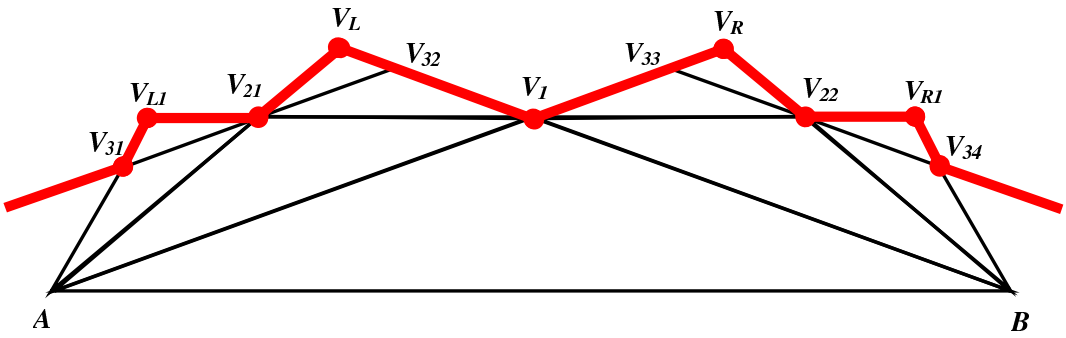


**Figure 3.3:** The forbidden zone of the edge $AB$, the boundary line (red) after first three iterations

Call $X$ the point of the set $S$ that is in the forbidden zone. The induction is going to be on $i$ – the order of the triangle (with respect to the construction of the forbidden zone) within whose closure the point $X$ lies. The same variable $i$ is used for the distance from $AB$ in the triangulation $T_{AB}$. We call the part of $T_{AB}$ consisting of all triangles of distance up to $i$ from $AB$ the **traced part** of $T_{AB}$.

We are going to prove inductively that the triangles of $T_{AB}$ of distance up to $i$ from $AB$ completely cover up to $i$-th order triangles of the forbidden zone.

The base case is $i = 1$ and we have a single $1^{\text{st}}$ order triangle – $\triangle ABV_1$. We are going to prove that if $X$ lies within $\triangle ABV_1$ then any triangulation containing the edge $AB$ has to have angles smaller than $\alpha$. We have already assumed the contrary, i.e. that the edge $AB$ is part of some $\alpha$-triangulation of $S$, denoted by $T_{AB}$. Given the placement of $X$ inside $\triangle ABV_1$ there are three possibilities as shown in Figure 3.4 on the next page:

First, $X$ can be connected to both $A$ and $B$ in $T_{AB}$, which means that $\triangle ABX$ will be part of the triangulation $T_{AB}$. This will immediately violate the angular constraint, as at least one of the angles $\angle XAB$ and $\angle XBA$ is smaller than $\alpha$. Second, the point X can be connected to only one of the ends of $AB$ in $T_{AB}$, say to $A$. Then the edge $XB$ is not in the triangulation $T_{AB}$, and therefore it should be intersected by at least one edge incident to $A$, thus forming angles of less than $\alpha$ (remember that $\angle XAB$ itself is at most $\alpha$). Third possibility is that $X$ is not connected to either of the points $A$ or $B$ in $T_{AB}$. Then, there is an edge in the triangulation $T_{AB}$ that properly intersects the interior of the triangle $\triangle ABX$, thus separating $X$ from $AB$. If there are multiple edges with this property, consider the lowest of them, call it $YZ$. By lowest we mean the one that cuts off from $\triangle ABX$ a part adjacent to $AB$ with the smallest area. The edges $AB$ and $YZ$ are in the triangulation $T_{AB}$, and by our choice of $YZ$ no other edge of $T_{AB}$ intersects the interior of the quadrilateral $ABZY$ without being incident to $A$ or $B$. Thus, one of the diagonals of this quadrilateral, either $AZ$ or $BY$ is part of the triangulation $T_{AB}$. This also violates the angular

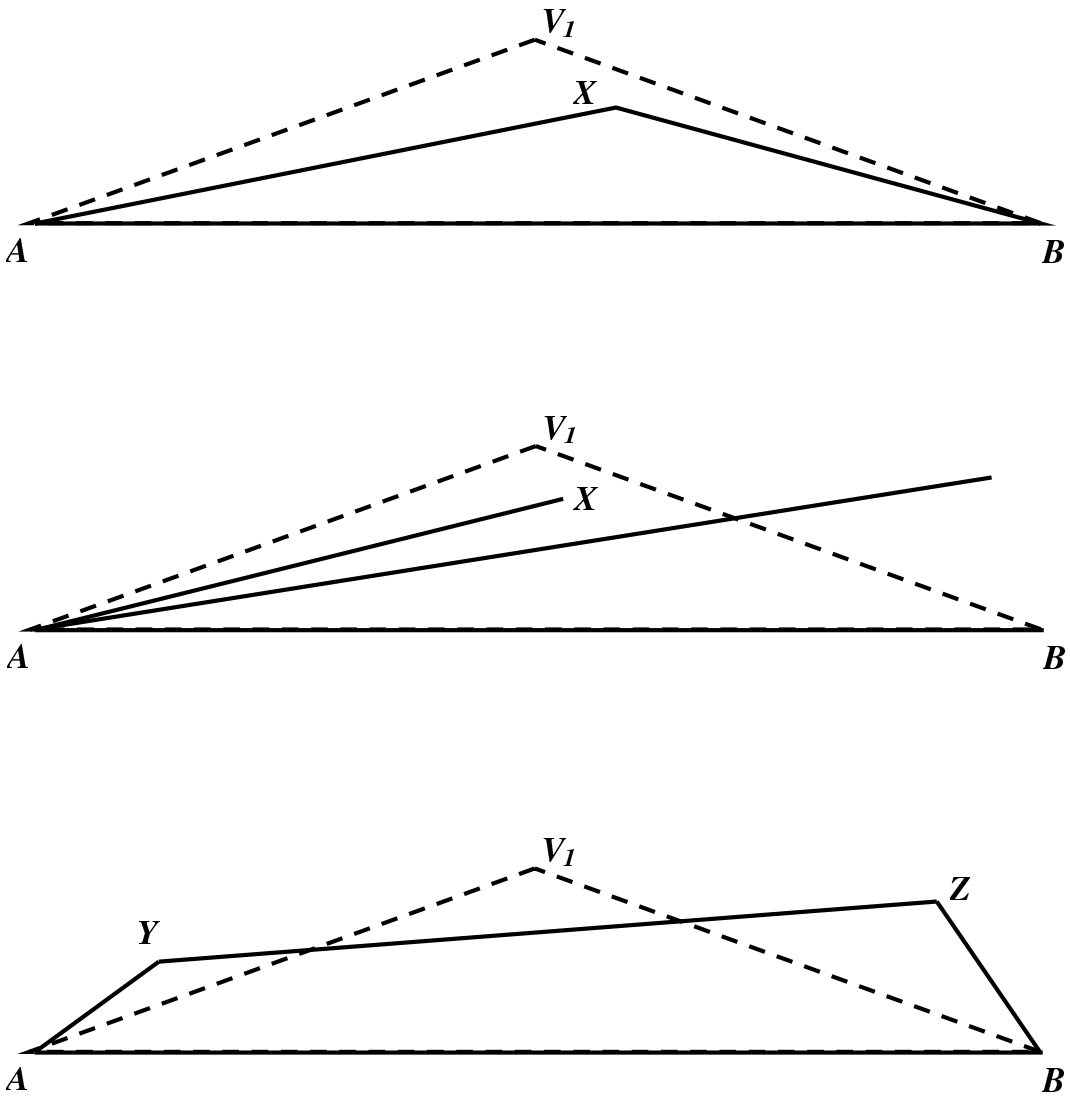


**Figure 3.4:** Possible placements of the point $X$ with respect to the triangulation $T_{AB}$ in the base case of Property 57 on page 56

constraint as both $AZ$ and $BY$ lie inside the angles $\angle XAB$ and $\angle XBA$, respectively. If so, any of them will form with the edge $AB$ angles of less than $\alpha$. Figure 3.4 on the preceding page illustrates the three subcases of the base case.

To summarize our findings, we have shown in the base case analysis that if a point $X$ from the set $S$ lies within the first order triangle $\triangle ABV_1$, then the edge $AB$ is not in any $\alpha$-triangulation of $S$. Additionally we have shown that if $AB$ is in some $\alpha$-triangulation $T_{AB}$ of $S$, then no edge of this triangulation properly intersects the interior of $\triangle ABV_1$. There is one more important thing to notice. The point of $S$ to which the edge $AB$ is connected in $T_{AB}$ can only lie in the free wedge, i.e. the angle of $180° - 2\alpha$ opposite $\angle AV_1B$. Denote this point by $W_1$, please refer to Figure 3.5 on the next page. If we consider the $2^{\text{nd}}$ order triangles, the $\triangle ABW_1$ can have edges coinciding with the base edges of these triangles: $AW_1$ coinciding with $AV_1$, or $BW_1$ coinciding with $BV_1$. Another possibility is that the edges $AW_1$ and $BW_1$ intersect the interior of the triangles $\triangle AV_{21}V_1$ and $\triangle V_1V_{22}B$, respectively. And the last possible case is that $\triangle ABW_1$ contains an entire $2^{\text{nd}}$ order triangle in its interior.

There can be points of $S$ inside the angles $\angle V_1AB$ and $\angle V_1BA$, outside $\triangle ABV_1$, but they cannot be connected to the edge $AB$ in the triangulation $T_{AB}$.

Our inductive hypothesis is that $X$ does not lie inside any of the triangles of up to $i$-th order. In addition, we assume the traced part of the triangulation $T_{AB}$ up to distance $i$ from $AB$ completely includes the part of the forbidden zone up to $i$-th order in its interior. For the sake of notation completeness we are going to denote the vertices of the traced part of $T_{AB}$ by $W_{ij}$, where $i$ is the same as the induction variable (i.e. the order of the triangles in the construction of the forbidden zone) and $j$ is an index, assigned in clockwise order. As $W_{ij}$ are vertices of $T_{AB}$, it should be noted that they are points of the set $S$ ($W_{ij} \in S$), unlike $V_{ij}$ which are auxiliary points having no connection to the set $S$. Note that here we may need more or less than $2^{i-1}$ triangles, depending on the position of the points in $S$, to cover the forbidden zone up to $i$-th order. This means that the outer edges of the traced part of $T_{AB}$, i.e. those edges that have only one triangle adjacent to them in the traced part of $T_{AB}$ can interact with the $(i+1)$-th order triangles in one of the following four ways:

(1) they can be aligned or coincide with the base edge of an $i+1$-th order triangle

(2) they can intersect the interior of an $(i+1)$-th order triangle being incident to one of its base vertices

(3) they can intersect the interior of an $(i+1)$-th order triangle without being incident to one of its base vertices

(4) the traced part of $T_{AB}$ can completely enclose in its interior an $(i+1)$-th order triangle.

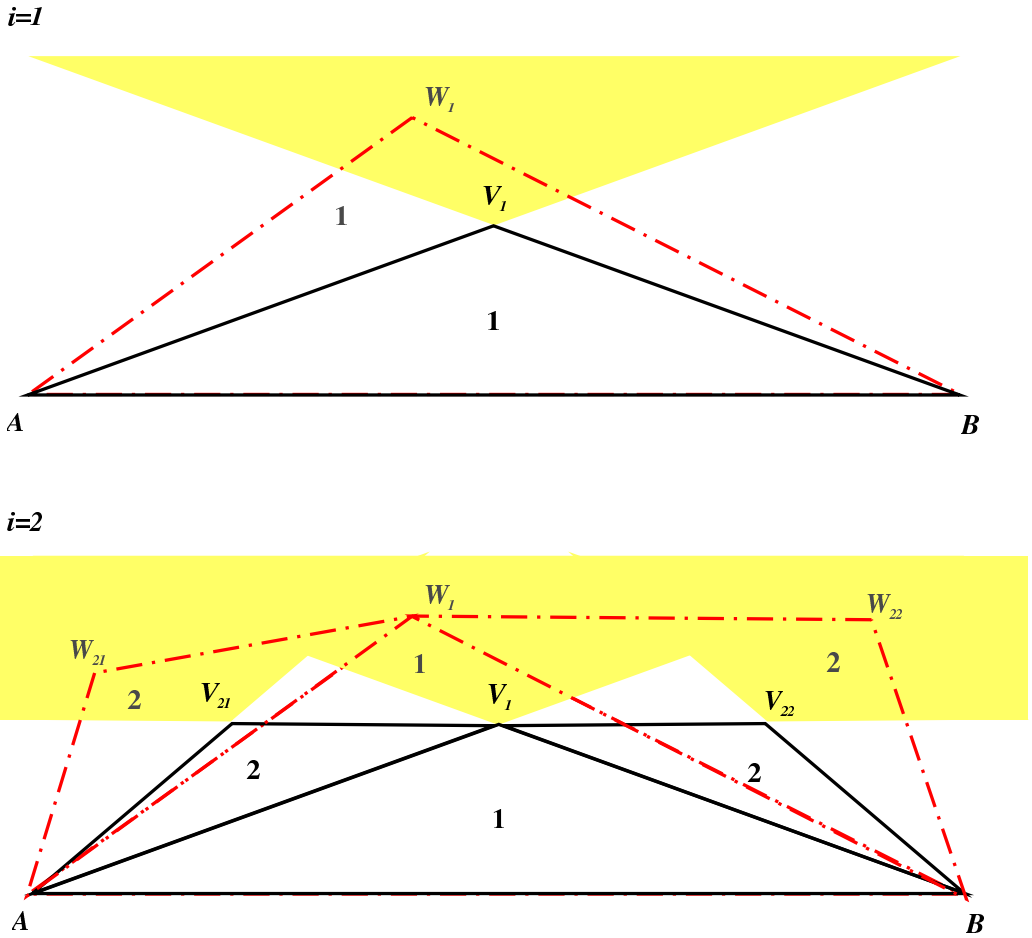


**Figure 3.5:** The part of the forbidden zone of the edge $AB$ up to $i$-th order triangles and the traced part of the triangulation $T_{AB}$ up to distance $i$ in the proof of Property 57 on page 56

For the inductive step, we have to show that if the point $X$ lies in some $(i+1)$-th order triangle, with respect to the construction of the forbidden zone of the edge $AB$, then the edge $AB$ cannot be part of any $\alpha$-triangulation of $S$. The method is the same, as for the base case, i.e., we are going to show that this leads to the violation of the angular constraint. Consider the four possible cases as per the inductive hypothesis. In case (4), we have a direct violation of the definition of triangulation, as $X$ would lie inside one of the triangles of $T_{AB}$. Thus $T_{AB}$ cannot exist. Cases (1), (2) and (3) correspond to the three situations resolved in the base case analysis. We have to consider three possibilities for $X$ - being directly connected to an edge of $T_{AB}$ (here we talk about the edge that shares points with the $(i+1)$-th order triangle in which $X$ lies), to only one of its endpoints, or not being connected to it. The violations of the angular constraints are derived in the same manner. The three possibilities correspond to the three situations presented in Figure 3.4 on page 58, in this order. It remains to note that if we go outside of the convex hull of $S$ in building the forbidden zone, the property claimed is trivially true – there are no points of $S$ inside the part of the forbidden zone that is outside the convex hull of $S$. □

Forbidden zones are used in computational geometry under different names in variety of situations, e.g., for defining different subgraphs of triangulations. They were extensively investigated in connection with MWT as a tool for rejection of edges. Here we have in mind slightly different approach. If we know that a certain triangle is in some $\alpha$-triangulation of $S$, then we can derive constraints on the positions of the other points of $S$, in other words we are guaranteed some empty space around the triangle in question.

## 3.2 Parameters of the forbidden zone

### 3.2.1 Size, shape and analytical form

In this section, we are going to describe the forbidden zone of an edge $AB$ in terms of analytical geometry. For this purpose, and for the rest of this section, we will assume that the edge $AB$ has a length of $2a$, where $a$ is a positive real number. The edge will be aligned with the $x$–axis of a two–dimensional Cartesian coordinate system in a way that its midpoint coincides with the origin $O(0,0)$. Thus the endpoints of $AB$ have coordinates $A(-a,0)$ and $B(a,0)$. We consider an angle $\alpha \leq 30°$. The reason for this further restriction on the value of $\alpha$ is the following: while the forbidden zone was described for any $\alpha \leq 60°$, in our algorithmic approach we are going to use only the values of $\alpha \leq 30°$. This will be discussed in detail at the appropriate place further in this chapter.

From the proof of Property 56 on page 55 it follows that:

**Property 58** *The forbidden zone of the edge AB properly contains the trapezoid $ABV_{R1}V_{L1}$ (see Figure 3.3 on page 57). Base angles of the trapezoid, adjacent to the side AB, are equal to $3\alpha$, and the angles adjacent to the side $V_{L1}V_{R1}$ are equal to $180^\circ - 3\alpha$. The height of the trapezoid is $(AB/2)\tan\alpha = a\tan\alpha$. Additionally, the forbidden zone of the edge AB properly contains the triangles $\triangle V_{21}V_LV_1$ and $\triangle V_1V_RV_{22}$, placed on the top of the trapezoid $ABV_{R1}V_{L1}$.*

Next, we are going to compute the coordinates of $V_L$, $V_R$, $V_{L1}$, and $V_{R1}$ under the current assumptions.

By the construction of the forbidden zone:

$$\angle BAV_1 = \angle ABV_1 = \angle V_1AV_L = \angle V_1BV_R = \angle V_LAV_{L1} = \angle V_RBV_{R1} = \angle V_{L1}V_1V_L = \angle V_{R1}V_1V_R = \alpha$$

Recalling that the midpoint of $AB$ is $O(0,0)$, the point $V_1$ is a vertex of the right triangle $\triangle OBV_1$ with $OB = a$, $\angle BOV_1 = 90^\circ$ and $\angle OBV_1 = \alpha$, therefore $OV_1 = a\tan\alpha$ and the point $V_1$ has coordinates $(0, a\tan\alpha)$. The line $V_1V_R$ has a slope of $\tan\alpha$, and using the fact that the point $V_1$ is on the line, the equation of the line is:

$$AV_R \equiv V_1V_R : y = x\tan\alpha + a\tan\alpha = (x+a)\tan\alpha$$

Analogously, the line $V_1V_L$ has a slope of $-\tan\alpha$, and using that the point $V_1$ is on the line, the equation of the line is:

$$BV_L \equiv V_1V_L : y = -x\tan\alpha + a\tan\alpha = (a-x)\tan\alpha$$

It is easy to verify the above equations by substituting the coordinates of $A$ into the equation for $V_1V_R$ and the coordinates of $B$ into the equation for $V_1V_L$.
The line $AV_L$ has a slope of $\tan 2\alpha$, and using the fact that the point $A$ lies on the line we obtain the equation:

$$AV_L : y = (x+a)\tan 2\alpha$$

Similarly, for the line $BV_R$ we obtain the equation:

$$BV_R : y = (a-x)\tan 2\alpha$$

Now we are ready to determine the coordinates of the points $V_L$ and $V_R$ by intersecting the pairs of lines $AV_L$ and $BV_L$, and $AV_R$ and $BV_R$, respectively. For example, for $V_L$ we have:

$$(x+a)\tan 2\alpha = (a-x)\tan\alpha \Leftrightarrow x(\tan\alpha + \tan 2\alpha) = a(\tan\alpha - \tan 2\alpha) \Leftrightarrow x = \frac{a(\tan\alpha - \tan 2\alpha)}{\tan\alpha + \tan 2\alpha}$$

We are going to use the following two well-known trigonometric identities:

$$\sin\theta_1\cos\theta_2 \pm \sin\theta_2\cos\theta_1 = \sin(\theta_1 \pm \theta_2)$$

to transform the fraction as follows:

$$\frac{\tan\alpha - \tan 2\alpha}{\tan\alpha + \tan 2\alpha} = \frac{(\sin\alpha\cos 2\alpha - \sin 2\alpha\cos\alpha)/(\cos\alpha\cos 2\alpha)}{(\sin\alpha\cos 2\alpha + \sin 2\alpha\cos\alpha)/(\cos\alpha\cos 2\alpha)} = \frac{\sin(-\alpha)}{\sin 3\alpha} = -\frac{\sin\alpha}{\sin 3\alpha}$$

Thus, the $x$–coordinate of the point $V_L$ is $-a\sin\alpha/\sin 3\alpha$. The $y$–coordinate of $V_L$ is found by substituting the above $x$–coordinate into one of the equations, for example:

$$y = (a - x)\tan\alpha = a\left(1 + \frac{\sin\alpha}{\sin 3\alpha}\right)\tan\alpha = \frac{a(\sin\alpha + \sin 3\alpha)\tan\alpha}{\sin 3\alpha}$$

Here, we use another well-known trigonometric formula:

$$\sin\theta_1 + \sin\theta_2 = 2\sin\frac{\theta_1 + \theta_2}{2}\cos\frac{\theta_1 - \theta_2}{2}$$

to transform the expression into:

$$\frac{a(\sin\alpha + \sin 3\alpha)\tan\alpha}{\sin 3\alpha} = \frac{2a\sin 2\alpha\cos\alpha\tan\alpha}{\sin 3\alpha} = \frac{2a\sin 2\alpha\sin\alpha}{\sin 3\alpha}$$

Finally, the coordinates of the point $V_L$ are $(-a\sin\alpha/\sin 3\alpha, 2a\sin 2\alpha\sin\alpha/\sin 3\alpha)$. Because of the symmetry with respect to the $y$–axis, the coordinates of $V_R$ are $(a\sin\alpha/\sin 3\alpha, 2a\sin 2\alpha\sin\alpha/\sin 3\alpha)$. Next, we will find the coordinates of the points $V_{21}$ and $V_{22}$. The line $V_{21}V_{22} \equiv V_{L1}V_{R1}$ is parallel to the $x$–axis and passes through the point $V_1$, therefore it has equation:

$$V_{L1}V_{R1} : y = a\tan\alpha$$

To find the $x$–coordinate of $V_{21}$, we have to substitute the above $y$ in the equation of the line $AV_L$.

$$a\tan\alpha = (x + a)\tan 2\alpha \Leftrightarrow x = \frac{a(\tan\alpha - \tan 2\alpha)}{\tan 2\alpha}$$

Developing the expression further, we get:

$$x = \frac{a(\tan\alpha - \tan 2\alpha)}{\tan 2\alpha} = \frac{a(\sin\alpha\cos 2\alpha - \cos\alpha\sin 2\alpha)}{\cos\alpha\cos 2\alpha\tan 2\alpha} = \frac{a\sin(-\alpha)}{\cos\alpha\sin 2\alpha} = -\frac{a\sin\alpha}{2\sin\alpha\cos^2\alpha} = -\frac{a}{2\cos^2\alpha}$$

Therefore the coordinates of the two points are: $V_{21}(-a/2\cos^2\alpha, a\tan\alpha)$ and symmetrically with respect to the $y$–axis $V_{22}(a/2\cos^2\alpha, a\tan\alpha)$. The equations of the non-parallel sides of the trapezoid, $AV_{L1}$ and $BV_{R1}$ are obtained similarly:

$$AV_{L1} : y = (x + a)\tan 3\alpha \qquad BV_{R1} : y = (a - x)\tan 3\alpha$$

From these two equations, taking into account that both $V_{L1}$ and $V_{R1}$ have an $y$–coordinate of $a\tan\alpha$ we can determine their $x$–coordinates, for $V_{L1}$ we have:

$$a\tan\alpha = (x + a)\tan 3\alpha \Leftrightarrow x = \frac{a(\tan\alpha - \tan 3\alpha)}{\tan 3\alpha} = \frac{a(\sin\alpha\cos 3\alpha - \cos\alpha\sin 3\alpha)}{\cos\alpha\cos 3\alpha\tan 3\alpha}$$

Further development yields:

$$x = \frac{a\sin(-2\alpha)}{\cos\alpha\sin 3\alpha} = -\frac{2a\sin\alpha}{\sin 3\alpha}$$

The coordinates are: $V_{L1}(-2a\sin\alpha/\sin 3\alpha, a\tan\alpha)$ and $V_{R1}(2a\sin\alpha/\sin 3\alpha, a\tan\alpha)$. It is interesting to note that the $x$–coordinate of $V_{L1}$ is exactly twice the $x$–coordinate of $V_L$.

In our further considerations we are going to use the part of the forbidden zone consisting of the trapezoid $ABV_{R1}V_{L1}$ and the two triangles $\triangle V_{21}V_1V_L$ and $\triangle V_1V_{22}V_R$. It is useful to describe analytically the boundary of this region. We denote the boundary by $B(x)$.

$$B(x) = \begin{cases} (x+a)\tan 3\alpha & \text{for } -a \le x \le -2a\sin\alpha/\sin 3\alpha \text{ (the segment } AV_{L1}) \\ a\tan\alpha & \text{for } -2a\sin\alpha/\sin 3\alpha \le x \le -a/2\cos^2\alpha \text{ (the segment } V_{L1}V_{21}) \\ (x+a)\tan 2\alpha & \text{for } -a/2\cos^2\alpha \le x \le -a\sin\alpha/\sin 3\alpha \text{ (the segment } V_{21}V_L) \\ (a-x)\tan\alpha & \text{for } -a\sin\alpha/\sin 3\alpha \le x \le 0 \text{ (the segment } V_LV_1) \\ (x+a)\tan\alpha & \text{for } 0 \le x \le a\sin\alpha/\sin 3\alpha \text{ (the segment } V_1V_R) \\ (a-x)\tan 2\alpha & \text{for } a\sin\alpha/\sin 3\alpha \le x \le a/2\cos^2\alpha \text{ (the segment } V_RV_{22}) \\ a\tan\alpha & \text{for } a/2\cos^2\alpha \le x \le 2a\sin\alpha/\sin 3\alpha \text{ (the segment } V_{22}V_{R1}) \\ (a-x)\tan 3\alpha & \text{for } 2a\sin\alpha/\sin 3\alpha \le x \le a \text{ (the segment } V_{R1}B) \end{cases} \tag{3.1}$$

**Corollary 59** *For $\alpha = 30°$, the forbidden zone of the edge $AB = 2a$ includes the rectangle $ABV_{R1}V_{L1}$ with height $a/\sqrt{3}$. On top of this rectangle the forbidden zone includes two right triangles $\triangle V_{21}V_LV_1$ and $\triangle V_1V_RV_{22}$ with bases of $\frac{2a}{3}$ and angles of $30°$ at $V_1$. Refer to Figure 3.6.*

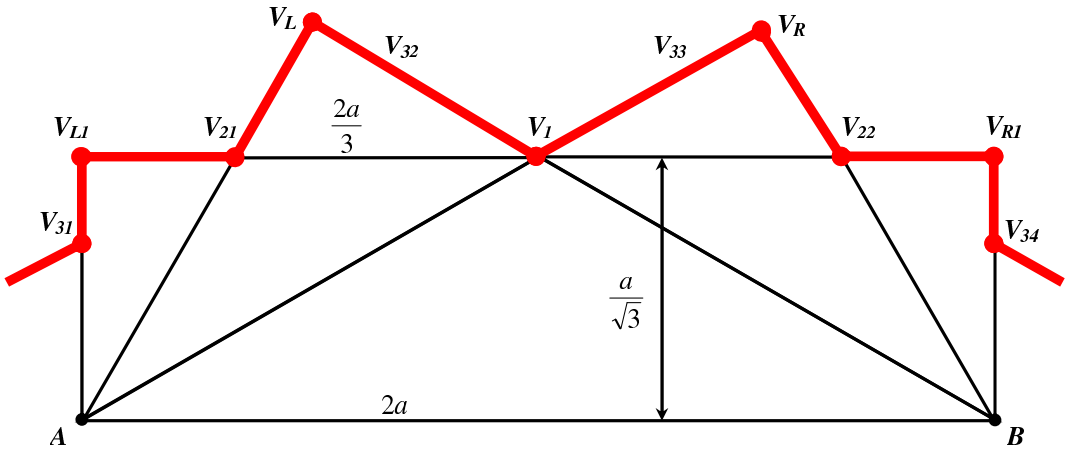


**Figure 3.6:** Parameters of the forbidden zone of the edge $AB = 2a$ for $\alpha = 30°$

We are going to use the $30°$ forbidden zone in the proof of Lemma 72 on page 74, therefore we rewrite the analytical form of its boundary (the rectangle and two triangles part) for $\alpha = 30°$. Note that in this case the segments $AV_{L1}$ and $V_{R1}B$ are vertical, and thus vanish from the expression

for the boundary. Trivially they have the equations:

$$AV_{L1} : x = -a \qquad V_{R1}B : x = a$$

The boundary is given by:

$$B(x) = \begin{cases} a/\sqrt{3} & \text{for } -a \le x \le -2a/3 \text{ (the segment } V_{L1}V_{21}) \\ \sqrt{3}(x+a) & \text{for } -2a/3 \le x \le -a/2 \text{ (the segment } V_{21}V_L) \\ (a-x)/\sqrt{3} & \text{for } -a/2 \le x \le 0 \text{ (the segment } V_LV_1) \\ (x+a)/\sqrt{3} & \text{for } 0 \le x \le a/2 \text{ (the segment } V_1V_R) \\ \sqrt{3}(a-x) & \text{for } a/2 \le x \le 2a/3 \text{ (the segment } V_RV_{22}) \\ a/\sqrt{3} & \text{for } 2a/3 \le x \le a \text{ (the segment } V_{22}V_{R1}) \end{cases}$$

We mentioned several times that the boundary of the forbidden zone will intersect the line $AB$ outside of the segment $AB$. It is interesting to know exactly when this is going to happen, that is for what value of $i$ does the boundary of the free wedge of the leftmost (or the rightmost) $i$-th order triangle intersect the line $AB$. This depends on the value of $\alpha$. Denote by $n_\alpha$ the number with the property that $n_\alpha \cdot \alpha \ge 180°$, but $(n_\alpha - 1)\alpha < 180°$. Therefore $n_\alpha$ is the smallest number of angles $\alpha$ that are necessary to fill but not exceed an angle of 180°. In our considerations of matching triangles it is also important to know how many angles of magnitude $\alpha$ are enough to fill a right angle, we denote this number by $n_1$. Of course this number is equal to the half of $n_\alpha$ when $n_\alpha$ is even and to the half of $n_\alpha + 1$, otherwise. Explicitly:

$$n_\alpha = \left\lceil \frac{180°}{\alpha} \right\rceil \qquad n_1 = \left\lfloor \frac{n_\alpha + 1}{2} \right\rfloor$$

Note that in an $i$-th order triangle, the lengths of each of the two equal sides are equal to the length of the base multiplied by a factor of $1/2\cos\alpha$. Thus $d_i$ the length of the side of the $i$-th order triangle is:

$$d_i = \frac{AB}{2^i \cos^i \alpha}$$

This parameter is also important for our future considerations as it represents the distance from the endpoints of the segment $AB$ to the parts of the forbidden zone that lie outside of the trapezoid near the intersection with the line $AB$. It is easy to see that the point of intersection of the boundary of the forbidden zone is at a distance $d^*$ which satisfies the inequality

$$d_{n_\alpha} \le d^* \le d_{n_\alpha + 1}$$

### 3.2.2 Transformations of the forbidden zone

Here we are going to study and describe the properties of the forbidden zone of the edge $AB$ under various planar transformations such as extension of the base edge, contraction of the base edge, and rotation about one of the endpoints.

**Corollary 60** *If a segment $A'B'$ properly contains another segment $AB$ then the forbidden zone of $A'B'$ properly contains the forbidden zone of $AB$.*

**Proof.** To begin we show the containment of the trapezoid and the two top triangles.
From the analytical geometry approach taken in previous subsection 3.2.1, we can use Equation 3.1 on page 64 which describes the boundary of the forbidden zone of a segment of length $2a$ with respect to a point that is at a distance $x$ from the midpoint of that segment. Now, consider extension of the segment to the right by a length of $2h$, where $h$ is a positive real number. This means that the new coordinates of the midpoint $O'$ are $(0, h)$ and the length of the segment has changed, so its half length is now $a + h$ instead of $a$. Note that the coordinate system is relative to the new midpoint $O'$. Thus if we want to return to the original coordinate system centered at $O$ – the midpoint of $AB$ we need to translate it back by $h$ units, which corresponds in analytical form to the substitution:

$$\{a \leftarrow a + h, x \leftarrow x - h\}$$

It can now be verified by Equation 3.1 on page 64 that each point that was in the forbidden zone of the original segment is also in the forbidden zone of the extended segment.
We can also use our knowledge of the geometry of the forbidden zone to see that the described extension of the segment results in the following: the left endpoint $A \equiv A'$ stays the same, so do the lines $AV_1$, $AV_L$ and $AV_{L1}$. The points $V_1'$, $V_L'$ and $V_{L1}'$ move along these lines farther from $A$. The point $B'$ is strictly to the right of $B$, therefore the lines $B'V_1'$, $B'V_R'$ and $B'V_{R1}'$ are parallel to $BV_1$, $BV_R$ and $BV_{R1}$, respectively and strictly to the right of them. Hence, the claimed containment of the forbidden zones.
Similarly, an extension of the segment to the left by a length of $2h$ is equivalent to the substitution:

$$\{a \leftarrow a + h, x \leftarrow x + h\}$$

Again, Equation 3.1 on page 64 verifies that any point that was in the forbidden zone of the segment before its extension is still in the forbidden zone after the extension. Figure 3.7 on the following page presents an illustration.

To complete the proof we must mention that the larger segment $A'B'$ can be obtained by its proper part $AB$ by two extensions – one to the right and one to the left, by appropriate lengths (not necessarily equal). Each of these extensions was shown to have the claimed property.
So far we have only proven the containment of the parts of the forbidden zones that we are using in our considerations – the trapezoid and the two top triangles. However, it is easy to see how the proof can be generalized to include the other parts of the forbidden zone. One way to see this is by using the boundary chain representation of the forbidden zone. As all the vertices along the chain are defined by intersection of lines from $A$ and $B$, when the edge is extended, say to the

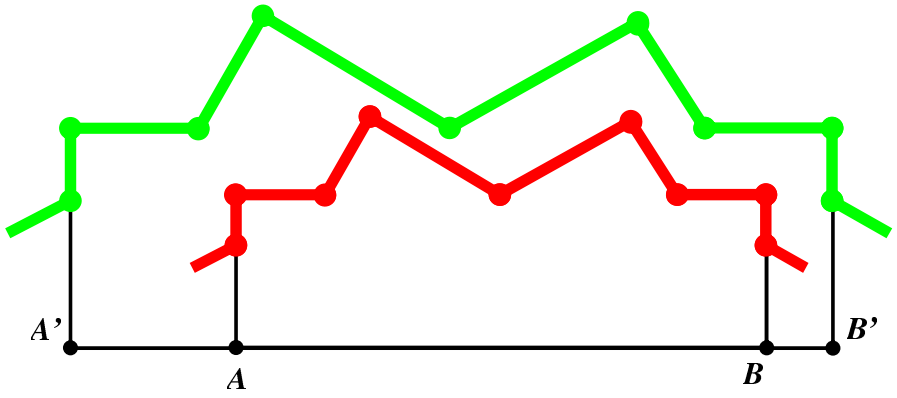


**Figure 3.7:** Segments $AB$ and $A'B'$ and their respective forbidden zone boundaries

right (outwards from $B$), all the vertices of the new chain will move outwards on their respective lines relative to their previous positions. As a result the boundary segments will alternatingly slide outwards or move outwards parallel to themselves. To conclude the argument we have to use the fact that the forbidden zone is monotone in the $y$-coordinate direction. This is true whenever $\alpha \leq 30°$. The $y$-monotonicity of the trapezoidal part can be derived directly from its analytical expression. For the outside parts we can use the fact that they correspond to trapezoidal parts of higher order edges. □

Note that the contrapositive of the statement of Corollary 60 is also useful. If we shrink an edge, as opposed to extending it, all the points that were outside of the forbidden zone of the original edge remain outside of the forbidden zone of the shorter edge.

Before we consider the rotation of the entire forbidden zone resulting from a rotation of the base edge about one of its endpoints, we are going to consider a simpler case. Let triangle $\triangle ABX$ be such that the angle at $B$, $\angle ABX = \alpha$ is acute. Consider a clockwise rotation of $\triangle ABX$ about $B$ at an angle $0 < \varphi < \alpha$. We are interested in the relative position of the points from the interior of $\triangle ABX$ relative to the interior of the triangle $\triangle A'BX'$ – the image of $\triangle ABX$ under the described rotation. This is the subject of the next lemma.

**Lemma 61** *Given a triangle $\triangle ABX$ with an acute angle at $B$, $\angle ABX = \alpha$, a rotation of $\triangle ABX$ about $B$ in clockwise direction at an angle $0 < \varphi < \alpha$ will keep the points of the interior of $\triangle ABX$ in the interior of the rotated triangle $\triangle A'BX'$ or on the other side of the segment $BA'$ when the angle at $X$, $\angle AXB$, is non–acute.*

**Proof.** To prove this lemma we need to use the property of a circle stating that a line perpendicular to the diameter at its endpoint is tangent to the circle (i.e., it has only one point in common

with the circle), and any other line that forms a smaller than the right angle with the diameter at its endpoint intersects the circle on the same side where the acute angle is formed. Amazingly, this proposition appears in Book III of Euclid's *"Elements"* [27].

Please refer to Figure 3.8 on the next page. Because of the fact that $\angle AXB$ is not acute, the point $A$ lies outside of the circle centered at $B$ with a radius of $BX$. We are going to prove first that the point $X$ lies inside the rotated triangle $\triangle A'BX'$. To see that this is true consider the position of the segment $BX$. It forms an angle of $\varphi$ with its image $BX'$, therefore it lies in the interior of the angle $\angle A'X'B$. Moreover, $X$ and $X'$ are on the circle by construction and $A'$ is outside of the circle as is the entire segment $A'X'$ according to Euclid's above mentioned proposition. This means that the extension of the segment $BX$ intersects $A'X'$, which establishes our claim. Also note that the point $A$ lies below the line $A'B$ by the properties of the rotation. Thus, the side $AX$ intersects the side $A'B$ at a point $U$, which is internal for both segments. Therefore, the triangle $\triangle UBX$ is contained in the interior of $\triangle A'BX'$, and the rest, triangle $\triangle AUB$ is on the other side of the segment $BA'$. It is easy to construct a counterexample for the case when $\angle AXB$ is acute. We need to use again Euclid's proposition and based on the fact that $AX$ intersects the circle, position $X'$ (i.e. choose $\varphi$) so that $X$ is not inside $\triangle A'BX'$, i.e. the segment $BX$ properly intersects the segment $A'X'$. □

**Corollary 62** *Consider a rotation of the segment $AB$ in a clockwise direction about the point $B$ at an angle $0° < \varphi < 180°$. Let the image of $A$ under this rotation be $A'$. For $\alpha \leq 25°$, all the points of the forbidden zone of $AB$ lying to the right (in the same half–plane as point $B$) of the line $AV_{L1}$ are either inside the forbidden zone of $A'B$ or on the other side of the segment $A'B$. When $\alpha > 25°$, the same property is guaranteed for the part of the forbidden zone that lies to the right (in the same half–plane as point $B$) of the line $AV_L$.*

**Proof.** First we will establish the claim for the trapezoidal part plus the two triangles on top of it. We are going to triangulate this part of the forbidden zone, using triangles incident to $B$ and use the result of Lemma 61 on the preceding page. One way to triangulate is to consider the triangles $\triangle AV_LB$, $\triangle V_1V_RB$, and $\triangle V_{22}V_{R1}B$. Together they form the part of the forbidden zone lying to the right of the line $AV_L$. Given that $\angle AV_LB = \angle V_1V_RB = \angle V_{22}V_RB = 180° - 3\alpha$ and that $180° - 3\alpha \geq 90°$ for $\alpha \leq 30°$, we can directly use the previous lemma and conclude that the points inside the described part of the forbidden zone of $AB$ will either remain inside the forbidden zone of $A'B$ or fall below the line $A'B$.
Under certain conditions, the entire forbidden zone may have this property. To see this, we need to use a different triangulation. This time it includes the triangles $\triangle AV_{L1}B$, $\triangle V_{L1}V_{21}B$, $\triangle V_{21}V_LB$, $\triangle V_1V_RB$, and $\triangle V_{22}V_{R1}B$. The last two triangles were shown to have the necessary property for

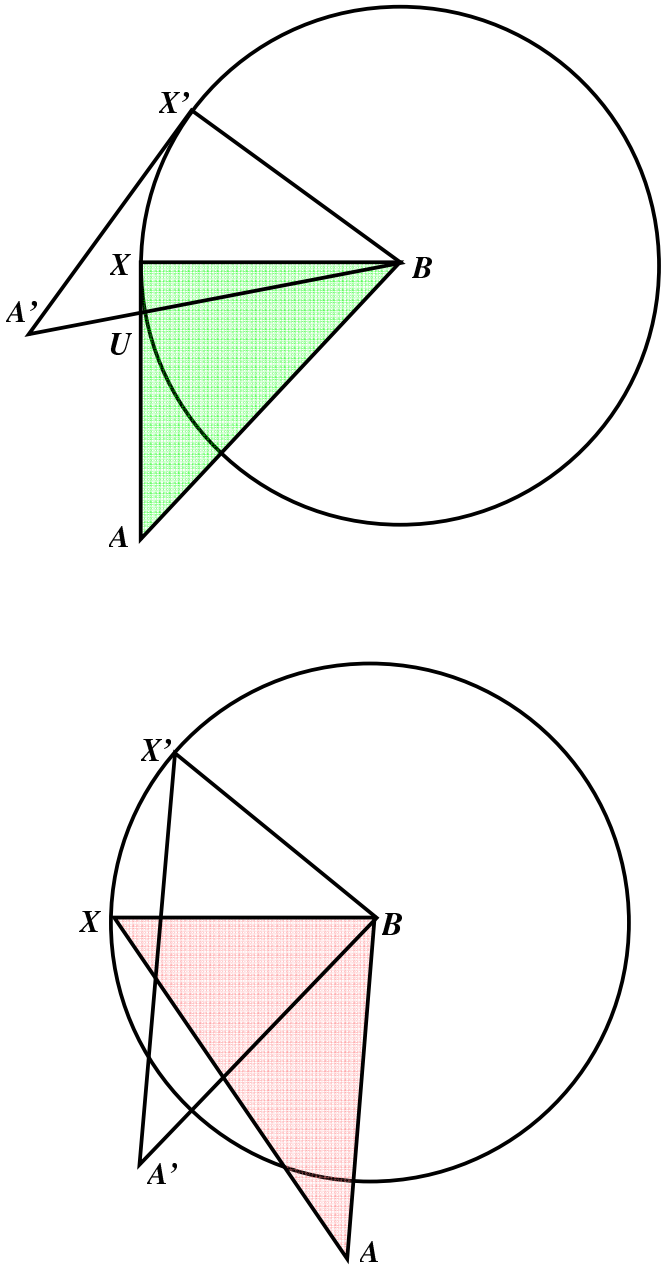


**Figure 3.8:** Lemma 61 on page 67. Top: $\angle AXB \geq 90°$, Bottom: $\angle AXB < 90°$

any value of $\alpha$. The triangles $\triangle V_{L1}V_{21}B$ and $\triangle V_{21}V_LB$ have angles, respectively, $\angle V_{L1}V_{21}B = 180^\circ - \angle V_1V_{21}B = 180^\circ - \angle V_{21}BA$ and $\angle V_{21}V_LB = 180^\circ - 3\alpha$. But $\angle V_{21}BA < \angle V_1BA = \alpha$, it follows then that $\angle V_{L1}V_{21}B > 180^\circ - \alpha > 150^\circ$. Thus, the two triangles satisfy the premises of Lemma 61 on page 67. The only triangle remaining to consider is $\triangle AV_{L1}B$. Its angle $\angle AV_{L1}B$ is not guaranteed to be right or obtuse. Numerical calculations show that the measure decreases with the increase of $\alpha$ over the interval $[0^\circ, 30^\circ]$. At a value of approximately $25.2987058^\circ$ this angle becomes acute. Therefore, for all the values of $\alpha \in [0^\circ, 25^\circ]$, the premises of Lemma 61 on page 67 are satisfied and the trapezoidal part of the forbidden zone plus the two top triangles has the claimed rotational property. Using the same argument as in the proof of Corollary 60 on page 66, i.e., the fact that the parts of the forbidden zone, outside of the trapezoid plus the two triangles on top, are trapezoidal parts of higher order edges, we can verify the claim of this corollary. For the entire part of the forbidden zone surrounding the point $B$, we can claim the containment property, regardless of the value of $\varphi$. This is true because this part of the forbidden zone is tiled by triangles adjacent to $B$ and having top angles of $180^\circ - 3\alpha$, in fact connecting $B$ to all convex vertices on the right part of the boundary chain will generate the desired triangulation. It is also clear from the approach taken in this proof that in the vicinity of $A$, we will have smaller angles as we connect $B$ to the chain vertices of higher order close to $A$. Thus, we cannot claim that entire part of the forbidden zone there will have this rotational property. Depending on the value of $\alpha$ the coverage will vary. □

Here the contrapositive of the statement of Corollary 62 on page 68 is also meaningful. If we rotate an edge, in counterclockwise direction about one of its endpoints, all the points that were outside of the forbidden zone of the original edge remain outside of the forbidden zone of the rotated edge.

The transformational properties of the forbidden zone established in this subsection are going to be useful in the case analysis carried out in the subsequent sections.

## 3.3 Subgraphs of the Delaunay triangulation

**Definition 63** *For a given planar set of points $S$, the **minimum spanning tree** is defined as the straight edge tree connecting all the points in $S$ and having minimum total edge length amongst all spanning trees of $S$. We denote the minimum spanning tree of $S$ by $MST(S)$.*

**Definition 64** *For a given planar set of points $S$, the **relative neighbourhood graph** of $S$, denoted by $RNG(S)$ consists of all edges $AB$, where $A, B \in S$, such that there is no point $X$ from $S$ such that $XA < AB$ and $XB < AB$. In other words, there is no point of $S$ that is closer to both $A$ and $B$ than they are to each other.*

This definition is equivalent to saying that the region formed by the intersection of the circles with radii $|AB|$ centered at $A$ and $B$ is empty of points of $S$. This region is known in the literature as a **lune** of the edge $AB$. The lune is illustrated in Figure 3.9.

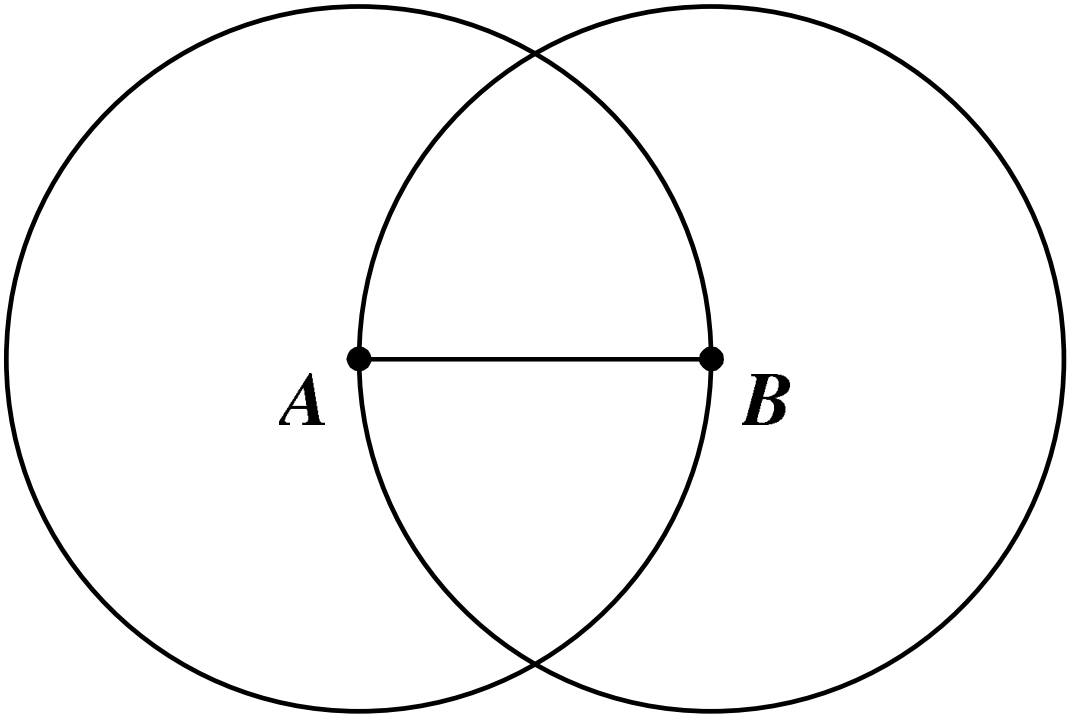


**Figure 3.9:** The construction of the lune of the edge $AB$

**Corollary 65 ([36])** *Every edge of $MST(S)$ is an edge of $RNG(S)$.*

**Proof.** To see the validity of the claim, assume that there is some point $X$ of $S$ in the lune of an edge $AB$ of $MST(S)$. $X$ cannot be connected to both $A$ and $B$ in the $MST(S)$ because it will form a cycle in $MST(S)$, which is a tree, i.e. has no cycles. Therefore we can replace $AB$ with a shorter edge - $XA$ or $XB$, thus obtaining a spanning tree of smaller overall length. □

**Definition 66** *For a given planar set of points $S$, the **Gabriel graph** of $S$, denoted by $GG(S)$ consists of all edges $AB$, where $A, B \in S$, such that there is no point from $S$ in the circle with diameter $AB$.*

**Corollary 67** *Every edge of $RNG(S)$ is an edge of $GG(S)$.*

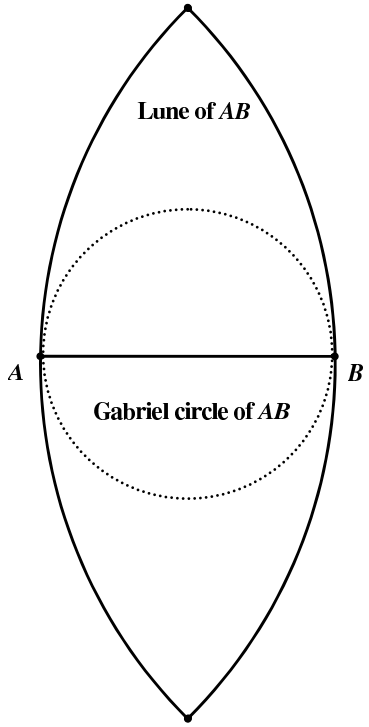


**Figure 3.10:** The lune and the Gabriel circle of the edge $AB$

**Proof.** The lune of an edge properly includes the circle with a diameter this edge as shown in Figure 3.10. Thus, if the lune of an edge is empty of points of $S$, so will be the circle defining the Gabriel graph for this edge. □

**Corollary 68** *Every edge of $GG(S)$ is an edge of $DT(S)$, where $DT(S)$ denotes the Delaunay triangulation of $S$ considered as a graph.*

**Proof.** It is one of the properties of the Delaunay triangulation, not mentioned earlier, that an edge is a Delaunay edge if and only if there exists a circle passing through its endpoints that does not enclose any other point from $S$. If an edge is a Gabriel edge, by its definition such a circle exists, therefore it is also a Delaunay edge. □

Thus, we have established the following important relationship between the subgraphs of the Delaunay triangulation.

**Property 69 ([48])** *For a planar point set $S$:*

$$MST(S) \subseteq RNG(S) \subseteq GG(S) \subseteq DT(S)$$

**Corollary 70 ([48])** *Given a planar point set $S$, the graphs $MST(S)$, $RNG(S)$, $GG(S)$, and $DT(S)$ are all planar and connected.*

**Proof.** The planarity of the four graphs follows from the planarity of the Delaunay triangulation, $DT(S)$, which is a supergraph of the other three. The connectedness follows from the connectedness of the minimum spanning tree, $MST(S)$, which is a subgraph of the other three. □

It is important to mention that all four graphs can be computed within $O(n \log n)$ time and $O(n)$ space [19].

Corollary 70 has two important implications. First, because of the connectedness of these subgraphs of the Delaunay triangulation, it is enough to establish that any of them is a part of an optimal triangulation, in order to claim polynomial time computability of the same. In fact, a connected graph, spanning the point set $S$, together with its convex hull edges will subdivide the interior of the convex hull into disjoint simple polygons whose union is exactly the convex hull of $S$. Second, because of the planarity, all the subgraphs of the Delaunay triangulation have linear complexity (linear number of edges with respect to the size of the point set). Therefore, there will be a linear number of regions in the subdivision, as each internal edge can be part of at most two simple polygon boundaries. A major consequence of this is the applicability of the Klincsek's algorithm to finding the optimal triangulation with respect to the quality measure considered. As each of the diagonals considered in the Klincsek's algorithm will be considered at most once, and each of the polygons has linear (in $n$, the size of $S$) number of vertices, the optimal triangulation will be computed within $O(n^3)$ time and $O(n^2)$ space. Our algorithmic approach will exploit this result, as in certain cases the relative neighbourhood graph will be part of our approximating triangulation as proven in Theorem 74 on page 78.

Before proving Theorem 74 on page 78, we recall another of Tan's results in [54] that is important to this particular setting.

**Corollary 71** *The relative neighbourhood graph, $RNG(S)$, of a point set $S$ subdivides the convex hull of the point set into a linear number of interior disjoint simple polygons. Each of these polygons contains at most one edge of the convex hull of $S$.*

As it was mentioned at the beginning of the chapter, we intend to develop good approximation algorithms for the MaxMin and MinMax area of a general point set. Our approach relies on the following observation: the RNG is a part of every 30°-triangulation. We are going to show that the RNG is a part of every 30°-triangulation by showing that the forbidden zone of any possible edge that could intersect a given edge $AB$ of the RNG contains at least one of the points $A$ or $B$ in its interior. Thus, in an 30°-triangulation, if such exists, the RNG edges cannot be intersected by other legal edges.

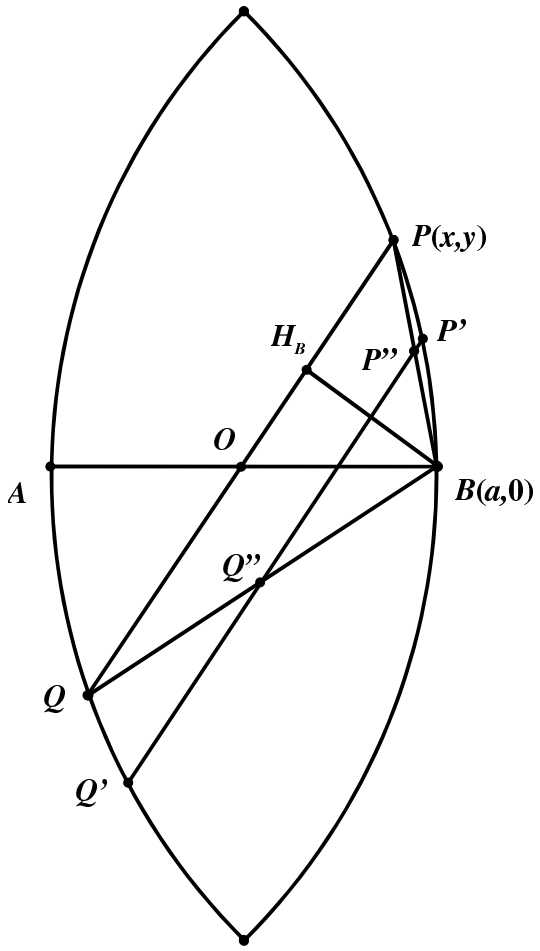


**Figure 3.11:** Edges $PQ$ and $P'Q'$ intersecting the RNG edge $AB$ in Lemma 72 and Lemma 73 on page 77

Keeping the assumptions of the previous section, let us denote the midpoint of the considered edge $AB$ by $O$. Further, let us place the edge $AB$ on the $x$-axis of a coordinate system with an origin in its midpoint $O$. The points $A$ and $B$ have coordinates $(-a, 0)$ and $(a, 0)$, respectively, where $a$ is a positive real number.

**Lemma 72** *Let $PQ$ be a segment that goes through $O$ such that the points $P$ and $Q$ are on the boundary of the lune of $AB$. Then the point $B$ is in the $30°$-forbidden zone of the segment $PQ$.*

**Proof.** Without loss of generality we can assume that the point $P$ lies in quadrant I. Given $P(x, y)$, denote the orthogonal projection of the point $B$ onto the segment $PQ$ by $H_B$. Please, refer to Figure 3.11.

The idea is to compute the distance $BH_B$ and the depth of the forbidden zone of $PQ$ at $H_B$ and show that the first is less than or equal to the second quantity, thus establishing the claim. First, note that the point $O$ is in fact the midpoint of $PQ$, because of the central symmetry. It is easy to see that $H_B$ is a point that lies in the interior of the segment $OP$: the angles of triangle $\triangle OBP$ are all acute and $BH_B$ is an altitude in this triangle. Also remember that we are using a 30° forbidden zone, thus $\alpha = 30°$, $\sin\alpha = 1/2, \cos\alpha = \sqrt{3}/2, \tan\alpha = 1/\sqrt{3}$. Denote the distance between $O$ and $P$ by $p$, and the distance between $O$ and $H_B$ by $d$. We can write the depth $B(d)$ of the forbidden zone of the segment $PQ$ as a function of $d$ and $p$ as follows:

$$B(d) = \begin{cases} (p+d)/\sqrt{3} & \text{for } 0 \le d \le p/2 \\ \sqrt{3}(p-d) & \text{for } p/2 \le d \le 2p/3 \\ p/\sqrt{3} & \text{for } 2p/3 \le d \le p \end{cases} \tag{3.2}$$

The point $P$ lies on the circle centered at $A(-a, 0)$ with a radius of $2a$, the equation of this circle is, therefore, $(x+a)^2 + y^2 = 4a^2$. Solving for $y$ we have:

$$y^2 = 4a^2 - x^2 - 2ax - a^2 = 3a^2 - 2ax - x^2 = (3a+x)(a-x)$$

taking into account that $y$ has a non–negative value because of our choice of $P$, and so do $3a + x$ and $a - x$, we can take a square root of both sides of the above equation and express $y$ as a function of $x$ and $a$ as follows:

$$y = \sqrt{(3a+x)(a-x)}$$

Further, for the length of $OP$, as a function of $x$ and $a$ we have:

$$OP = \sqrt{x^2 + y^2} = \sqrt{3a^2 - 2ax} = \sqrt{a(3a-2x)} = p$$

Again, note that $3a - 2x$ is a strictly positive term. Now we can obtain the length of $BH_B$ as a function of $x$ and $a$ by expressing the area of $\triangle OBP$ in two different ways. Namely:

$$A_{\triangle OBP} = \frac{OB \cdot y}{2}, A_{\triangle OBP} = \frac{OP \cdot BH_B}{2}$$

These equalities give:

$$\frac{OB \cdot y}{2} = \frac{OP \cdot BH_B}{2} \Leftrightarrow BH_B = \frac{OB \cdot y}{OP} = \frac{a\sqrt{(3a+x)(a-x)}}{\sqrt{a(3a-2x)}} = \sqrt{\frac{a(3a+x)(a-x)}{3a-2x}}$$

Finally, for the length of $OH_B$ as a function of $x$ and $a$ we have:

$$OH_B = OB \cdot \cos\angle BOP = \frac{OB \cdot x}{OP} = \frac{ax}{\sqrt{a(3a-2x)}} = \sqrt{\frac{a}{3a-2x}} \cdot x = d$$

We have to verify, therefore, that $BH_B \le B(d)$ for all values of $x$ and $a$. Strictly speaking, there is only one variable here, $x$, as $a$ is a parameter. This is rather lengthy, but only involves basic

mathematics.

The first possibility for $d$ according to Equation 3.2 on the previous page is $0 \leq d \leq p/2$. The right part of this double inequality, $d \leq p/2$ is equivalent to:

$$\sqrt{\frac{a}{3a-2x}} \cdot x \leq \frac{1}{2}\sqrt{a(3a-2x)} \Leftrightarrow 2x \leq 3a - 2x \Leftrightarrow x \leq \frac{3}{4}a$$

Note that $d \geq 0$ is always true for $0 \leq x \leq a$. Thus, we have to check that for $x \in [0, \frac{3}{4}a]$ the inequality $BH_B \leq (p+d)/\sqrt{3}$ holds. This is equivalent to:

$$\sqrt{\frac{a(3a+x)(a-x)}{3a-2x}} \leq \frac{1}{\sqrt{3}}\left(\sqrt{a(3a-2x)} + \sqrt{\frac{a}{3a-2x}} \cdot x\right)$$

We can divide both sides by the common factor $\sqrt{a}$, which is non–zero, followed by the multiplication of both sides by the (non–zero) factor of $\sqrt{3(3a-2x)}$, the result is:

$$\sqrt{3(3a+x)(a-x)} \leq 3a - x$$

Taking into account the fact that $3a - x > 0$, we can square both sides and obtain:

$$3(3a+x)(a-x) \leq (3a-x)^2 \Leftrightarrow 9a^2 - 6ax - 3x^2 \leq 9a^2 - 6ax + x^2 \Leftrightarrow 4x^2 \geq 0$$

Consequently, for all $x \in [0, \frac{3}{4}a]$ the point $B$ is in the forbidden zone of the segment $PQ$. The second possibility for $d$ according to Equation 3.2 on the preceding page is $p/2 \leq d \leq 2p/3$. The right part of this double inequality, $d \leq 2p/3$, is equivalent to:

$$\sqrt{\frac{a}{3a-2x}} \cdot x \leq \frac{2}{3}\sqrt{a(3a-2x)} \Leftrightarrow 3x \leq 2(3a-2x) \Leftrightarrow 7x \leq 6a \Leftrightarrow x \leq \frac{6}{7}a$$

Note that according to our previous case calculations $p/2 \geq d$ is equivalent to $x \geq \frac{3}{4}a$. Thus, we have to check that for $x \in [\frac{3}{4}a, \frac{6}{7}a]$ the inequality $BH_B \leq \sqrt{3}(p-d)$ holds. This is equivalent to:

$$\sqrt{\frac{a(3a+x)(a-x)}{3a-2x}} \leq \sqrt{3}\left(\sqrt{a(3a-2x)} - \sqrt{\frac{a}{3a-2x}} \cdot x\right)$$

We are going to divide both sides by the common factor $\sqrt{a}$, which is non–zero, and then multiply both sides by the (non–zero) factor of $\sqrt{(3a-2x)}$, the result is:

$$\sqrt{(3a+x)(a-x)} \leq 3\sqrt{3}(a-x)$$

Taking into account the fact that $a - x > 0$, we can square both sides and obtain:

$$(3a+x)(a-x) \leq 27(a-x)^2$$

Further, we can divide by $a - x$, which gives us:

$$3a + x \leq 27(a-x) \Leftrightarrow 3a + x \leq 27a - 27x \Leftrightarrow 28x \leq 24a \Leftrightarrow x \leq \frac{6}{7}a$$

Consequently, for all $x \in [\frac{3}{4}a, \frac{6}{7}a]$ the point $B$ is in the forbidden zone of the segment $PQ$. The third and final possibility for $d$, according to Equation 3.2 on page 75, is $2p/3 \leq d \leq p$. The right part of this double inequality, $d \leq p$, is equivalent to:

$$\sqrt{\frac{a}{3a-2x}} \cdot x \leq \sqrt{a(3a-2x)} \Leftrightarrow x \leq 3a - 2x \Leftrightarrow 3x \leq 3a \Leftrightarrow x \leq a$$

which was assumed to be true. Note that according to our previous case calculations $d \geq 2p/3$ is equivalent to $x \geq \frac{6}{7}a$. Thus, we have to check that for $x \in [\frac{6}{7}a, a]$ the inequality $BH_B \leq p/\sqrt{3}$ holds. This is equivalent to:

$$\sqrt{\frac{a(3a+x)(a-x)}{3a-2x}} \leq \frac{1}{\sqrt{3}}\sqrt{a(3a-2x)}$$

We are going to divide both sides by the common factor $\sqrt{a}$, which is non–zero, and then multiply both sides by the (non–zero) factor of $\sqrt{3(3a-2x)}$, the result is:

$$\sqrt{3(3a+x)(a-x)} \leq (3a-2x)$$

Given the fact that both sides of the inequality are positive, we are going to square them, obtaining:

$$3(3a+x)(a-x) \leq (3a-2x)^2 \Leftrightarrow 9a^2 - 6ax - 3x^2 \leq 9a^2 - 12ax + 4x^2 \Leftrightarrow 6ax \leq 7x^2 \Leftrightarrow \frac{6}{7}a \leq x$$

Consequently, for all $x \in [\frac{6}{7}a, a]$ the point $B$ is in the forbidden zone of the segment $PQ$.
This completes the proof. □

The result of this lemma was suggested by computational experiments done by my supervisor using the software package *Cinderella*©.

Further, we have to consider the edges that cross $AB$ and do not pass through its midpoint $O$.

**Lemma 73** *Let $P'Q'$ be a segment such that the points $P'$ and $Q'$ are on the boundary of the lune of $AB$. Let $P'Q'$ intersect $AB$ at a point $R$ such that $R$ is between $O$ and $B$. Then the point $B$ is in the forbidden zone of the segment $P'Q'$.*

**Proof.** As in the proof of Lemma 72 on page 74, assume that the point $P'$ is in quadrant I. Further, let $PQ$ be a segment parallel to the edge $P'Q'$, such that $PQ$ contains $O$ with $P$ and $Q$ on the boundary of the lune. The situation is illustrated in Figure 3.11 on page 74. The segment $BP$ lies entirely inside the lune of $AB$. Thus, $BP$ intersects $P'Q'$ in an internal point, which we denote by $P''$. Similarly, if we construct the segment $BQ$ it will intersect $P'Q'$ at an internal point which we denote by $Q''$. By construction $\triangle PBQ \sim \triangle P''BQ''$ because of the fact that $PQ$ and $P''Q''$ are parallel. Because of the similarity of the two triangles and the scaling property the fact that $B$ is in the forbidden zone of $PQ$ (established in Lemma 72 on page 74) implies that $B$ is also in the forbidden zone of $P''Q''$. Thus, we have two segments, namely $P''Q''$ and $P'Q'$ that satisfy the

premises of Corollary 60 on page 66. We conclude that $B$ is in the forbidden zone of the edge $P'Q'$. Since any edge crossing $AB$ is parallel to an edge crossing $AB$ and going through its midpoint, the claim of this lemma is established. □

**Theorem 74** *Given a planar set of points $S$, the relative neighbourhood graph of $S$ is part of every 30°-triangulation (if such a triangulation exists).*

**Proof.** It is evident form Lemma 72 on page 74 and Lemma 73 on the previous page that the edges of the relative neighbourhood graph of a planar point set $S$ cannot be intersected by any other edge in a 30°-triangulation, if such a triangulation exists. Therefore, they must be in every 30°-triangulation, if such a triangulation exists. □

The result of Theorem 74 is tight. In other words, there is no guarantee that for an angle $\alpha < 30°$ the relative neighbourhood graph will be part of every (or any) $\alpha$-triangulation. A four-point example can be constructed that shows this. Consider a pair of points $A$ and $B$ as per the notation used throughout this section, and two other points $C$ and $D$ "slightly" outside the lune of $AB$, placed on the right side of the perpendicular bisector of $AB$ infinitesimally close to it. Analysis shows that we can make the angles $\angle DCB$ and $\angle CDB$ as close to 30° as we want, while keeping the point $B$ outside of the forbidden zone of the edge $CD$.

## 3.4 Approximations to the MaxMin and MinMax area triangulations

As we have mentioned earlier, there are no guarantees for the angle quality of the optimal area triangulation, and conversely for the area qualities of "fat" triangulations. Therefore, we consider an approximation approach:

**Algorithm 75**

***Input:*** *Planar set of points $S$ in general position.*

***Output:*** *Triangulations $\tilde{T}_1$ and $\tilde{T}_2$ of $S$ that approximate, respectively, the MaxMin and MinMax area triangulations of $S$.*

*(1.) Compute the Delaunay triangulation of $S$, $DT(S)$. Denote by $\alpha^*$ the smallest angle in $DT(S)$.*

*(2.)* ***if*** $\alpha^* < 30°$ ***then***

$\tilde{T}_1 := DT(S)$, $\tilde{T}_2 := DT(S)$

*(3.)* ***else***

*Compute the optimal area 30°-triangulations, $T_1^{30°}$ (MaxMin) and $T_2^{30°}$ (MinMax), of $S$ by Klincsek's algorithm, using the results of Corollary 70 on page 73 and*

*Corollary 71 on page 73.*
$\tilde{T_1} := T_1^{30^\circ}$ *and* $\tilde{T_2} := T_2^{30^\circ}$.

**Time and Space Analysis.** In step (1.) we compute the Delaunay triangulation of $S$. As we mentioned in Section 1.5, this takes $O(n \log n)$ time. The Delaunay angle, i.e., the smallest angle in the Delaunay triangulation of the point set, is denoted by $\alpha^*$. It can be found in linear time, $O(n)$, for example by brute force. Depending on the value of $\alpha^*$, we have two cases, treated in steps (2.) and (3.), respectively:
If $\alpha^* < 30^\circ$, then no 30°-triangulation of $S$ is possible, as by Property 13 on page 8 the Delaunay triangulation maximizes the minimum angle. Thus, we are going to use the Delaunay triangulation as an approximation for both optimal area triangulations.
If $\alpha^* \geq 30^\circ$, then the set $S$ admits 30°-triangulation(s). By Theorem 74 on the preceding page, the relative neighbourhood graph is part of any 30°-triangulation. Additionally, the relative neighbourhood graph is connected by Corollary 70 on page 73, implying that if we draw the relative neighbourhood graph and the convex hull, the point set (the interior of its convex hull, that is) will be subdivided into a set of simple polygons. In addition, any of these polygons has at most one convex hull edge as shown in Corollary 71 on page 73 [54]. Now we can apply Klincsek's algorithm to compute the optimal 30°-triangulations. This computation requires a cubic time, $O(n^3)$. The optimization is done separately for MaxMin and MinMax area and we have two different optimal triangulations. We use the optimal area 30°-triangulations as an approximation for the optimal area triangulations.
This algorithm has a cubic worst-case running time and subcubic expected running time. It uses quadratic space, $O(n^2)$, in the case we have to perform step (3.), and linear space, $O(n)$, otherwise.

Whether we can compute a specific 30°-triangulation, for example the MinMax area one, in subcubic time is not a trivial question. One approach to a strictly subcubic algorithm would be to obtain one of the locally optimal 30°-triangulations, in no more than quadratic time, by performing all area equalizing flips that preserve all angles above 30° in the Delaunay triangulation, and then use this locally area optimal 30°-triangulation as an approximation to the globally optimal. This approach can be generalized to obtain a locally optimal $\alpha$-triangulation for any $\alpha < 30^\circ$ by relaxing the Delaunay triangulation as much as possible by edge flips that equalize the area of the two triangles inside the convex quadrilateral, while preserving the angular constraint imposed.

If, for practical reasons, we need to approximate the optimal area triangulations by triangulations of certain angular quality, we can introduce a parameter to our algorithm. We need to modify the algorithm as follows:

**Algorithm 76**

***Input:*** *Planar set of points $S$ in general position, and an angle $\alpha$.*

***Output:*** *Triangulation $\tilde{T}_3$ of $S$ that approximates the MaxMin and MinMax area triangulations of $S$.*

*(1'.) Compute the Delaunay triangulation of $S$, $DT(S)$. Denote by $\alpha^*$ the smallest angle in $DT(S)$.*

*(2'.)* ***if*** $\alpha \leq \alpha^*$ ***then***

$T_{current} := DT(S)$

***repeat***

$T_{temp} := flip(T_{current})$

$T_{current} := T_{temp}$

***until*** *no flip in $T_{current}$ is possible*

$\tilde{T}_3 := T_{current}$

***return*** $\tilde{T}_3$

*(3'.)* ***else***

***return*** *"No $\alpha$-triangulation of $S$ exists"*

**Time and Space Analysis.** Step (1'.) is the same as step (1.) of the previous algorithm. Thus, it is performed within $O(n \log n)$ time, using linear space, $O(n)$. For the step (2'.) we assume that we have an implementation of the function $flip(T)$. This function performs a single reverse Delaunay flip in the triangulation $T$. This reverse Delaunay flip has two additional properties: it is area equalizing, and it yields two new triangles whose angles are greater than or equal to the input parameter $\alpha$. We perform as many flips of this type as possible. The resulting triangulation is locally optimal with respect to both MaxMin and MinMax triangulation. This is due to the fact that the flip we perform optimizes both quality measures at the same time, as it was explained previously. Step (2'.) is performed within $O(n^2)$ time, using linear space, $O(n)$. Justification for this was given in Section 1.5, where we considered the properties of the Delaunay triangulation with respect to the Delaunay flip. Step (3'.) requires constant time and space.
Therefore, this algorithm has a quadratic, $O(n^2)$, worst-case running time and subquadratic expected running time. It uses linear space, $O(n)$.

To evaluate the practicality of these two algorithmic approaches, we need to know how well the Delaunay triangulation, the locally area-optimized Delaunay triangulation, and the optimal 30°-triangulations approximate the optimal area triangulations. More generally, we want to derive the following result.

**Property 77** *Given a planar set of points $S$, two angles $\alpha$ and $\beta$, $\alpha > \beta$ in the interval $(0°, 60°)$, and two triangulations of $S$ – $T_\alpha$ (which is an $\alpha$-triangulation) and $T_\beta$ (which is a $\beta$-triangulation).*

*Consider a perfect matching between triangles in $T_\alpha$ and $T_\beta$. Let $\frac{A_\alpha}{A_\beta}$ be the ratio of the areas of a pair of matched triangles from $T_\alpha$ and $T_\beta$, respectively. Then there are functions $f_1(\alpha, \beta)$ and $f_2(\alpha, \beta)$ such that*

$$f_1(\alpha, \beta) \leq \frac{A_\alpha}{A_\beta} \leq f_2(\alpha, \beta)$$

*for all choices of the pair of triangulations $T_\alpha$ and $T_\beta$, and the matched pair of triangles within $T_\alpha$ and $T_\beta$. Furthermore, for fixed $\alpha$:*

$$\lim_{\beta \to 0^\circ} f_1(\beta) = 0 \qquad \lim_{\beta \to 0^\circ} f_2(\beta) = +\infty$$

The objective of our study is to find the analytical form of the bounding functions $f_1(\alpha, \beta)$ and $f_2(\alpha, \beta)$. This is going to be achieved by a case analysis of the matched pairs of triangles, using forbidden zones and other obvious geometric constraints that arise in these situations.

From the description of the two algorithmic approaches above, it is clear that we are actually going to deal with $\alpha \leq 30^\circ$. In Algorithm 75, we compute the minimum angle of the approximating triangulations, it is either $30^\circ$ or $\alpha^* < 30^\circ$. In Algorithm 76, we get this angle as a parameter. Thus, it can be considered constant from here onwards, and the two bounding functions become functions of a single variable, $\beta$. It is further clear that if we have a reason to believe that the optimal area triangulations are "fat" enough, we would not need to approximate them. Thus, we will need to run the approximating algorithms only if $\beta$ is small compared to what we need in practise. Assuming that we know the value of $\beta$, the two bounding functions are now two constants, and we can find the approximation factors as follows: the double inequality has the form $c_1 \leq \frac{A_\alpha}{A_\beta} \leq c_2$. Consider for example the MinMax area triangulation. The worst (largest area) triangle in the $\alpha$-triangulation, call it $\Delta^\alpha_{\max}$, is matched to some triangle in the $\beta$-triangulation, denoted by $\Delta'$. Using the right hand side of the double inequality we have:

$$\frac{A(\Delta^\alpha_{\max})}{A(\Delta')} \leq c_2 \Rightarrow A(\Delta^\alpha_{\max}) \leq c_2 \cdot A(\Delta') \leq c_2 \cdot A(\Delta^\beta_{\max})$$

or in terms of the quality measures of the two compared triangulations $T_\alpha$ and $T_\beta$ we have $\lambda(T_\alpha) \leq c_2 \cdot \lambda(T_\beta)$. We can assume that $T_\beta$ is the optimal MinMax area triangulation, and thus for **any** $\alpha$-triangulation $T_\alpha$ we are guaranteed to be not worse than $c_2$ times $T_\beta$. Hence, the approximation factor is $c_2$. Similarly, using the left hand side of the double inequality we can see that any $\alpha$-triangulation approximates the optimal MaxMin area triangulation by factor of not more than $\frac{1}{c_1}$. Further, it is very interesting to determine the behaviour of the functions when $\alpha = \beta$ or in other words how good is, in terms of area, any $\alpha$-triangulation compared to any other $\alpha$-triangulation for a given value of $\alpha$. This may lead to reasonable probabilistic approaches to approximation of the optimal area triangulations. Again, the expected behaviour of these two functions as functions of

a single argument is:

$$\lim_{\alpha \to 0^\circ} f_1(\alpha) = 0, \quad \lim_{\alpha \to 0^\circ} f_2(\alpha) = +\infty, \quad \text{and} \quad \lim_{\alpha \to 60^\circ} f_1(\alpha) = \lim_{\alpha \to 60^\circ} f_2(\alpha) = 1$$

## 3.5 Matching triangles, cases

To evaluate the approximation ratio between a known $\alpha$-triangulation and the unknown optimal $\beta$-triangulation, we are going to use a result by Aichholzer et al. [2] that establishes the existence of one-to-one matching between the triangles of any two triangulations of a point set.

**Property 78 (Matching, [2])** *Given a planar set of points $S$ and two triangulations $T_1$ and $T_2$ of $S$, there exists a perfect matching (bijective mapping) between the triangles of $T_1$ and $T_2$ such that each pair of matched triangles have:*

- *at least one shared vertex*
- *shared interior points.*

This is a very strong theoretical result. Algorithmically, matching of this type can be computed by using general algorithms for matchings in bipartite graphs. There are algorithms that achieve this in quadratic time with respect to the size of the graph. It is not known whether we can compute such matchings more efficiently based on the geometric properties of triangulations, although some research has recently been done in this area [3]. Neither is it known how many different matchings with this property exist between a given two triangulations of a point set.
As it will become clear from further analysis, we intend to use perfect matchings to compare two triangulations, the optimal MaxMin or MinMax area triangulations that we cannot efficiently compute and a specific triangulation that is computable within reasonable time.

We are also going to use the angular constraints that we introduced. Recall that in an $\alpha$-triangulation, all the angles are in the interval $[\alpha, 180^\circ - 2\alpha]$.

**Lemma 79** *Given a triangle with a side $a$, all the angles of which are greater than or equal to $\alpha$, the minimal and maximal area of such a triangle are given by:*

$$A_{\min} = \frac{a^2}{4} \cdot \tan \alpha$$

*(occurring when the triangle is an isosceles with both base angles equal to $\alpha$) and*

$$A_{\max} = \frac{a^2}{4} \cdot \cot \frac{\alpha}{2} = \frac{a^2}{4} \cdot \frac{1}{\tan \frac{\alpha}{2}}$$

*(occurring when the triangle is an isosceles with a top angle of $\alpha$).*

**Proof.** Consider the angle of the triangle opposite the side of length $a$. For a fixed value of this angle, the vertices of all such triangles lie on a part of a circular arc going through the endpoints of the side of length $a$. Therefore the maximum area of the triangle is obtained for the isosceles triangle (corresponding to the highest point on the circular arc), and the minimum area is obtained for the triangles with a base angle of $\alpha$ (corresponding to the two lowest points on the arc when there is a constraint on the smallest angle). Therefore the maximum area is obtained when the isosceles triangle is as tall as possible, which is when the angle opposite the side of length $a$ is $\alpha$, and the minimum area is obtained when both of the base angles are equal to $\alpha$. □

We will denote, for the rest of the section, a triangle of the $\alpha$-triangulation by $\triangle ABC$ and will use the standard notation for its side lengths $a, b, c$. Similarly the matching triangle of the $\beta$-triangulation will be $\triangle A_1B_1C_1$ and the sides are going to be $a_1, b_1, c_1$. We use the following two formulae for area of a triangle, either two sides and the angle between them:

$$A_\triangle = \frac{ab}{2}\sin\theta$$

or a side and three angles:

$$A_\triangle = \frac{a^2}{2}\cdot\frac{\sin\phi\sin\psi}{\sin\theta}$$

(here $\phi$, $\psi$, $\theta$ are the angles opposite sides $a$, $b$, $c$, of the triangle, respectively) which is equivalent to:

$$A_\triangle = \frac{a^2}{2}\cdot\frac{\sin\phi\sin\psi}{\sin(\phi+\psi)}$$

We now consider the cases as to how the matched triangles from an $\alpha$-triangulation and a $\beta$-triangulation interact. Based on the angular constraints, we identify the "forbidden zone" around each edge of the triangulation – the region of the plane that is empty of points from the original point set. For an edge of length $a$, the forbidden zone properly includes a trapezoid of height $(a/2)\tan\alpha$ that has base angles of $3\alpha$. The non–parallel sides of this trapezoid are, therefore, of length $(a\tan\alpha)/(2\sin 3\alpha)$. With respect to an edge (of length $a$) of an $\alpha$-triangulation, any other point from the set can be either outside of the strip of height $(a/2)\tan\alpha$ (Zone 1), inside a circle with radius $(a\tan\alpha)/(2\sin 3\alpha)$ centered at one of its endpoints but outside the trapezoid (Zone 2), or inside the strip and outside the circles (Zone 3). The situation is illustrated in Figure 3.12 on the next page.

The structure of the cases has two levels. The first level is based on the number of vertices that the triangles of the $\alpha$-triangulation ($\triangle ABC$) and the $\beta$-triangulation ($\triangle A_1B_1C_1$) share. There can be

- three shared vertices

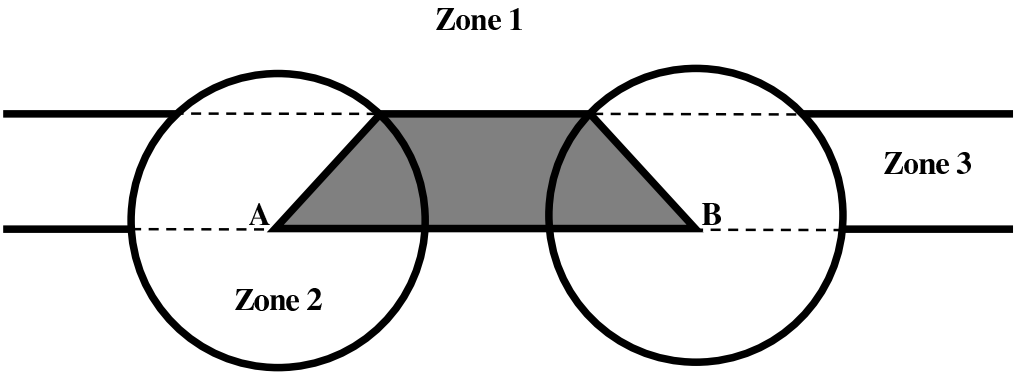


**Figure 3.12:** The forbidden zone of the edge $AB$ and zones 1, 2, and 3

- two shared vertices
- one shared vertex

Cases are considered in the given order. Within the last case, there are subcases based on the positions of the non-shared vertices relative to the edges of the other triangle (the triangle to which they do not belong). There are, again, three possible subcases

- point(s) in Zone 1
- point(s) in Zone 2
- point(s) in Zone 3

The detailed structure of the different subcases is explained within the appropriate subsection where they are considered. Note that in all cases none of the points $A, B, C, A_1, B_1, C_1$ can lie in the interior of either $\triangle ABC$ or $\triangle A_1B_1C_1$. This is due to the fact that both $\triangle ABC$ and $\triangle A_1B_1C_1$ are triangles of valid triangulations of $S$, and thus, by Definition 1 on page 1, are empty of points of $S$. This property will be important for analyzing the possible placements of the considered points with respect to the considered triangles. Also note, that each vertex (each one of the six points named above) is in Zone 1 with respect to the opposite edge of the triangle in which it is a vertex. This is another consequence of the fact that the triangles $\triangle ABC$ and $\triangle A_1B_1C_1$ are triangles of valid triangulations, respectively $\alpha$-triangulation and $\beta$-triangulation, of $S$.

The rest of this section is technical, it derives the bounding functions for all possible cases of matching triangles. It can be skipped, through Section 3.6 on page 103, on the first reading.

### 3.5.1 Three shared vertices

In this case the triangles are the same, $\triangle ABC \equiv \triangle A_1B_1C_1$, and the ratio of areas is equal to one.

### 3.5.2 Two shared vertices (shared edge)

Assume that the two matched triangles share the edge $BC \equiv B_1C_1$, which has length $a$. According to Lemma 79 on page 83:

$$(A_\alpha)_{\min} = \frac{a^2}{4} \cdot \tan\alpha, \quad (A_\alpha)_{\max} = \frac{a^2}{4} \cdot \frac{1}{\tan\frac{\alpha}{2}}, \quad (A_\beta)_{\min} = \frac{a^2}{4} \cdot \tan\beta, \quad \text{and} \quad (A_\beta)_{\max} = \frac{a^2}{4} \cdot \frac{1}{\tan\frac{\beta}{2}}$$

Therefore, we can compute:

$$\left(\frac{A_\alpha}{A_\beta}\right)_{\min} \geq \frac{(A_\alpha)_{\min}}{(A_\beta)_{\max}} \geq \tan\alpha \cdot \tan\frac{\beta}{2}$$

and

$$\left(\frac{A_\alpha}{A_\beta}\right)_{\max} \leq \frac{(A_\alpha)_{\max}}{(A_\beta)_{\min}} \leq \frac{1}{\tan\beta \cdot \tan\frac{\alpha}{2}}$$

### 3.5.3 Exactly one shared vertex

Assume that the two matched triangles share the vertex $A$, $A \equiv A_1$. Then, depending on the mutual position of the vertices $B, C, B_1, C_1$, we can have two different situations, as illustrated in Figure 3.13.

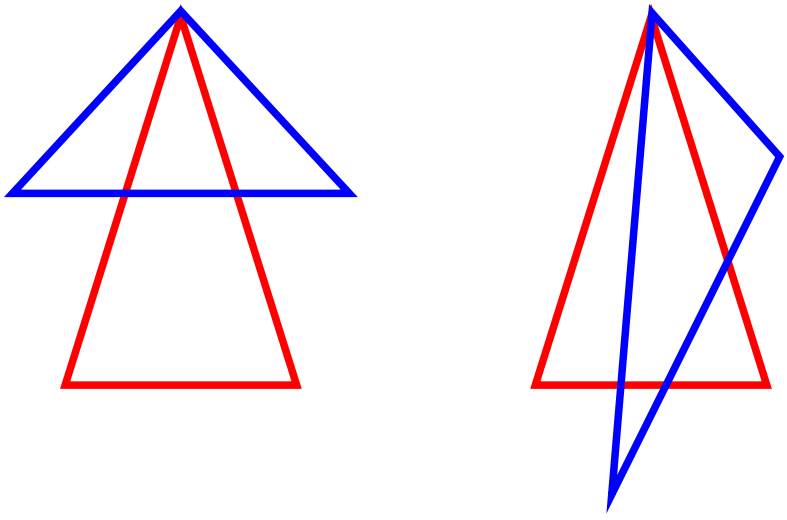

**Figure 3.13:** Exactly one shared vertex

Namely, one of the angles $\angle BAC$ and $\angle B_1AC_1$ can contain the other (as shown on the left), or it neither of them will contain the other (as shown on the right). Additionally, here it is very important to consider the positions of the points with respect to the forbidden zones of the edges of the matched triangle, as the lengths of the edges, and subsequently the bounds obtained will depend on this. Note, that in the two previous subsections, the results hold regardless of the mutual position of the points.

Crucial for all subcases that arise in this case is the intersection between a pair of sides, one from each of the matched triangles.

### A pair of intersecting sides

Let the sides $AC = b$ and $B_1C_1 = a_1$ intersect at the point $X$, and in addition both pairs of vertices are outside the strip of the other edge (Zone 1). Please refer to Figure 3.14 for an illustration.

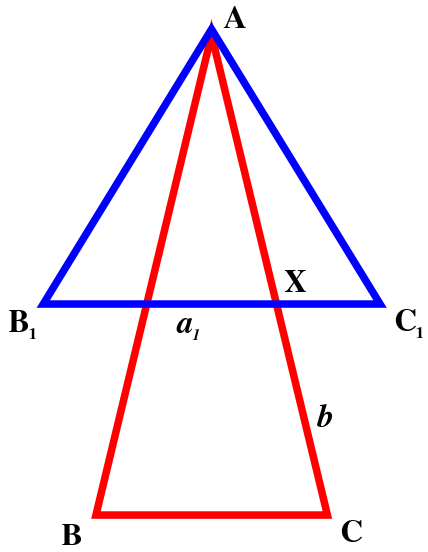


**Figure 3.14:** A pair of intersecting sides $B_1C_1$ and $AC$

Then, using the fact that the points $C$ and $A$ are outside of the forbidden zone of the edge $B_1C_1$, and the fact that the forbidden zone has width of $\frac{a_1}{2} \cdot \tan\beta$, we have $XC > \frac{a_1}{2} \cdot \tan\beta$ and $XA > \frac{a_1}{2} \cdot \tan\beta$. But $XC + XA = CA = b$, so $b > a_1 \tan\beta$. We can rewrite this as $a_1 < b/\tan\beta$. Similarly, because of the fact that points $C_1$ and $B_1$ are outside of the forbidden zone of the edge $AC$, and the fact that the forbidden zone has width of $(b/2)\tan\alpha$, we have $XB_1 > (b/2)\tan\alpha$ and $XC_1 > (b/2)\tan\alpha$. But $XB_1 + XC_1 = B_1C_1 = a_1$, so $a_1 > b\tan\alpha$. We can rewrite this as $b < a_1/\tan\alpha$. Thus, we have bounded $a_1$ from below and above:

$$b\tan\alpha < a_1 < \frac{b}{\tan\beta}$$

Using these inequalities, we can obtain the following bounds for the area of the $\beta$-triangle:

$$(A_\beta)_{\min} = \frac{a_1^2}{4} \cdot \tan\beta \geq \frac{b^2}{4} \cdot \tan^2\alpha \cdot \tan\beta, \qquad (A_\beta)_{\max} = \frac{a_1^2}{4} \cdot \frac{1}{\tan\frac{\beta}{2}} \leq \frac{b^2}{4} \cdot \frac{1}{\tan^2\beta \cdot \tan\frac{\beta}{2}}$$

Then, using the results of Lemma 79 on page 83 for $(A_\alpha)_{\min}$ and $(A_\alpha)_{\max}$ we can compute the bounds for the ratio of the areas as follows:

$$\left(\frac{A_\alpha}{A_\beta}\right)_{\min} \geq \frac{(A_\alpha)_{\min}}{(A_\beta)_{\max}} \geq \frac{\frac{b^2}{4} \cdot \tan\alpha}{\frac{b^2}{4} \cdot \frac{1}{\tan^2\beta \cdot \tan\frac{\beta}{2}}} \geq \tan\alpha \cdot \tan^2\beta \cdot \tan\frac{\beta}{2}$$

and

$$\left(\frac{A_\alpha}{A_\beta}\right)_{\max} \leq \frac{(A_\alpha)_{\max}}{(A_\beta)_{\min}} \leq \frac{\frac{b^2}{4} \cdot \frac{1}{\tan\frac{\alpha}{2}}}{\frac{b^2}{4} \cdot \tan^2\alpha \cdot \tan\beta} \leq \frac{1}{\tan\beta \cdot \tan^2\alpha \cdot \tan\frac{\alpha}{2}}$$

Here the upper and the lower bound are symmetric again:

$$f_2(\alpha, \beta) = \frac{1}{f_1(\beta, \alpha)}$$

This means that the bounds do not depend on which of the angles $\angle BAC$ and $\angle B_1AC_1$ contains the other. To verify that, we can use the double inequality for $b$ expressed in terms of $a_1$:

$$a_1 \tan\beta < b < \frac{a_1}{\tan\alpha}$$

Repeating the calculations will yield the same bounds.

These are the best bounds that we are going to be able to obtain for the case when one of the angles $\angle BAC$ and $\angle B_1AC_1$ contains the other as shown on the left in Figure 3.13 on page 85 and in Figure 3.14 on the previous page.

We are going to show that the bounds derived here are worse than the bounds for the shared edge case. For the lower bounds we have:

$$\tan\alpha\tan^2\beta\tan\frac{\beta}{2} < \tan\alpha\tan\frac{\beta}{2} \Leftrightarrow \tan^2\beta < 1 \Leftrightarrow \tan\beta < 1 \Leftrightarrow \beta < 45^\circ$$

For the upper bounds we have:

$$\frac{1}{\tan\beta\tan\frac{\alpha}{2}} < \frac{1}{\tan\beta\tan^2\alpha\tan\frac{\alpha}{2}} \Leftrightarrow \tan^2\alpha < 1 \Leftrightarrow \tan\alpha < 1 \Leftrightarrow \alpha < 45^\circ$$

Remember that earlier we have specified that $0^\circ < \beta < \alpha \leq 30^\circ$, so the two inequalities above hold.

**Neither of the angles $\angle BAC$ and $\angle B_1AC_1$ contains the other**

As Figure 3.15 on the following page and the right part of Figure 3.13 on page 85 show, there is a possibility that neither of the angles $\angle BAC$ and $\angle B_1AC_1$ contains the other. Now, we are going

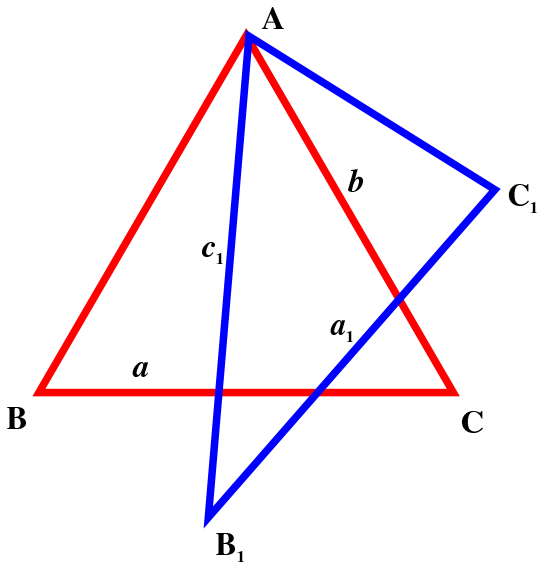


**Figure 3.15:** Neither of the angles $\angle BAC$ and $\angle B_1AC_1$ contains the other

to obtain better bounds – based on the formula for area that uses the product of two sides and the included angle. As shown in Figure 3.15, assume the sides $BC = a$ and $A_1B_1 = c_1$ intersect. Again, assuming that both pairs of vertices are in Zone 1 with respect to the edge formed by the other two, we are going to have: $c_1 \tan\beta < a < c_1/\tan\alpha$ and $a\tan\alpha < c_1 < a/\tan\beta$. The sides $AC = b$ and $B_1C_1 = a_1$ intersect as well. We can assume that since the situation when $B_1C_1$ intersects $AB$ is symmetric – we can interchange the names of the points $B$ and $C$. Additionally, we cannot have a situation where either of the points $B$ or $C$ lies inside the triangle $\triangle A_1B_1C_1$, as $\triangle A_1B_1C_1$ is part of a triangulation, and therefore is empty of points of $S$. Thus we have: $a_1\tan\beta < b < a_1/\tan\alpha$ and $b\tan\alpha < a_1 < b/\tan\beta$

Also, for an $\alpha$-triangle with sides $a, b$ and angles restricted to be larger than $\alpha$, the minimum and maximum area are given by $(ab/2)\sin\alpha \le A_\alpha \le ab/2$, i.e., the minimum area is $(ab/2)\sin\alpha$, when the angle at point $C$ is exactly $\alpha$; and when the angle at $C$ is a right angle, we have the maximum area of $ab/2$. Similarly, for the $\beta$-triangle $\triangle A_1B_1C_1$: $(a_1c_1/2)\sin\beta \le A_\beta \le a_1c_1/2$. Substituting, we obtain:

$$(A_\beta)_{\min} \ge \frac{ab}{2}\cdot\tan^2\alpha\cdot\sin\beta, \qquad (A_\beta)_{\max} \le \frac{ab}{2}\cdot\frac{1}{\tan^2\beta}$$

Thus, the bounds in this case are:

$$\left(\frac{A_\alpha}{A_\beta}\right)_{\min} \ge \frac{(A_\alpha)_{\min}}{(A_\beta)_{\max}} \ge \frac{\frac{ab}{2}\cdot\sin\alpha}{\frac{ab}{2}\cdot\frac{1}{\tan^2\beta}} \ge \sin\alpha\cdot\tan^2\beta$$

and

$$\left(\frac{A_\alpha}{A_\beta}\right)_{\max} \le \frac{(A_\alpha)_{\max}}{(A_\beta)_{\min}} \le \frac{\frac{ab}{2}}{\frac{ab}{2}\cdot\tan^2\alpha\cdot\sin\beta} \le \frac{1}{\sin\beta\cdot\tan^2\alpha}$$

In this case, upper and lower bound are symmetric in terms of $\alpha$ and $\beta$, regardless of the choice of triangles, i.e., regardless of whether $B$ lies inside $\angle B_1AC_1$ or $B_1$ lies inside $\angle BAC$. This is true because in both possible arrangements to compute the bounds we use two pairs of intersecting sides and in each pair one of the sides is form the $\alpha$–triangle and the other is from the $\beta$–triangle.

Recall that we are assuming $\beta \leq 30°$. To show that these bounds are better than the ones derived on the basis of only one pair of intersecting sides (the previously analysed case), consider the inequalities:

$$\tan\alpha \cdot \tan^2\beta \cdot \tan\frac{\beta}{2} < \sin\alpha \cdot \tan^2\beta \Leftrightarrow \tan\frac{\beta}{2} < \cos\alpha,$$

which is true whenever $\alpha < \arccos(\tan 15°) \simeq 74.45°$, since $\tan\frac{\beta}{2} < \tan 15° < \cos\alpha$, for the lower bound, and

$$\frac{1}{\sin\beta \cdot \tan^2\alpha} < \frac{1}{\tan\beta \cdot \tan^2\alpha \cdot \tan\frac{\alpha}{2}} \Leftrightarrow \tan\beta \cdot \tan^2\alpha \cdot \tan\frac{\alpha}{2} < \sin\beta \cdot \tan^2\alpha \Leftrightarrow \tan\frac{\alpha}{2} < \cos\beta,$$

which is true whenever $\beta < \arccos(\tan 30°) \simeq 54.74°$, since $\tan\frac{\alpha}{2} < \tan 30° < \cos\beta$, for the upper bound.

This concludes the cases when all the vertices of the two triangles are situated so that they lie in Zone 1 with respect to the edges of the other triangle. From this point on, at least one of the points will be in Zone 2 or Zone 3 with respect of some edge of the other triangle.

We can fix one of the triangles, for example the $\alpha$–triangle $\triangle ABC$, and consider all possible positions of the points $B_1$ and $C_1$ with respect to the forbidden zones of the edges of $\triangle ABC$. The case when we have exactly one of the points in Zone 2 is postponed because its consideration will depend on the developments in the following section. The same is done with the case when at least one point is in Zone 3. Next, we consider the cases when exactly two points lie in Zone 2.

**Placements of points in Zone 2**

In analysing the subsequent cases we are going to need inequalities involving distances between points placed in circles. To facilitate this, we introduce the following lemma:

**Lemma 80**

*(i) Given two circles $c_1(O_1, r_1)$ and $c_2(O_2, r_2)$ whose centres are at a distance $O_1O_2 = d$ from each other, the distance between a point $X$ lying within the closure of $c_1$, and another point $Y$ lying within the closure of $c_2$ satisfies the following inequalities:*

$$d - r_1 - r_2 \leq XY \leq d + r_1 + r_2$$

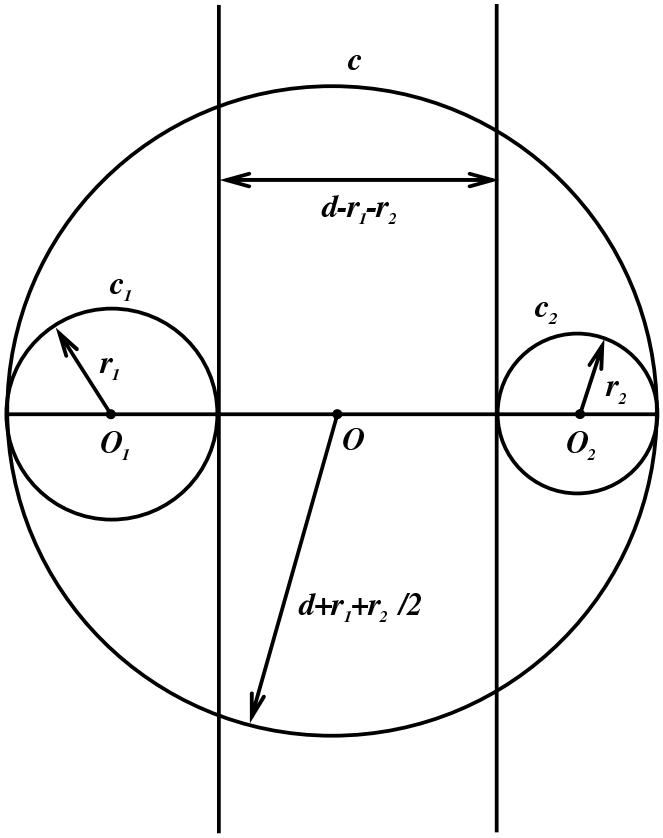


**Figure 3.16:** Lemma 80, the construction in case (i)

*(ii) Given a circle $c_1(O, r_1)$ and a point $X$ in the plane at a distance $OX = d$ from the centre of the circle, the distance between $X$ and any other point $Y$ lying within the closure of $c_1$ satisfies the following inequalities:*

$$d - r_1 \leq XY \leq d + r_1$$

**Proof.** First, we are going to prove part (i). The interesting case is $r_1 + r_2 < d$, i.e. interior disjoint circles. We can construct a circle $c(O, r)$ that is internally tangent to both $c_1$ and $c_2$. The center of $c$ lies on the central axis of $c_1$ and $c_2$. The diameter of $c$ is equal to $2r = d + r_1 + r_2$. Both $X$ and $Y$ lie within the closure of $c$, therefore $XY \leq d + r_1 + r_2$. Consider the tangents to $c_1$ and $c_2$ at their points of intersection with the central axis, inside $c$. The distance between these two parallel lines is $d - r_1 - r_2$. The points $X$ and $Y$ lie on different sides of the parallel strip defined by these two tangent lines, therefore $d - r_1 - r_2 \leq XY$. The construction is illustrated in Figure 3.16.
When the circles $c_1$ and $c_2$ intersect, the construction of the tangent circle is the same, hence the upper bound. The lower bound is trivial, because $d - r_1 - r_2$ is negative.

Note that part (ii) follows from part (i) when $r_2 = 0$. □

When the vertex $A$ is shared, the two points $B_1$ and $C_1$ can be placed in the circles defining Zone 2, centered at $A$, $B$, and $C$, in four different ways. Here we recall, that the radius of the circle defining Zone 2 for an edge of length $a$ is:

$$r = \frac{a}{2} \cdot \frac{\tan\alpha}{\sin 3\alpha}$$

For convenience, we will introduce the constant

$$k = \frac{1}{2} \cdot \frac{\tan\alpha}{\sin 3\alpha}$$

thus $r = k \cdot a$. The four possible distributions of the points in the circles are illustrated in Figure 3.17 on the following page. We are going to consider the possible placements and derive bounds for the ratio of the areas.

We start with the placement **(a)**. Here we can constrain two of the sides, $AC_1 = b_1$ and $AB_1 = c_1$, of the $\beta$-triangle, with respect to two of the sides of the $\alpha$-triangle, $AC = b$ and $AB = c$, respectively, using the result of Lemma 80 on the previous page, part (ii). Namely, $b - r \le b_1 \le b + r$, and having in mind that $r = k \cdot b$ we obtain $b(1-k) \le b_1 \le b(1+k)$. Similarly $c(1-k) \le c_1 \le c(1+k)$. For the areas we have: $(bc/2)\sin\alpha \le A_\alpha \le bc/2$, $(b_1c_1/2)\sin\beta \le A_\beta \le b_1c_1/2$, and therefore

$$(A_\alpha)_{\min} = \frac{bc}{2} \cdot \sin\alpha, \;\; (A_\alpha)_{\max} = \frac{bc}{2}, \;\; (A_\beta)_{\min} \ge \frac{bc}{2}(1-k)^2 \cdot \sin\beta, \quad \text{and} \quad (A_\beta)_{\max} \le \frac{bc}{2}(1+k)^2$$

Thus, for the ratio of the areas we have:

$$\left(\frac{A_\alpha}{A_\beta}\right)_{\min} \ge \frac{(A_\alpha)_{\min}}{(A_\beta)_{\max}} \ge \frac{\frac{bc}{2} \cdot \sin\alpha}{\frac{bc}{2}(1+k)^2} \ge \frac{\sin\alpha}{(1+k)^2}$$

and

$$\left(\frac{A_\alpha}{A_\beta}\right)_{\max} \le \frac{(A_\alpha)_{\max}}{(A_\beta)_{\min}} \le \frac{\frac{bc}{2}}{\frac{bc}{2}(1-k)^2 \cdot \sin\beta} \le \frac{1}{(1-k)^2 \cdot \sin\beta}$$

In placement **(b)**, we can constrain two of the sides of the $\beta$-triangle, $AC_1 = b_1$ and $AB_1 = c_1$, with relation to only one side, $AC = b$, of the $\alpha$-triangle, using the result of Lemma 80 on the preceding page, part (ii): $b - r \le b_1 \le b + r$, $b - r \le c_1 \le b + r$, which leads to the following: $b(1-k) \le b_1 \le b(1+k)$, $b(1-k) \le c_1 \le b(1+k)$. Further $\frac{b^2}{4} \cdot \tan\alpha \le A_\alpha \le \frac{b^2}{4} \cdot \frac{1}{\tan\frac{\alpha}{2}}$, $\frac{b_1c_1}{2} \cdot \sin\beta \le A_\beta \le \frac{b_1c_1}{2}$, and therefore

$$(A_\beta)_{\min} \ge \frac{b^2}{2}(1-k)^2 \cdot \sin\beta, \qquad (A_\beta)_{\max} \le \frac{b^2}{2}(1+k)^2.$$

For the bounds we obtain:

$$\left(\frac{A_\alpha}{A_\beta}\right)_{\min} \ge \frac{(A_\alpha)_{\min}}{(A_\beta)_{\max}} \ge \frac{\frac{b^2}{4} \cdot \tan\alpha}{\frac{b^2}{2}(1+k)^2} \ge \frac{\tan\alpha}{2(1+k)^2}$$

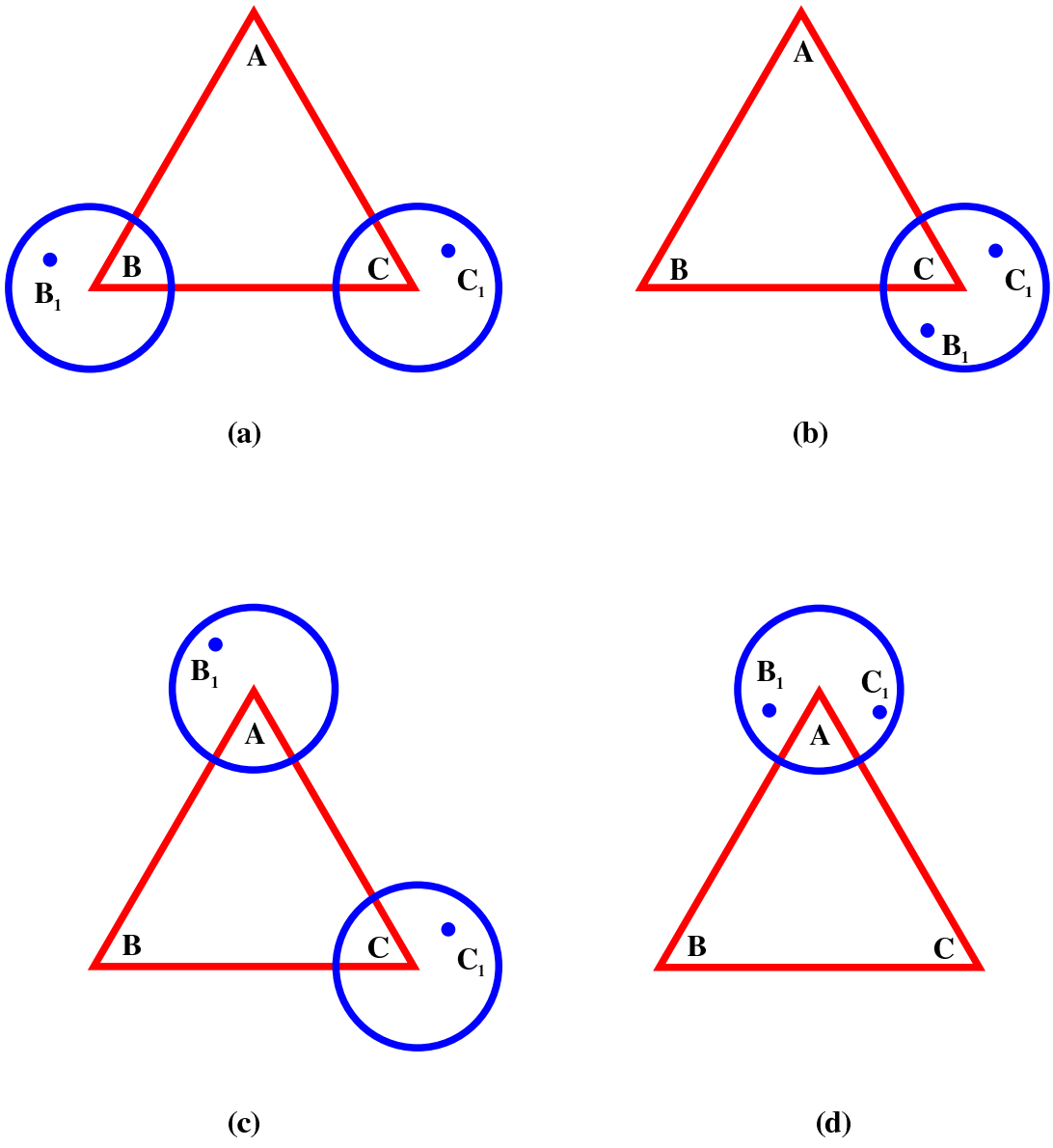


**Figure 3.17:** Possible placements of $B_1$ and $C_1$ in zone 2

and

$$\left(\frac{A_\alpha}{A_\beta}\right)_{\max} \leq \frac{(A_\alpha)_{\max}}{(A_\beta)_{\min}} \leq \frac{\frac{b^2}{4}\cdot\frac{1}{\tan\frac{\alpha}{2}}}{\frac{b^2}{2}(1-k)^2\cdot\sin\beta} \leq \frac{1}{2(1-k)^2\cdot\sin\beta\cdot\tan\frac{\alpha}{2}}$$

Comparing these bounds with the bounds for placement **(a)**, we can see that:

$$\frac{\tan\alpha}{2(1+k)^2} < \frac{\sin\alpha}{(1+k)^2} \Leftrightarrow \frac{1}{2} < \cos\alpha,$$

which is true whenever $\alpha < 60°$, for the lower bound, and

$$\frac{1}{(1-k)^2\cdot\sin\beta} < \frac{1}{2(1-k)^2\cdot\sin\beta\cdot\tan\frac{\alpha}{2}} \Leftrightarrow \tan\frac{\alpha}{2} < \frac{1}{2},$$

which is true whenever $\alpha < 2\arctan\left(\frac{1}{2}\right) \simeq 53.13°$, for the upper bound. Thus, the bounds in placement **(b)** are always worse than those in placement **(a)**.

In the third placement, **(c)**, we are going to relate two of the sides of the $\beta$-triangle, $B_1C_1 = a_1$ and $AC_1 = b_1$, to only one side, $AC = b$, of the $\alpha$-triangle. We do this using the result of Lemma 80 on page 90, part (i) and (ii), respectively: $b - 2r \leq a_1 \leq b + 2r$, $b - r \leq b_1 \leq b + r$, or equivalently: $b(1-2k) \leq a_1 \leq b(1+2k)$, $b(1-k) \leq b_1 \leq b(1+k)$. Similar to the analysis of the previous placement, for the areas we have: $\frac{b^2}{4}\cdot\tan\alpha \leq A_\alpha \leq \frac{b^2}{4}\cdot\frac{1}{\tan\frac{\alpha}{2}}$, $\frac{a_1b_1}{2}\cdot\sin\beta \leq A_\beta \leq \frac{a_1b_1}{2}$, and therefore

$$(A_\beta)_{\min} \geq \frac{b^2}{2}(1-k)(1-2k)\cdot\sin\beta, \qquad (A_\beta)_{\max} \leq \frac{b^2}{2}(1+k)(1+2k).$$

The bounds are:

$$\left(\frac{A_\alpha}{A_\beta}\right)_{\min} \geq \frac{(A_\alpha)_{\min}}{(A_\beta)_{\max}} \geq \frac{\frac{b^2}{4}\cdot\tan\alpha}{\frac{b^2}{2}(1+k)(1+2k)} \geq \frac{\tan\alpha}{2(1+k)(1+2k)}$$

and

$$\left(\frac{A_\alpha}{A_\beta}\right)_{\max} \leq \frac{(A_\alpha)_{\max}}{(A_\beta)_{\min}} \leq \frac{\frac{b^2}{4}\cdot\frac{1}{\tan\frac{\alpha}{2}}}{\frac{b^2}{2}(1-k)(1-2k)\cdot\sin\beta} \leq \frac{1}{2(1-k)(1-2k)\cdot\sin\beta\cdot\tan\frac{\alpha}{2}}$$

Again, we are going to compare these to the bounds obtained for placement **(b)**. We have:

$$\frac{\tan\alpha}{2(1+k)(1+2k)} < \frac{\tan\alpha}{2(1+k)^2} \Leftrightarrow 1+k < 1+2k,$$

which is true whenever $k > 0$, for the lower bound, and

$$\frac{1}{2(1-k)^2\cdot\sin\beta\cdot\tan\frac{\alpha}{2}} < \frac{1}{2(1-k)(1-2k)\cdot\sin\beta\cdot\tan\frac{\alpha}{2}} \Leftrightarrow 1-2k < 1-k,$$

which is true whenever $k > 0$ and

$$1 - 2k > 0 \Leftrightarrow k < \frac{1}{2}$$

The last inequality will be shown to be valid in the interval $\alpha \in (0°, 30°]$, which is sufficient for our considerations. Thus, the bounds in placement **(c)** are always worse than those in placement **(b)**. Note that for the three placements considered so far, the lower bound (the one that gives us the approximation constant for the MaxMin Area triangulation) does not depend on the angle $\beta$.

To show that $k < 1/2$, we are going to analyze the behaviour of $k$ as a function on $\alpha$ in the interval $(0°, 30°]$. We transform the expression for $k$ as a function of $\alpha$ as follows:

$$2k(\alpha) = \frac{\tan\alpha}{\sin 3\alpha} = \frac{\sin\alpha}{\cos\alpha \sin\alpha(3 - 4\sin^2\alpha)} = \frac{1}{\cos\alpha(4\cos^2\alpha - 1)} = \frac{1}{4\cos^3\alpha - \cos\alpha}$$

Here we used the known trigonometrical equalities:

$$\sin 3\alpha = 3\sin\alpha - 4\sin^3\alpha, \text{ and } \quad \sin^2\alpha + \cos^2\alpha = 1$$

Further, we are going to show that $k(\alpha)$ is monotonically increasing over $(0°, 30°]$. This is equivalent to showing that $\alpha_1 < \alpha_2 \leq 30° \Rightarrow k(\alpha_1) < k(\alpha_2)$, which follows:

$$k(\alpha_1) < k(\alpha_2) \Leftrightarrow \frac{1}{4\cos^3\alpha_1 - \cos\alpha_1} < \frac{1}{4\cos^3\alpha_2 - \cos\alpha_2} \Leftrightarrow 4\cos^3\alpha_2 - \cos\alpha_2 < 4\cos^3\alpha_1 - \cos\alpha_1$$

The cross multiplication above is valid since $k(\alpha)$ by its definition and geometric meaning is a positive value. We develop the inequality further:

$$4\cos^3\alpha_2 - 4\cos^3\alpha_1 < \cos\alpha_2 - \cos\alpha_1 \Leftrightarrow$$

$$\Leftrightarrow 4(\cos\alpha_2 - \cos\alpha_1)(\cos^2\alpha_1 + \cos^2\alpha_2 + \cos\alpha_1\cos\alpha_2) < \cos\alpha_2 - \cos\alpha_1 \Leftrightarrow$$

$$\Leftrightarrow 4(\cos\alpha_2 - \cos\alpha_1)\left(\cos^2\alpha_1 + \cos^2\alpha_2 + \cos\alpha_1\cos\alpha_2 - \frac{1}{4}\right) < 0$$

We know that $\cos x$ is a decreasing function over $(0°, 30°]$. Therefore $\alpha_1 < \alpha_2 \leq 30° \Rightarrow \cos\alpha_1 > \cos\alpha_2$. Thus, the term $4(\cos\alpha_2 - \cos\alpha_1)$ is strictly negative. Dividing by this term we obtain the following inequality:

$$\cos^2\alpha_1 + \cos^2\alpha_2 + \cos\alpha_1\cos\alpha_2 - \frac{1}{4} > 0$$

We are going to use one more time the fact that $\cos x$ is a decreasing function over $(0°, 30°]$. This means that $\cos\alpha_1 > \cos\alpha_2 \geq \cos 30° = \sqrt{3}/2$. Thus, $\cos^2\alpha_1 > 3/4$. This alone is enough to establish the validity of the above inequality as the terms $\cos^2\alpha_2$ and $\cos\alpha_1\cos\alpha_2$ are strictly positive.

As $k(0°)$ is well defined, and equal to $1/6$, and additionally $k(30°) = 1/2\sqrt{3}$ we have:

$$\frac{1}{6} < k(\alpha) \leq \frac{1}{2\sqrt{3}} \text{ for } \alpha \in (0°, 30°]$$

Thus $k(\alpha) < 1/2$.

Finally, the placement **(d)** should be considered. There, the points $B_1$ and $C_1$ are in the circle defining zone 2 for the shared vertex $A$. This is the worst case, as $B_1$ and $C_1$ can be "very close" to $A$, thus making the area of the $\beta$-triangle small, and increasing the upper bound (the one related to the approximation constant for the MinMax Area triangulation). However, if we include the forbidden zones of the edges in the vicinity of the point $A$, we can derive some constraints. Without loss of generality we can assume that $b \geq c$ for the two edges incident to $A$, $AB = c$ and $AC = b$. First, the angle of the $\alpha$-triangle at $A$, $\angle BAC \geq \alpha$ by our assumption. Moreover, the forbidden zones, the trapezoid part of them form angles of $3\alpha$ with the edges $BA$ and $CA$ at $A$. Therefore, there is a circular sector with a central angle of $7\alpha$ that is forbidden for the points $B_1$ and $C_1$. Hence, the top angle of the $\beta$-triangle is $\angle B_1AC_1 \geq 7\alpha$. The first constraint therefore is $2\beta + 7\alpha \leq 180°$, using the sum of the angles of the triangle $\triangle B_1AC_1$, which is a $\beta$-triangle. Recall that $\beta < \alpha$, thus this is only possible for $\beta < 20°$.

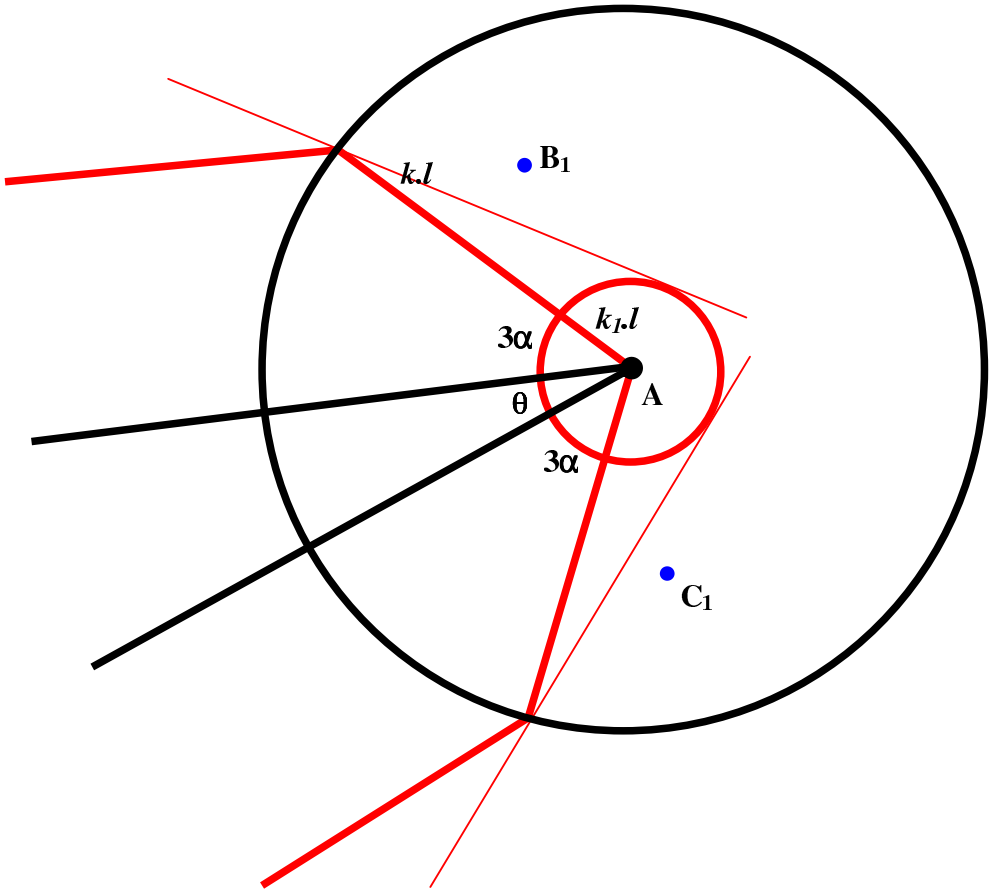


**Figure 3.18:** Two constraining circles in placement (d)

To constrain the lengths of the sides $B_1A$ and $C_1A$ of the $\beta$-triangle, we are going to use the fact that forbidden zones of edges $AB$ and $AC$ contain a circle around $A$. If $i = \left\lceil \frac{180^\circ}{2\alpha} - \frac{1}{2} \right\rceil$ it can be shown that the the radius of the forbidden circle is $k_1 b$ for the edge $AC$ (respectively $k_1 c$ for the edge $AB$), where

$$k_1 = \frac{d_i}{l} = \frac{1}{(2\cos\alpha)^i}$$

$l$ is the length of the base edge of the forbidden zone (either $b$ or $c$ here), and $d_i$ is the distance from an endpoint of an edge (in this case $A$) to the first $i$-th order vertex of its forbidden zone, as defined earlier in Section 3.2 on page 65. By the proof of Property 56 on page 55, angles at the vertices of the boundary of the forbidden zone are either $180^\circ - 3\alpha$ (non-acute when $\alpha \leq 30^\circ$) or $180^\circ + 2\alpha$ (reflex). Therefore, if we rotate the segment $AV_{i,1} = d_i = k_1 l$ towards the interior of the forbidden zone it stays inside according to Lemma 61 on page 67.

Recall that we assumed $b \geq c$. The lengths of the sides $B_1A$ and $C_1A$ of the $\beta$-triangle are therefore constrained to $k_1 c \leq b_1 \leq kb$, $k_1 c \leq c_1 \leq kb$. Therefore, for the areas of the two triangles we have: $\frac{b^2}{4} \cdot \tan\alpha \leq A_\alpha \leq \frac{c^2}{4} \cdot \frac{1}{\tan\frac{\alpha}{2}}$, $\frac{b_1 c_1}{2} \cdot \sin 2\beta \leq A_\beta \leq \frac{b_1 c_1}{2}$, and therefore

$$(A_\beta)_{\min} \geq \frac{c^2}{2} k_1^2 \cdot \sin 2\beta, \qquad (A_\beta)_{\max} \leq \frac{b^2}{2} k^2.$$

The bounds in this case are:

$$\left(\frac{A_\alpha}{A_\beta}\right)_{\min} \geq \frac{(A_\alpha)_{\min}}{(A_\beta)_{\max}} \geq \frac{\frac{b^2}{4} \cdot \tan\alpha}{\frac{b^2}{2} k^2} \geq \frac{\tan\alpha}{2k^2}$$

and

$$\left(\frac{A_\alpha}{A_\beta}\right)_{\max} \leq \frac{(A_\alpha)_{\max}}{(A_\beta)_{\min}} \leq \frac{\frac{c^2}{4} \cdot \frac{1}{\tan\frac{\alpha}{2}}}{\frac{c^2}{2} k_1^2 \cdot \sin 2\beta} \leq \frac{1}{2k_1^2 \cdot \sin 2\beta \cdot \tan\frac{\alpha}{2}}$$

Next we show that when, depending on $\alpha$ and $\beta$, this case is possible, the lower bound will be better than the lower bound found for placement **(c)**, and the upper bound is, as expected, worse than the upper bound for placement **(c)**. For the lower bounds we have:

$$\frac{\tan\alpha}{2k^2} > \frac{\tan\alpha}{2(1+k)(1+2k)} \Leftrightarrow 2k^2 + 3k + 1 > k^2 \Leftrightarrow k^2 + 3k + 1 > 0$$

which is true when $k > 0$. For the upper bounds we have:

$$\frac{1}{2k_1^2 \sin 2\beta \tan\frac{\alpha}{2}} > \frac{1}{2(1-k)(1-2k)\sin\beta \tan\frac{\alpha}{2}} \Leftrightarrow \frac{(1-k)(1-2k)}{2k_1^2} > \cos\beta$$

In simplifying the expression above we used the following trigonometric equality:

$$\sin 2\beta = 2\sin\beta\cos\beta$$

We will show that the two sides of the above inequality are separated by the unity. First we develop the left hand side:

$$\frac{(1-k)(1-2k)}{2k_1^2} = \frac{1 - 3k + 2k^2}{2k_1^2} = \frac{1-3k}{2k_1^2} + \frac{k^2}{k_1^2}$$

Now, consider the two additive terms on the left. We have shown that:

$$\frac{1}{6} < k < \frac{1}{2\sqrt{3}} \Rightarrow \frac{1}{2} < 3k < \frac{\sqrt{3}}{2} \Rightarrow 1 - \frac{\sqrt{3}}{2} < 1 - 3k < \frac{1}{2} \Rightarrow 1 - 3k > 0 \Rightarrow \frac{1-3k}{2k_1^2} > 0$$

Additionally, $k$ is the ratio of the length of the third order edge to the length of the base edge, while $k_1$ is the ratio of the length of the third or higher order edge to the length of the base edge, thus

$$k = \frac{d_3}{l}, k_1 = \frac{d_i}{l} \text{ for } i \geq 3 \Rightarrow k \geq k_1 \Rightarrow \frac{k}{k_1} \geq 1 \Rightarrow \frac{k^2}{k_1^2} \geq 1$$

Therefore

$$\frac{1-3k}{2k_1^2} + \frac{k^2}{k_1^2} > 1 > \cos\beta$$

**Exactly one point in Zone 2**

First we are going to assume that the point $B_1$ is in Zone 2 with respect to the edge $AB$, i.e., lies in the Zone 2 defining circle of the point $B$. The point $C_1$ by this assumption is not in Zone 2 with respect to any of the sides of $\triangle ABC$. We can constrain the side $AB_1$ of the $\beta$-triangle with relation to the side $AB$ of the $\alpha$-triangle, using the result of Lemma 80 on page 90, part (ii): $c - r \leq c_1 \leq c + r$, which leads to: $c(1-k) \leq c_1 \leq c(1+k)$. Further $\frac{c^2}{4}\tan\alpha \leq A_\alpha \leq \frac{c^2}{4}\frac{1}{\tan\frac{\alpha}{2}}$, $\frac{c_1^2}{4}\tan\beta \leq A_\beta \leq \frac{c_1^2}{4}\frac{1}{\tan\frac{\beta}{2}}$, and therefore

$$(A_\beta)_{\min} \geq \frac{c^2}{4}(1-k)^2\tan\beta, \qquad (A_\beta)_{\max} \leq \frac{c^2}{4}(1+k)^2\frac{1}{\tan\frac{\beta}{2}}.$$

For the bounds we obtain:

$$\left(\frac{A_\alpha}{A_\beta}\right)_{\min} \geq \frac{(A_\alpha)_{\min}}{(A_\beta)_{\max}} \geq \frac{\frac{c^2}{4}\tan\alpha}{\frac{c^2}{4}(1+k)^2\frac{1}{\tan\frac{\beta}{2}}} \geq \frac{\tan\alpha\tan\frac{\beta}{2}}{(1+k)^2}$$

and

$$\left(\frac{A_\alpha}{A_\beta}\right)_{\max} \leq \frac{(A_\alpha)_{\max}}{(A_\beta)_{\min}} \leq \frac{\frac{c^2}{4}\frac{1}{\tan\frac{\alpha}{2}}}{\frac{c^2}{4}(1-k)^2\tan\beta} \leq \frac{1}{(1-k)^2\tan\beta\tan\frac{\alpha}{2}}$$

Next, we consider the opposite situation, point $B$ lies in the Zone 2 with respect to the edge $AB_1$. Then, we can constrain the side $AB$ of the $\alpha$-triangle with relation to the side $AB_1$ of the $\beta$-triangle using the result of Lemma 80 on page 90, part (ii): $c_1 - r \leq c \leq c_1 + r$, which leads to: $c_1(1-k) \leq c \leq c_1(1+k)$. Further $\frac{c^2}{4}\tan\alpha \leq A_\alpha \leq \frac{c^2}{4}\frac{1}{\tan\frac{\alpha}{2}}$, $\frac{c_1^2}{4}\tan\beta \leq A_\beta \leq \frac{c_1^2}{4}\frac{1}{\tan\frac{\beta}{2}}$, and therefore

$$(A_\alpha)_{\min} \geq \frac{c_1^2}{4}(1-k)^2\tan\alpha, \qquad (A_\alpha)_{\max} \leq \frac{c_1^2}{4}(1+k)^2\frac{1}{\tan\frac{\alpha}{2}}.$$

For the bounds we obtain:

$$\left(\frac{A_\alpha}{A_\beta}\right)_{\min} \geq \frac{(A_\alpha)_{\min}}{(A_\beta)_{\max}} \geq \frac{\frac{c_1^2}{4}(1-k)^2\tan\alpha}{\frac{c_1^2}{4}\frac{1}{\tan\frac{\beta}{2}}} \geq \tan\alpha\tan\frac{\beta}{2}(1-k)^2$$

and

$$\left(\frac{A_\alpha}{A_\beta}\right)_{\max} \leq \frac{(A_\alpha)_{\max}}{(A_\beta)_{\min}} \leq \frac{\frac{c_1^2}{4}(1+k)^2\frac{1}{\tan\frac{\alpha}{2}}}{\frac{c_1^2}{4}\tan\beta} \leq \frac{(1+k)^2}{\tan\beta\tan\frac{\alpha}{2}}$$

We are going to compare the bounds obtained for the second case here to those for the first case.

For the lower bounds we have:

$$\tan\alpha\tan\frac{\beta}{2}(1-k)^2 < \frac{\tan\alpha\tan\frac{\beta}{2}}{(1+k)^2} \Leftrightarrow (1-k^2)^2 < 1$$

Which is true, based on our analysis for the values of $k$. Thus the lower bound for the second case is worse.

For the upper bounds we have:

$$\frac{(1+k)^2}{\tan\beta\tan\frac{\alpha}{2}} < \frac{1}{(1-k)^2\tan\beta\tan\frac{\alpha}{2}} \Leftrightarrow (1-k^2)^2 < 1$$

True, as shown above. Thus the upper bound for the first case is worse.

This raises the question of how do these bounds compare to the bounds obtained for the placements in the previous subsection, where two of the points were known to lie in Zone 2 with respect to the sides of the other triangle. We are going to show that these bounds are worse than the bounds obtained for the placement **(c)**. For the lower bounds we have:

$$\tan\alpha\tan\frac{\beta}{2}(1-k)^2 < \frac{\tan\alpha}{2(1+k)(1+2k)} \Leftrightarrow \tan\frac{\beta}{2} < \frac{1}{2(1-k^2)(1+k-2k^2)}$$

Thus we have to investigate the behaviour of the functions $1-k^2$ and $1+k-2k^2$ for the values of $k \in (1/6, 1/2\sqrt{3}]$. $1-k^2$ is a parabola growing downwards with a top at $k=0$, therefore $1-k^2$ is decreasing over the interval $(1/6, 1/2\sqrt{3}]$. The maximum value of $1-k^2$ over $(1/6, 1/2\sqrt{3}]$ is then attained at $k=1/6$ and equals $35/36$. $1+k-2k^2$ also is a parabola growing downwards with a top at $k=1/4$. The top of this parabola lies inside the interval $(1/6, 1/2\sqrt{3}]$ and the maximum value is therefore $9/8$. As the two functions do not attain their maxima for the same value of $k$, the maximum of their product is strictly less than the product of the respective maxima, which is $35/32$. The minimum value of $1-k^2$ over $(1/6, 1/2\sqrt{3}]$ is then attained at $k=1/2\sqrt{3}$ and equals $11/12$. The minimum value of $1+k-2k^2$ is attained at $k=1/6$ and equals $10/9$. As the two functions do not attain their minima for the same value of $k$, the minimum of their product is strictly less than the product of the respective minima, which is $55/54$.In other words we have:

$$2\cdot\frac{55}{54} < 2(1-k^2)(1+k-2k^2) < 2\cdot\frac{35}{32} \Leftrightarrow \frac{16}{35} < \frac{1}{2(1-k^2)(1+k-2k^2)} < \frac{27}{55}$$

Thus, we can maximally strenghten the inequality for $\beta$ requiring that

$$\tan\frac{\beta}{2} < \frac{16}{35} \Leftrightarrow \beta < 2\arctan\left(\frac{16}{35}\right) \simeq 49.134^\circ$$

For the upper bounds we have:

$$\frac{(1+k)^2}{\tan\beta\tan\frac{\alpha}{2}} > \frac{1}{2(1-k)(1-2k)\sin\beta\tan\frac{\alpha}{2}} \Leftrightarrow \cos\beta > \frac{1}{2(1-k^2)(1+k-2k^2)}$$

As $\cos\beta$ is a decreasing function in $(0°, 30°]$, we have to maximally strenghten the right hand side of the inequality. Based on the previous analysis, we require that:

$$\cos\beta > \frac{27}{55} \Leftrightarrow \beta < \arccos\left(\frac{27}{55}\right) \simeq 60.599°$$

The case that remains to be considered is when $B_1$ is in the circle defining Zone 2 of the point $A$ (the shared vertex). Consider the position of the point $C_1$. If $C_1$ is in Zone 3 with respect to any of the sides of $\triangle ABC$, this situation belongs to the case considered in the next subsection. Note that $C_1$ cannot belong to Zone 2 of any of the sides of $\triangle ABC$ by the assumption at the beginning of this subsection (if it were, the case is considered previously). It remains then for $C_1$ to be in Zone 1 of some of the sides of $\triangle ABC$. In this case, consider the side $B_1C_1$ of the $\triangle AB_1C_1$. It intersects either $AB$ or $AC$, or both of them. Further, $A \equiv A_1$ is in Zone 1 with respect to $B_1C_1$, as $\triangle AB_1C_1$ is a valid $\beta$-triangle. Now consider the positions of the points $B$ and $C$ with respect to the side $B_1C_1$. If either of $B$ or $C$ is in Zone 1 relative to $B_1C_1$, then we have a "pair of intersecting sides" ($(AB, B_1C_1)$ or $(AC, B_1C_1)$) as considered earlier. If either of the points $B$ or $C$ is in Zone 3 relative to $B_1C_1$, we are going to consider the case in the next subsection. If both $B$ and $C$ are in Zone 2 relative to $B_1C_1$, then this is a placement considered previously. This concludes the considerations under this subsection.

**At least one point in Zone 3**

Without loss of generality assume that $B_1$ is the point that is in Zone 3 with respect of one of the sides of $\triangle ABC$, i.e., $B_1$ is in Zone 3 of point $A$ or point $B$ (these are the only two distinct cases, as the points $B$ and $C$ can be renamed arbitrarily). First, we consider the case when $B_1$ is in Zone 3 with respect to the point $B$. Note that the point $C_1$ cannot belong to either Zone 2 or Zone 3 with respect to $B$. If $C_1$ is in Zone 2 with respect to $B$, this is a previously considered placement – one point in Zone 2. If $C_1$ is in Zone 3 with respect to $B$, this this will violate the convexity constraints, as $\angle B_1BC_1$ 180°, please refer to Figure 3.12 on page 84.

To constrain the length of the side $AB_1 = c_1$ we are going to use the minimum given by the position of $B_1$ at the intersection of the Zone 2 circle and the line defining Zone 1 and Zone 3. The maximum length of $c_1$ is given by the position of $B$ on the boundary of the forbidden zone of $AB_1$ such that $\angle BB_1A = \beta$. Note that $\angle BB_1A \geq \beta$, otherwise a $\beta$-triangulation will not exist. Also note that

$\angle BB_1A$ is always acute as $\triangle BB_1A$ has one obtuse angle, namely $\angle B_1BA \geq 180° - 3\alpha$. Angle $\angle BAB_1$ must obey the same requirement, it has to be greater than or equal to $\beta$. Furthermore, because of the fact that $\angle B_1BA$ is obtuse, the orthogonal projection of $B$ onto $AB_1$ is an internal point for the segment $AB_1$. We know that $B$ lies outside of the forbidden zone of $AB_1$. Since $B$ projects orthogonally in an internal point on $AB_1$, $B$ cannot lie in Zone 3 with respect to $AB_1$. If it lies in Zone 2 with respect to $AB_1$ then this case has been previously considered. Thus, we can assume that $B$ is in Zone 1 with respect to $AB_1$. Please refer to Figure 3.19 for an illustration of this placement of points.

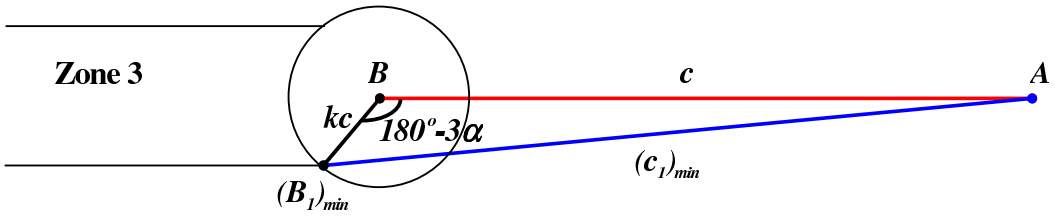


**Figure 3.19:** Placement of $B_1$ inside Zone 3, minimal length position

Consider the triangle $\triangle AB(B_1)_{\min}$. In this triangle $AB = c$, $B(B_1)_{\min} = kc$ and $\angle AB(B_1)_{\min} = 180° - 3\alpha$. Applying the law of cosines we find the third side, $A(B_1)_{\min}$:

$$(c_1)^2_{\min} = (A(B_1)_{\min})^2 = c^2 + k^2c^2 + 2kc^2\cos 3\alpha = c^2(1 + k^2 + 2k\cos 3\alpha)$$

$$\Rightarrow (c_1)_{\min} = c\sqrt{1 + k^2 + 2k\cos 3\alpha}$$

The maximum possible length of $c_1$ is obtained when the triangle $\triangle BB_1A$ is isosceles with $\angle B_1BA = 180° - 2\beta$. Then applying the law of sines, having in mind that $AB = BB_1 = c$ and $\angle BB_1A = \angle BAB_1 = \beta$ we obtain:

$$\frac{(c_1)_{\max}}{c} = \frac{\sin(180° - 2\beta)}{\sin\beta} = \frac{\sin 2\beta}{\sin\beta} = 2\cos\beta \Leftrightarrow (c_1)_{\max} = 2c\cos\beta$$

Therefore,

$$c\sqrt{1 + k^2 + 2k\cos 3\alpha} \leq c_1 \leq 2c\cos\beta$$

Finally, we can bound the area of the $\alpha$- and $\beta$-triangles as follows:

$$\frac{c^2}{4}\tan\alpha \leq A_\alpha \leq \frac{c^2}{4}\frac{1}{\tan\frac{\alpha}{2}}$$

$$\frac{c^2}{4}(1 + k^2 + 2k\cos 3\alpha)\tan\beta \leq \frac{c_1^2}{4}\tan\beta \leq A_\beta \leq \frac{c_1^2}{4}\frac{1}{\tan\frac{\beta}{2}} \leq c^2\frac{\cos^2\beta}{\tan\frac{\beta}{2}}$$

For the bounds we obtain:

$$\left(\frac{A_\alpha}{A_\beta}\right)_{\min} \geq \frac{(A_\alpha)_{\min}}{(A_\beta)_{\max}} \geq \frac{\frac{c^2}{4}\tan\alpha}{c^2\frac{\cos^2\beta}{\tan\frac{\beta}{2}}} \geq \frac{\tan\alpha\tan\frac{\beta}{2}}{4\cos^2\beta}$$

and

$$\left(\frac{A_\alpha}{A_\beta}\right)_{\max} \leq \frac{(A_\alpha)_{\max}}{(A_\beta)_{\min}} \leq \frac{\frac{c^2}{4}\frac{1}{\tan\frac{\alpha}{2}}}{\frac{c_1^2}{4}(1+k^2+2k\cos 3\alpha)\tan\beta} \leq \frac{1}{(1+k^2+2k\cos 3\alpha)\tan\beta\tan\frac{\alpha}{2}}$$

Next, we compare these bounds with the bounds obtained in the previous subsection. We have an interesting result here – the lower bound is worse than the previously obtained, while the upper bound is better. Comparing the lower bounds we have:

$$\frac{\tan\alpha\tan\frac{\beta}{2}}{4\cos^2\beta} < \tan\alpha\tan\frac{\beta}{2}(1-k)^2 \Leftrightarrow \cos^2\beta > \frac{1}{4(1-k)^2} \Leftrightarrow \cos\beta > \frac{1}{2(1-k)}$$

By the previous analysis

$$\frac{1}{6} < k < \frac{1}{2\sqrt{3}} \Leftrightarrow \frac{2\sqrt{3}-1}{2\sqrt{3}} < 1-k < \frac{5}{6} \Leftrightarrow \frac{6}{5} < \frac{1}{1-k} < \frac{2\sqrt{3}}{2\sqrt{3}-1} \Leftrightarrow$$

$$\Leftrightarrow \frac{3}{5} < \frac{1}{2(1-k)} < \frac{\sqrt{3}}{2\sqrt{3}-1} = \frac{6+\sqrt{3}}{11}$$

Thus we have to require that

$$\cos\beta > \frac{6+\sqrt{3}}{11} \Leftrightarrow \beta < 45.338^\circ$$

Comparing the upper bounds we have:

$$\frac{1}{(1+k^2+2k\cos 3\alpha)\tan\beta\tan\frac{\alpha}{2}} < \frac{(1+k)^2}{\tan\beta\tan\frac{\alpha}{2}} \Leftrightarrow \frac{1}{(1+k^2+2k\cos 3\alpha)} < (1+k)^2$$

which is true because the two sides of the inequality are separated by the unity:

$$\frac{1}{(1+k^2+2k\cos 3\alpha)} < 1 < (1+k)^2$$

Next, we have to consider the possibility of the point $B$ being in Zone 3 with respect to the side $AB_1$ of the $\beta$-triangle. Similarly to the previous case, we have:

$$c_1\sqrt{1+k^2+2k\cos 3\beta} \leq c \leq 2c_1\cos\alpha$$

Consequently, we can bound the area of the $\alpha$- and $\beta$-triangles as follows:

$$\frac{c_1^2}{4}(1+k^2+2k\cos 3\beta)\tan\alpha \leq \frac{c^2}{4}\tan\alpha \leq A_\alpha \leq \frac{c^2}{4}\frac{1}{\tan\frac{\alpha}{2}} \leq c_1^2\frac{cos^2\alpha}{\tan\frac{\alpha}{2}}$$

$$\frac{c_1^2}{4}\tan\beta \leq A_\beta \leq \frac{c_1^2}{4}\frac{1}{\tan\frac{\beta}{2}}$$

For the bounds we obtain:

$$\left(\frac{A_\alpha}{A_\beta}\right)_{\min} \geq \frac{(A_\alpha)_{\min}}{(A_\beta)_{\max}} \geq \frac{\frac{c_1^2}{4}(1+k^2+2k\cos 3\beta)\tan\alpha}{\frac{c_1^2}{4}\frac{1}{\tan\frac{\beta}{2}}} \geq (1+k^2+2k\cos 3\beta)\tan\alpha\tan\frac{\beta}{2}$$

and

$$\left(\frac{A_\alpha}{A_\beta}\right)_{\max} \leq \frac{(A_\alpha)_{\max}}{(A_\beta)_{\min}} \leq \frac{c_1^2\frac{\cos^2\alpha}{\tan\frac{\alpha}{2}}}{\frac{c_1^2}{4}\tan\beta} \leq \frac{\cos^2\alpha}{4\tan\beta\tan\frac{\alpha}{2}}$$

We show that these bounds are better than the bounds obtained for the case when a single point is placed in Zone 2 (previous subsection). Comparing the lower bounds we have:

$$\tan\alpha\tan\frac{\beta}{2}(1+k^2+2k\cos 3\beta) > \tan\alpha\tan\frac{\beta}{2}(1-k)^2 \Leftrightarrow 1+k^2+2k\cos 3\beta > 1+k^2-2k \Leftrightarrow$$

$$\Leftrightarrow 2k(\cos 3\beta+1) > 0$$

Comparing the upper bounds we have:

$$\frac{\cos^2\alpha}{4\tan\beta\tan\frac{\alpha}{2}} < \frac{(1+k)^2}{\tan\beta\tan\frac{\alpha}{2}} \Leftrightarrow \frac{\cos^2\alpha}{4} < (1+k)^2$$

which is true because the two sides of the inequality are separated by the unity:

$$\frac{\cos^2\alpha}{4} \leq \frac{1}{4} < 1 < (1+k)^2$$

It remains to consider the case when $B_1$ is in Zone 3 at $A$ (the shared vertex). The consideration is similar to the one at the end of the previous subsection. $C_1$ cannot be in either Zone 3 or Zone 2 with respect to any of the edges at $A$, because this will create non–convexity, $\angle B_1AC_1 > 180°$. Therefore $C1$ is in Zone 2 with respect to both $AB$ and $AC$. Further, if $C_1$ is in Zone 2 or Zone 3 with respect to the third side, $BC$ of $\triangle ABC$ this situation has already been considered. Thus, $C_1$ is in zone 1 of the side $BC$ as well. Remember that $B_1C_1$ intersects two of the sides of $\triangle ABC$. If $BC$ and $B_1C_1$ intersect we will have a "pair of intersecting sides" case considered earlier, as $B_1$ also lies in Zone 1 of $BC$. Otherwise, consider the location of points $B$ and $C$ with respect to $B_1C_1$. If either of them is in Zone 1 relative to $B_1C_1$, then we have a "pair of intersecting sides" ($(AB, B_1C_1)$ or $(AC, B_1C_1)$) as considered earlier. If either of the points $B$ or $C$ is in Zone 3 relative to $B_1C_1$, it was the case considered earlier in this subsection. Finally, if both $B$ and $C$ are in Zone 2 relative to $B_1C_1$, this is again a placement considered previously. These are all the cases possible within the premises of the current subsection.

## 3.6 Approximation factors

In Section 3.5 we considered all possible cases of matched triangles and positions of the points with respect to the forbidden zones. First, we considered the trivial case when the two matched triangles share three vertices. Second, we considered the case when they share an edge. Third, we considered the case when the matched triangles share only one vertex. In this case there are several subcases, depending on the mutual positions of the triangles and the non-shared points. Namely, the non-shared points can lie in Zones 1, 2 or 3 with respect to the triangles. Recall that

$$k = \frac{\tan\alpha}{2\sin 3\alpha}$$

We studied the behaviour of function $k(\alpha)$ within the case analysis. The bounds we derived for $f_1$ and $f_2$ are summarized in Table 3.1 on the following page. Recall that $f_1$ and $f_2$ were the respective lower and upper bounds for the ratio between the areas of the matched triangles

$$f_1(\alpha,\beta) \leq \frac{A_\alpha}{A_\beta} \leq f_2(\alpha,\beta)$$

Along with the derivation of the bounds, in the previous section we have determined some relations between them. We will briefly recall their relationship, using the abbreviated notation for the cases as per Table 3.1 on the following page. Both bounds for case (2s) are worse than those for case (3s). Both bounds for case (1p) are worse than those for case (2s). In addition, both bounds in case (1p) are worse than those in case (2p). For the placements of two points inside Zone 2, as per Figure 3.17 on page 92 we have established that upper bound for case (d) is worse than the upper bound for case (c), which in turn is worse than the upper bound for case (b), which in turn is worse than the upper bound in case (a). For the lower bounds in these four placements, we have established that the lower bound for case (c) is worse than both lower bounds for the cases (d) and (b). In turn, the lower bound in case (b) is worse than the lower bound in case (a). Comparing cases (2B) and ($2B_1$), we have shown that the lower bound for case ($2B_1$) is worse than the lower bound for case (2B), but the upper bound for case (2B) is worse than the upper bound for case ($2B_1$). Regarding the lower bounds for cases (3B) and ($3B_1$) we established that the lower bound for case (3B) is worse than the lower bound for case ($2B_1$), which in turn is worse than the lower bound for case ($3B_1$). Regarding the upper bounds for cases (3B) and ($3B_1$) we established that the upper bound for case ($2B_1$) is worse than the upper bounds for both of them. Thus, it remains to consider the relationships between the lower bounds for the cases (1p), (c) and (3B) in order to determine the value of $f_1$. To determine the value of $f_2$ we have to compare the upper bounds for cases (1p), (d) and (2B).

**Table 3.1:** Bounding functions $f_1$ and $f_2$ for the different cases considered in Section 3.5

| Case | Subcase | $f_1$ | $f_2$ |
|---|---|---|---|
| 3 shared vertices | (3s) | $1$ | $1$ |
| 2 shared vertices | (2s) | $\tan\alpha \tan\frac{\beta}{2}$ | $\frac{1}{\tan\beta \tan\frac{\alpha}{2}}$ |
| 1 shared vertex, both points in Zone 1 | 1 pair only (1p), one angle contains the other | $\tan\alpha \tan^2\beta \tan\frac{\beta}{2}$ | $\frac{1}{\tan\beta \tan^2\alpha \tan\frac{\alpha}{2}}$ |
| | 2 pairs (2p), no angle containment | $\sin\alpha \tan^2\beta$ | $\frac{1}{\sin\beta \tan^2\alpha}$ |
| 2 points in Zone 2, Figure 3.17 on page 92 | (a) | $\frac{\sin\alpha}{(1+k)^2}$ | $\frac{1}{(1-k)^2 \sin\beta}$ |
| | (b) | $\frac{\tan\alpha}{2(1+k)^2}$ | $\frac{1}{2(1-k)^2 \sin\beta \tan\frac{\alpha}{2}}$ |
| | (c) | $\frac{\tan\alpha}{2(1+k)(1+2k)}$ | $\frac{1}{2(1-k)(1-2k) \sin\beta \tan\frac{\alpha}{2}}$ |
| | (d) | $\frac{\tan\alpha}{2k^2}$ | $\frac{1}{2k_1^2 \sin 2\beta \tan\frac{\alpha}{2}}$ |
| Only 1 point in Zone 2 | (2B) | $\frac{\tan\alpha \tan\frac{\beta}{2}}{(1+k)^2}$ | $\frac{1}{(1-k)^2 \tan\beta \tan\frac{\alpha}{2}}$ |
| | ($2B_1$) | $\tan\alpha \tan\frac{\beta}{2}(1-k)^2$ | $\frac{(1+k)^2}{\tan\beta \tan\frac{\alpha}{2}}$ |
| Point in Zone 3 | (3B) | $\frac{\tan\alpha \tan\frac{\beta}{2}}{4\cos^2\beta}$ | $\frac{1}{(1+k^2+2k\cos 3\alpha)\tan\beta \tan\frac{\alpha}{2}}$ |
| | ($3B_1$) | $(1+k^2+2k\cos 3\beta)\tan\alpha \tan\frac{\beta}{2}$ | $\frac{\cos^2\alpha}{4\tan\beta \tan\frac{\alpha}{2}}$ |

We start with the lower bounds. First we show that the lower bound for (1p) is worse than the lower bound for (c):

$$\tan\alpha\tan^2\beta\tan\frac{\beta}{2} < \frac{\tan\alpha}{2(1+k)(1+2k)} \Leftrightarrow \tan^2\beta\tan\frac{\beta}{2} < \frac{1}{4k^2+6k+2}$$

We will show that this is true, by showing that the two sides of the inequality are separated by $1/5$

$$\tan^2\beta\tan\frac{\beta}{2} < \frac{1}{5} < \frac{1}{4k^2+6k+2}$$

First, consider the left hand side. As $\tan\beta$ is an increasing function over the interval $(0°, 30°]$, we have

$$\tan^2\beta\tan\frac{\beta}{2} < \tan^3\beta < \tan^3 30° = \frac{1}{3\sqrt{3}} = \frac{1}{\sqrt{27}} < \frac{1}{\sqrt{25}} = \frac{1}{5}$$

Consider now the right hand side. The denominator is a quadratic function of $k$ (the graph of which is a parabola that is concave upwards), with roots $k = -1$ and $k = -1/2$. Recall that $k \in (1/6, 1/2\sqrt{3}]$. Therefore, in this interval the function $4k^2 + 6k + 2$ is strictly increasing, and attains its maximum value at $k = 1/2\sqrt{3}$. The maximum value is $(7 + 3\sqrt{3})/3$. Thus, we have

$$4k^2+6k+2 \leq \frac{7+3\sqrt{3}}{3} \Leftrightarrow \frac{1}{4k^2+6k+2} \geq \frac{3}{7+3\sqrt{3}}$$

It remained to verify that

$$\frac{1}{5} < \frac{3}{7+3\sqrt{3}} \Leftrightarrow 7+3\sqrt{3} < 15 \Leftrightarrow 3\sqrt{3} < 8 \Leftrightarrow \sqrt{27} < \sqrt{64}$$

which is now evident.

Next we show that the lower bound for (1p) is worse than the lower bound for (3B):

$$\tan\alpha\tan^2\beta\tan\frac{\beta}{2} < \frac{\tan\alpha\tan\frac{\beta}{2}}{4\cos^2\beta} \Leftrightarrow \sin^2\beta < \frac{1}{4} \Leftrightarrow \sin\beta < \frac{1}{2} \Leftrightarrow \beta < 30°$$

The results of the case analysis for the lower bounds are summarized in Figure 3.20 on the following page. The top level corresponds to the worst bound, links correspond to comparisons between bounds such that the top of the two linked cases has worse lower bound than the bottom one.

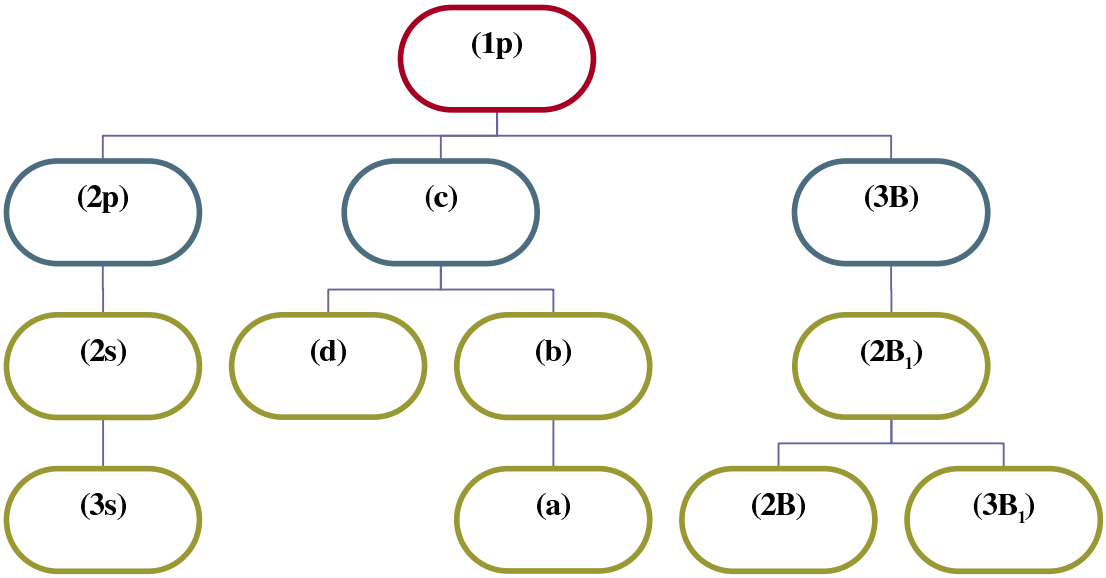


**Figure 3.20:** Comparison between the lower bounds, $f_1$

For the upper bounds, three cases remain to be considered: (1p), (d) and (2B). We show that the upper bound for (1p) is worse than the upper bound for (2B), as follows:

$$\frac{1}{\tan\beta\tan^2\alpha\tan\frac{\alpha}{2}} > \frac{1}{(1-k)^2\tan\beta\tan\frac{\alpha}{2}} \Leftrightarrow (1-k)^2 > \tan^2\alpha \Leftrightarrow 1-k > \tan\alpha$$

Previously we have shown that:

$$\frac{1}{6} < k < \frac{1}{\sqrt{12}} \Rightarrow \frac{6-\sqrt{3}}{6} < 1-k < \frac{5}{6}$$

and additionally

$$\tan\alpha < \frac{6-\sqrt{3}}{6} \Leftrightarrow \alpha < \arctan\left(\frac{6-\sqrt{3}}{6}\right) \simeq 32.42^\circ$$

The upper bounds for the cases (1p) and (d) can be compared analytically, but this is not necessary. Remember that the case (d) is possible only when $2\beta+7\alpha \leq 180^\circ$, which is a considerable constraint on the values of $\beta$. As it will be seen further, the lower bound for case (d) is much worse (when this case is possible) because of the fact that it contains a high power ($3^{\text{rd}}$ and above) of a very small number.

The results of the case analysis for the upper bounds are shown in Figure 3.21 on the next page. The dashed link corresponds to the comparison between the cases (1p) and (d). Case (d) is not always possible, but when possible is worse than (1p).

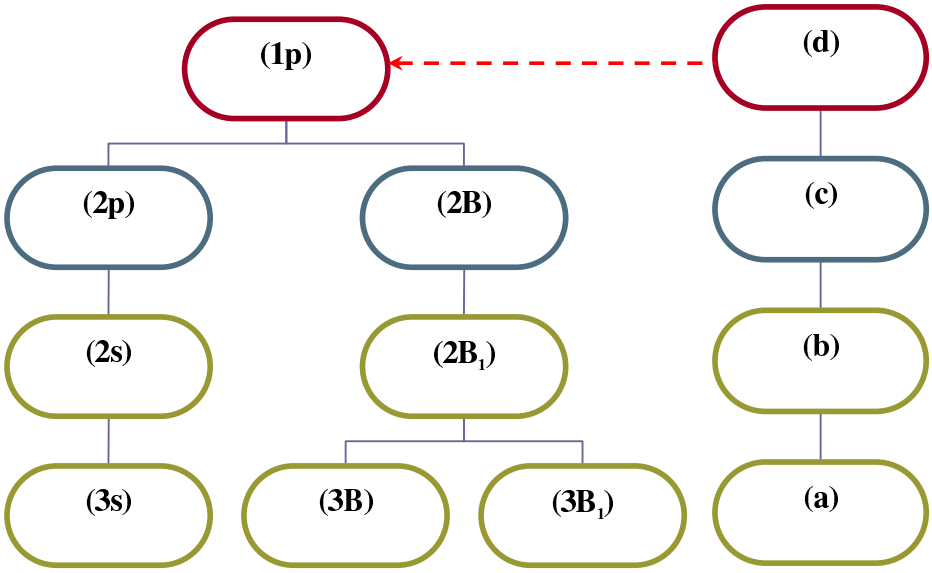


**Figure 3.21:** Comparison between the upper bounds, $f_2$

**Theorem 81** *For $0° < \beta < \alpha \leq 30°$ the bounding functions for the ratio of the area of the matched triangles from $T_\alpha$ and $T_\beta$ are:*

$$f_1 = \tan\alpha \tan^2\beta \tan\frac{\beta}{2}$$

*and*

$$f_2 = max\left(\frac{1}{\tan\beta \tan^2\alpha \tan\frac{\alpha}{2}}\ ,\ \frac{1}{2k_1^2 \sin 2\beta \tan\frac{\alpha}{2}}\right)$$

As discussed previously, the approximation factor $1/f_1$ shows how many times the smallest area triangle in the approximating $\alpha$ -triangulation can be smaller than the smallest area triangle in the optimal (MaxMin area) triangulation. Similarly, $f_2$ gives the ratio of the largest area triangle in the approximating triangulation, compared to the largest area triangle in the optimal (MinMax area) triangulation. Sample values of the approximation factors are presented in Table 3.2.

**Table 3.2:** Sample values of the approximation factors

| $\alpha$ | $\beta$ | $1/f_1$ | $f_2$ |
|---|---|---|---|
| 30° | 28° | 24.57 | 21.06 |
| 30° | 26° | 31.54 | 22.96 |
| 30° | 24° | 41.11 | 25.15 |
| 30° | 22° | 54.59 | 27.71 |

**Table 3.2:** Sample values of the approximation factors (continued)

| $\alpha$ | $\beta$ | $1/f_1$ | $f_2$ |
|---|---|---|---|
| 30° | 20° | 74.15 | 30.76 |
| 28° | 26° | 34.25 | 29.09 |
| 28° | 24° | 44.64 | 31.86 |
| 28° | 22° | 59.27 | 35.11 |
| 28° | 20° | 80.51 | 38.98 |
| 28° | 18° | 112.48 | 43.66 |
| 26° | 24° | 48.66 | 40.90 |
| 26° | 22° | 64.62 | 45.07 |
| 26° | 20° | 87.77 | 50.03 |
| 26° | 18° | 122.62 | 56.04 |
| 26° | 16° | 177.43 | 63.50 |
| 24° | 22° | 70.79 | 58.74 |
| 24° | 20° | 96.15 | 65.21 |
| 24° | 18° | 134.32 | 73.04 |
| 24° | 16° | 194.37 | 82.77 |
| 24° | 14° | 294.26 | 95.19 |
| 22° | 20° | 105.96 | 86.59 |
| 22° | 18° | 148.02 | 97.00 |
| 22° | 16° | 214.19 | 109.91 |
| 22° | 14° | 324.27 | 126.40 |
| 22° | 12° | 521.22 | 884.24 |
| 20° | 18° | 164.31 | 750.86 |
| 20° | 16° | 237.76 | 832.85 |
| 20° | 14° | 359.96 | 940.09 |
| 20° | 12° | 578.58 | 1085.09 |
| 20° | 10° | 1010.05 | 1290.41 |
| 18° | 16° | 266.34 | 3693.27 |
| 18° | 14° | 403.22 | 4168.80 |
| 18° | 12° | 648.12 | 4811.80 |
| 18° | 10° | 1131.45 | 5722.28 |
| 18° | 8° | 2228.31 | 7100.40 |
| 16° | 14° | 456.90 | 19320.47 |

**Table 3.2:** Sample values of the approximation factors (continued)

| $\alpha$ | $\beta$ | $1/f_1$ | $f_2$ |
|---|---|---|---|
| 16° | 12° | 734.40 | 22300.46 |
| 16° | 10° | 1282.08 | 26520.11 |
| 16° | 8° | 2524.96 | 32907.05 |
| 16° | 6° | 6023.76 | 43626.28 |
| 14° | 12° | 844.62 | 28557.64 |
| 14° | 10° | 1474.48 | 33961.27 |
| 14° | 8° | 2903.89 | 42140.29 |
| 14° | 6° | 6927.76 | 55867.17 |
| 14° | 4° | 23488.63 | 83460.37 |
| 12° | 10° | 1729.56 | 167255.17 |
| 12° | 8° | 3406.25 | 207535.87 |
| 12° | 6° | 8126.23 | 275139.11 |
| 12° | 4° | 27552.07 | 411032.29 |
| 12° | 2° | 221022.46 | 820062.07 |
| 10° | 8° | 4106.13 | 4126162.52 |
| 10° | 6° | 9795.92 | 5470228.84 |
| 10° | 4° | 33213.14 | 8172013.99 |
| 10° | 2° | 266435.54 | 16304214.75 |
| 8° | 6° | 12290.27 | 116323732.58 |
| 8° | 4° | 41670.26 | 173776855.99 |
| 8° | 2° | 334278.46 | 346707088.60 |

The approximation factors were calculated for each even value of $\alpha \in (0°, 30°]$ and for the even values of $\alpha - 10° \leq \beta \leq \alpha - 2°$. Numerical values confirm that if the optimal area triangulations are relatively "fat" then they can be approximated well by a triangulation that is "fat", such as the Delaunay Triangulation. The opposite is also evident, as the smallest angle in the optimal triangulation becomes smaller, we cannot have practical theoretical bounds. Both observations suggest that in approximating optimal area, it might be useful to employ a randomized algorithm, but no research in this direction is reported here. We also observe that the approximation factor for the MaxMin Area triangulation ($1/f_1$) grows slower with the decrease of $\alpha$, but for same $\alpha$ it grows faster with the decrease of $\beta$, compared to the respective growth of the approximation factor for the MinMax Area triangulation ($f_2$) under the same circumstances. In addition to the relatively faster growth of $f_2$ with the decrease of $\alpha$, this approximation factor grows by orders of magnitude,

when the worst case (d) is possible. In the table, this is first present between $\alpha = 22°, \beta = 14°$ and $\alpha = 22°, \beta = 12°$, there the increase is by a factor of 8. The difference between $1/f_1$ and $f_2$ for $\alpha = 2°, \beta = 1°$, which is not presented in the table, is 22 orders of magnitude – $10^8$ against $10^{30}$.

In conclusion, we hope that our approaches and results shed some light and serve as a basis for further developments on the nature, complexity and computation of the exact MaxMin and MinMax area triangulations of a general point set.

# Chapter 4

# Conclusions

The research presented in this thesis focuses on computing the MaxMin and the MinMax area triangulations (collectively called optimal area triangulations) of a set of points in the plane. This problem has not been studied in depth previously. However, it is mentioned that the the MinMax area triangulation is a hard open problem in one of the recent surveys of open problems in Computational Geometry presented (see the last chapter in Edelsbrunner's book [25]).

The first main contribution of this thesis is the development of algorithms that compute the exact optimal area triangulations of a convex polygon in $O(n^2 \log n)$ time and $O(n^2)$ space. This is an improvement of almost a linear factor over the best previously known algorithm by Klincsek [37]. Although the two optimal area triangulation of a convex polygon are of equal computational complexity, the MaxMin decision problem admits better solution – $O(n^2 \log \log n)$ due to the specific properties of this quality measure and using efficient data structures. This constitutes another contribution of the thesis, that has already been published [32].

In the case when the point set is in general position, the problem of finding the exact MinMax and MaxMin area triangulation is still of unknown complexity. The third main contribution of this study is the development of subcubic time algorithm that approximates the optimal triangulations within practical factors. The algorithmic approach combines two well-known concepts in the computational geometry literature – matchings between two different triangulations [2], and exclusion regions [7, 18]. The novelty is the introduction of angular constraints on the approximating triangulation, the definition of a forbidden zone (exclusion region) based on these constraints, and then the derivation of the bounds on the approximation factors [33]. Another contribution is the property that the relative neighbourhood graph is a part of every 30°-triangulation of a general point set, presented in Theorem 74 on page 78 of this thesis, and in [34].

The new results presented in this thesis allow some rows of the table presented in Chapter 1 to be updated as follows:

**Table 4.1:** Comparison between the known optimal triangulation algorithms, updated

| **Optimal Triangulation** | **General Point Set** | **Convex polygon** | **Algorithms** |
|---|---|---|---|
| MaxMin Area | $O(n^3)$ time, $O(n)$ space approximation algorithm | $O(n^2 \log n)$ time, $O(n^2)$ space, $O(n^2 \log\log n)$ time, $O(n^2)$ space for the decision problem | Modified dynamic programming for the convex case, angular constraints for the approximation algorithm in the general case |
| MinMax Area | $O(n^3)$ time, $O(n)$ space approximation algorithm | $O(n^2 \log n)$ time, $O(n^2)$ space | Modified dynamic programming for the convex case, angular constraints for the approximation algorithm in the general case |

The future research in this area can be directed towards strengthening the geometric and algorithmic properties of the optimal area triangulation in the convex case. A quadratic time algorithm might be possible for the two optimal triangulations considered in Chapter 2. Further, it is interesting to know whether there is a quadratic lower bound on the complexity of such an algorithm.

The approximation results presented in Chapter 3 of this thesis can be extended in two directions. First, the bounds derived here are worst-case bounds, based on a strongly localized notion of matching. De-localizing the matching might help, because in fact the worst triangles do not need to be close to each other in two different triangulations. Also, a precise analysis of the matching using the local optimality might improve the bounds on the approximation factors. Another interesting extension will be to look at the possibility of a randomized algorithm for generation of an approximating triangulation. The major problem, whether the exact MaxMin and MinMax area triangulations of a general point set are computable in polynomial time, is still open. Further structural properties of the optimal triangulations may help to settle this question.

It is also interesting to look at the generalization of these two problems in three dimensions. Namely, to consider the MinMax and MaxMin volume tetrahedralizations, or near-average volume terahedralizations, of a point set in the three-dimensional space. The solution to one of these three problems will lead to a speed-up of the existing algorithms for approximate weighted shortest tours in three-dimensional scenes with obstacles. The exact solution of the last problem is NP-complete

[19].

# References


[1] A. Agarwal, L. J. Guibas, J. Saxe, and P. W. Shor. A linear-time algorithm for computing the Voronoi diagram of a convex polygon. *Discrete Computational Geometry*, 4:591–604, 1989.

[2] O. Aichholzer, F. Aurenhammer, S.-W. Cheng, N. Katoh, G. Rote, M. Taschwer, and Y.-F. Xu. Triangulations intersect nicely. *Discrete and Computational Geometry*, 16(4):339–359, 1996.

[3] O. Aichholzer, F. Aurenhammer, P. Gonzalez-Nava, T. Hackl, C. Huemer, F. Hurtado, H. Krasser, S. Ray, and B. Vogtenhuber. Matching edges and faces in polygonal partitions. In *Proceedings of the* $17^{th}$ *Canadian Conference on Computational Geometry*, pages 123–126, 2005.

[4] O. Aichholzer, F. Hurtado, and M. Noy. A lower bound on the number of triangulations of planar point sets. *Computational Geometry: Theory and Applications*, 29(2):135–145, 2004.

[5] E. Anagnostou and D. Corneil. Polynomial-time instances of the minimum weight triangulation problem. *Computational Geometry: Theory and Applications*, 3:247–259, 1993.

[6] T. J. Baker and P. P. Pebay. A comparison of triangle quality measures. In *Proceedings of the* $10^{th}$ *International Meshing Roundtable*, pages 327–340, October 2001.

[7] R. Beirouti and J. Snoeyink. Implementations of the LMT heuristic for minimum weight triangulation. In *Proceedings of the* $14^{th}$ *Annual ACM Symposium on Computational Geometry*, pages 96–105, 1998.

[8] P. Belleville, M. Keil, M. McAllister, and J. Snoeyink. On computing edges that are in all minimum–weight triangulations. In *Proceedings of the* $12^{th}$ *Annual ACM Symposium on Computational Geometry*, pages V7–V8, 1996.

[9] M. Bern, H. Edelsbrunner, D. Eppstein, S. Mitchell, and T. S. Tan. Edge insertion for optimal triangulations. *Discrete and Computational Geometry*, 10:47–65, 1993.

[10] B. N. Boots. *Voronoi (Thiessen) Polygons*. Geo Books, Norwich, UK, 1986.

[11] P. Bose, P. Morin, I. Stojmenović, and J. Urrutia. Routing with guaranteed delivery in ad hoc wireless networks. *Wireless Networks*, 7(6):609–616, 2001.

[12] O. Bottema, R. Ž. Djordjevič, R. R. Janič, D. S. Mitrinovič, and P. M. Vasič. *Geometric Inequalities*. Wolters-Noordhoff Publishing, Groningen, The Netherlands, 1969.

[13] P. M. Camerini, F. Maffioli, S. Martello, and P. Toth. Most and least uniform spanning trees. *Discrete Applied Mathematics*, 15:181–197, 1986.

[14] R. C. Chang and R. C. T. Lee. On average length of the Delaunay triangulations. *BIT*, 24:269–273, 1984.

[15] S. W. Cheng, M. J. Golin, and J. C. F. Tsang. Expected case analysis of $\beta$-skeletons with applications to the construction of minimum–weight triangulations. In *Proceedings of the* $7^{th}$ *Canadian Conference on Computational Geometry*, pages 279–284, 1995.

[16] S.-W. Cheng and Y.-F. Xu. Approaching the largest $\beta$-skeleton within a minimum weight triangulation. In *Proceedings of the* $12^{th}$ *Annual ACM Symposium on Computational Geometry*, pages 196–203, 1996.

[17] Y. Dai, N. Katoh, and S.-W. Cheng. LMT-skeleton heuristics for several new classes of optimal triangulations. *Computational Geometry: Theory and Applications*, 17:51–68, 2000.

[18] G. Das and D. Joseph. Which triangulations approximate the complete graph? In *Proceedings of the International Symposium on Optimal Algorithms, Lecture Notes in Computer Science*, volume 401, pages 168–192. Springer–Verlag, 1989.

[19] M. de Berg, M. van Kreveld, M. Overmars, and O. Schwarzkopf. *Computational Geometry: Algorithms and Applications, 2nd Edition*. Springer-Verlag, February 2000.

[20] M. T. Dickerson, R. L. S. Drysdale, S. A. McElfresh, and E. Welzl. Fast greedy triangulation algorithms. *Computational Geometry: Theory and Applications*, 8:67–86, 1997.

[21] M. T. Dickerson, J. M. Keil, and M. H. Montague. A large subgraph of the minimum weight triangulation. *Discrete and Computational Geometry*, 18:289–304, 1997.

[22] M. T. Dickerson, S. McElfresh, and M. Montague. New algorithms and empirical findings on minimum weight triangulation heuristics. In *Proceedings of the* $11^{th}$ *Annual ACM Symposium on Computational Geometry*, pages 238–247, 1995.

[23] M. T. Dickerson and M. H. Montague. A (usually?) connected subgraph of the minimum weight triangulation. In *Proceedings of the* $12^{th}$ *Annual ACM Symposium on Computational Geometry*, pages 204–213, 1996.

[24] R. L. Drysdale, S. McElfresh, and J. S. Snoeyink. On exclusion regions for optimal triangulations. *Discrete Applied Mathematics*, 109:49–65, 2001.

[25] H. Edelsbrunner. *Geometry and Topology for Mesh Generation*. Cambridge University Press, UK, 2001.

[26] H. Edelsbrunner, T. S. Tan, and R. Waupotitsch. An $O(n^2 \log n)$ time algorithm for the minmax angle triangulation. *SIAM J. Sci. Stat. Comput.*, 13(4):994–1008, July 1992.

[27] Euclid. *Elements, Book III*. circa 280 BC.

[28] P. D. Gilbert. New results on planar triangulations. Master's thesis, University of Illinois at Urbana-Champaign, Urbana, 1979.

[29] L. S. Heath and S. V. Pemmaraju. New results for the minimum weight triangulation problem. *Agorithmica*, 12:533–552, 1994.

[30] S. Hu. A constant approximation algorithm for maximum weight triangulation. In *Proceeding of the* $15^{th}$ *Canadian Conference on Computational Geometry*, pages 150–154, August 2003.

[31] J. M. Keil. Computing a subgraph of the minimum weight triangulation. *Computational Geometry: Theory and Applications*, 4:13–26, 1994.

[32] J. M. Keil and T. S. Vassilev. An algorithm for the MaxMin area triangulation of a convex polygon. In *Proceeding of the* $15^{th}$ *Canadian Conference on Computational Geometry*, pages 145–149, August 2003.

[33] J. M. Keil and T. S. Vassilev. Optimal area triangulation wit angular constraints. In *Proceedings of the XI Encuentros de Geometría Computacional*, pages 15–22, June 2005.

[34] J. M. Keil and T. S. Vassilev. The relative neighbourhood graph is a part of every 30°–triangulation. In *Proceedings of the* $21^{st}$ *European Workshop on Computational Geometry*, pages 9–12, March 2005.

[35] D. G. Kirkpatrick. A note on Delaunay and optimal triangulations. *Information Processing Letters*, 10(3):127–128, 18 April 1980.

[36] D. G. Kirkpatrick and J. D. Radke. A framework for computational morphology. In G. T. Toussaint, editor, *Computational Geometry*, pages 217–248. Elsevier Science Publishers B.V. (North Holland), 1985.

[37] G. T. Klincsek. Minimal triangulations of polygonal domains. *Annals of Discrete Mathematics*, 9:121–123, 1980.

[38] T. Lambert. *Empty-Shape Triangulation Algorithms*. PhD thesis, University of Manitoba, Winnipeg, August 1994.

[39] C. Levcopoulos. An $\Omega(\sqrt{n})$ lower bound for the nonoptimality of the greedy triangulation. *Information Processing Letters*, 25:247–251, 17 June 1987.

[40] C. Levcopoulos and A. Lingas. On approximation behaviour of the greedy triangulation for convex polygon. *Algorithmica*, 2:175–193, 1987.

[41] C. Levcopoulos and A. Lingas. Fast algorithms for the greedy triangulation. *Proceedings of the* $2^{nd}$ *Scandinavian Workshop on Algorithm Theory, in Lecture Notes in Computer Science*, 447:238–250, 1990.

[42] C. Levcopoulos, A. Lingas, and J.-R. Sack. Heuristics for optimum binary search trees and minimum weight triangulation problems. *Theoretical Computer Science*, 66(2):181–203, August 1989.

[43] E. L. Lloyd. On triangulations of a set of points in the plane. In *Proceedings of the* $18^{th}$ *Annual IEEE Symposium on Foundations of Computer Science*, pages 228–240, 1977.

[44] G. K. Manacher and A. L. Zobrist. Neither the greedy nor the Delaunay triangulation of a planar point set approximates the optimal triangulation. *Information Processing Letters*, 9(1):31–34, 20 July 1979.

[45] J. S. B. Mitchell and J. O'Rourke. Computational geometry column 42. *International Journal of Computational Geometry and Applications*, 11(5):573–582, 2001.

[46] T. Ono, Y. Kyoda, T. Masada, K. Hayase, T. Shibuya, M. Nakade, M. Inaba, H. Imai, K. Imai, and D. Avis. A package for triangulations. Technical report, University of Tokyo, Japan, 2000.

[47] D. A. Plaisted and J. Hong. A heuristic triangulation algorithm. *Journal of Algorithms*, 8:405–437, 1987.

[48] F. Preparata and M. Shamos. *Computational Geometry: An Introduction*. Springer-Verlag, 1985.

[49] V. T. Rajan. Optimality of the Delaunay triangulation in $\Re^d$. *Discrete and Computational Geometry*, 12:189–202, 1994.

[50] O. Schwarzkopf. The extensible drawing editor Ipe. In *Proceedings of the* $11^{th}$ *Annual ACM Symposium on Computational Geometry*, pages C10–C11, 1995.

[51] M. I. Shamos and D. Hoey. Closest points problems. In *Proceedings of the* $16^{th}$ *Annual IEEE Symposium on Foundations of Computer Science*, pages 151–162, 1975.

[52] J. R. Shewchuk. What is a good linear element? Interpolation, conditioning, and quality measures. In *Proceedings of the* $11^{th}$ *International Meshing Roundtable*, pages 115–126, September 2002.

[53] W. D. Smith. *Studies in Computational Geometry Motivated by Mesh Generation*. PhD thesis, Princeton University, Princeton, NJ, 1989.

[54] T. S. Tan. *Optimal Two-dimensional Triangulations*. PhD thesis, University of Illinois at Urbana-Champaign, Urbana, 1993.

[55] G. Toussaint. Complexity, convexity and unimodality. *International Journal of Computer and Information Sciences*, 13(3):197–217, June 1984.

[56] G. Toussaint. Solving geometric problems with the rotating calipers. In *Proceedings of IEEE MELECON'83*, pages A10.02/1–4, May 1983.

[57] P. van Emde-Boas. Preserving order in a forest in less than logarithmic time and linear space. *Information Processing Letters*, 6(3):80–82, June 1977.

[58] P. van Emde-Boas, R. Kaas, and E. Zijlstra. Design and implementation of an efficient priority queue. *Mathematical Systems Theory*, 10:99–127, 1977.

[59] C. A. Wang. An optimal algorithm for greedy triangulation of a set of points. In *Proceedings of* $6^{th}$ *Canadian Conference on Computational Geometry*, pages 332–338, 1994.

# Index